Development of adaptive gaze-based human-machine interface for enhancing assisted daily living

Parasto Azizinezhad

A thesis submitted for the degree of

Doctor of Philosophy

at the

School of Computer Science and Electronic Engineering

University of Essex

April 2025

Abstract

The efficacy of gaze-based assistive technologies for individuals with severe motor impairments is often limited by a dual challenge: the cognitive inefficiency of rigid interfaces and the practical inaccessibility of costly hardware. This thesis presents the design, implementation, and validation of an integrated assistive system engineered to solve this dual problem. The core of the system is an adaptive, intention-based interface that utilizes a machine learning model to interpret pupillometry in real-time. By classifying the user's data into 'decision-making' and 'focus' events, this method replaces static dwell-time with a control mechanism that responds dynamically to user's intend, creating a more fluid and intuitive user experience. This intelligent software is paired with an accessible hardware solution: a low-cost, 3D-printable robotic controller. This mechanism retrofits standard powered wheelchairs through the mechanical actuation of the existing joystick, making advanced gaze-based navigation widely deployable without requiring extensive modifications or specialized installation. The system's functionality is further extended to semi-autonomous robotic manipulation by integrating an object detection layer, which offloads the profound cognitive load of the task by allowing users to execute complex pick-and-place actions with a single gaze command.

The performance of this integrated system was evaluated through a series of user studies focusing on realistic navigation and manipulation tasks. The evaluation employed a mixed-methods approach, analyzing objective performance metrics, such as task completion time and command frequency, alongside subjective feedback on usability and workload. The results provide strong

evidence for the success of this approach, showing that the adaptive interface was significantly more efficient and was subjectively preferred by participants over traditional dwell-based methods. The overall outcomes demonstrate that by concurrently addressing the fundamental challenges of usability and accessibility, this work provides a powerful and practical framework for enhancing assisted daily living, offering a validated pathway towards more adaptive and affordable assistive technologies.

Acknowledgements

First and foremost, I want to thank my parents, Amir & Mozhgan and my brother, Pedram, for their unwavering support throughout my life. Your financial help, emotional strength, constant advice, and belief in me have been the foundation of this journey. I truly couldn't have done this without you, and I'm endlessly grateful for the sacrifices you've made along the way.

I am also sincerely grateful to my supervisor, Dr. Anirban Chowdhury, for his academic guidance and support throughout the course of this research. His expertise and feedback have been valuable in shaping the direction and quality of this work.

I'm also sincerely thankful to my aunt for always being there with her support, kindness, and motivation. Your presence has meant so much to me.

To my friends, I extend my heartfelt thanks. A special mention goes to my beloved friend, who has been a steady source of support through countless coffee breaks, conversations, focused work sessions, and troubleshooting marathons. Your presence, encouragement, and insight have meant more than I can put into words.

I'd also like to express my appreciation to my extended family, especially my cousins, for their emotional support. The conversations, video calls, walks, and uplifting moments we shared helped me stay grounded and brightened the more challenging days.

Finally, thank you to everyone who helped, encouraged, advised, or inspired me throughout this journey. Every bit of support has made a difference, and I'm truly grateful.

Contents

x

List of Figures

xiv

xvii

List of Tables

List of Abbreviations

Chapter 1

Introduction

According to statistics published by the World Health Organization (WHO), approximately 16% of the global population, or approximately 1.3 billion individuals, are said to be experiencing a severe disability [8]. The estimate takes into consideration the extensive impact of disability on populations and societies worldwide. In addition, it is estimated that over 2.5 billion people worldwide rely on an assistive product to enable their daily living and improve their quality of life [9]. These figures emphasize the growing demand for accessible and inclusive technology that will empower individuals with disabilities and optimize their independence.

Assistive Technologies (ATs) play a significant role in attempts to enhance the quality of life of persons with disabilities as they enable them to conduct daily activities with greater autonomy and efficiency. The WHO is quoting that approximately 3.5 billion people globally are expected to require an assistive device by 2030 [9] that suggests that it makes us aware of the increasing requirement for such technologies and for their further improvement and development [10]. This growing reliance on ATs highlights not only their value in achieving autonomy and accessibility but also the necessity of innovating and refining their design so that they can efficiently cater to the range of users' needs. Based on this, the innovation of ATs is an imperative in addressing the issues being faced by people with disabilities and allowing them to integrate into society.

There are various modalities for interacting with assistive devices, as well as a wide range of device types tailored to the nature of an individual's disability and specific needs. Among these, mobility assistance is a particularly common requirement, and wheelchairs are widely used to support individuals with diverse conditions.

However, for individuals with severe mobility impairments—such as those with motor disabilities, upper-limb impairments, locked-in syndrome [11], amputations, or other conditions that limit hand function—the range of suitable assistive technologies becomes significantly narrower. Standard control methods for wheelchairs, which typically rely on manual or joystick input, are often inaccessible to these users. As a result, more specialised and adaptive interaction methods are necessary to accommodate their needs and ensure effective and independent use of such assistive technologies.

There are a variety of assistive and autonomous wheelchairs that have been developed, each with different methods of user interaction and command input. They vary from Electroencephalogram (EEG), Electromyogram (EMG), joystick, eye-tracking, and Graphic User Interfaces (GUIs) [12]. Some utilize a single mode of interaction, whilst others use a combination of modalities in an effort to enhance both functionality and usability for the user. For example, the RoboChair [13], which was introduced in 1997, combines a joystick for movement control with a GUI for more natural control.

In another recent study, Liu et al. [14] utilized a combination of eye-tracking and Inertial Measurement Unitss (IMUs) in movement intention detection to improve the safety and reliability of lower-limb exoskeletons for mobility assistance. Besides, Meena et al. [15] developed a gaze-controlled virtual keyboard, combining eye-tracking with other modalities to support learning for dyslexic children.

With the use of Eye-tracking alongside other biosignal-driven approaches such as brain-computer interfaces (BCIs) [16, 17], the combined modalities are being developed such as hybrid BCI architectures [18] which aim to enhance the accuracy, use and accommodative of user needs.

EEG signals have also been widely used as a control modality in several autonomous wheelchair projects, e.g., those presented in [19]. A case in point is the study conducted by [20], which explored a hybrid BCI using EEG and Electrooculogram (EOG) signals to control a wheelchair-mounted robotic arm system.

While such systems have much potential to assist individuals with mobility impairments, their deployment in the real world is beset by numerous challenges. They include the need for frequent calibration, which is time-consuming and inconvenient for users, greater user fatigue due to extended cognitive load, and great variability in signal responses between individuals. These issues hamper the scalability and generalizability of EEG-based control systems for assistive technologies and necessitate further research to enhance system robustness and user experience.

As a result, modalities like eye-tracking technology provide a more practical and user-friendly solution for controlling mobility assistance devices, especially for individuals with both upper and lower limb disabilities. For example, a wheelchair-mounted robotic arm controlled by a screen-based eye-tracker was introduced in [21]. This system likewise features an intuitive interface with buttons and options that enable both the mobility of the wheelchair and the robotic arm to be commanded, enabling greater integrated interaction.

Similarly, the research in [22] also presented a comparable robotic system designed to assist individuals with mobility impairments, though employing an alternative control method. They refer to the ability of eye-tracking technology to enhance the independence of users, offering an alternative to traditional solutions like the utilization of joysticks or EEG-based interfaces that may be less easy for certain users to operate effectively.

Today's ATs are mostly focused on fixing physical functionality. However, computing, artificial intelligence, and robotics are advancing very rapidly and open new avenues to making ATs more interactive and adaptive [23]. Future ATs will not only have to cater to users' physical requirements but also dynamically adapt to their mental and emotional states, including cognit-

ive load [24], fatigue [25], and emotional well-being. Advance solutions can enhance system response, and accommodation to the user, particularly in individuals who are severely physically disabled and are totally reliant upon assistive technology to interact daily and communicate effectively.

For instance, ATs that have been developed to aid human-computer or human-robot interaction for daily living activities must adjust their behaviour in line with the user's shifting mental and physical state. Dynamic adaptability is important in an effort to make such systems intuitive, efficient, and capable of providing an unobtrusive user experience.

For this to be done, it is critical to research ways in which cognitive states and feelings of humans may be communicated efficiently to assistive devices and ways in which these devices can become adaptable in real-time to accommodate personalized support. Development of human-machine interaction models that are high-level and that consider such variables will be fundamental. Such models will ensure the next-generation ATs are personalized to specific needs and enhance the usability and efficiency of the technologies. This approach will make all of them invaluable resources to promote accessibility and bring greater autonomy to the user.

Eye-tracking technology has become a widely utilized tool, particularly in psychological research, where it offers valuable insights into human cognition and areas of interest [26, 27]. Some of the vast studies have centered on mental workload estimation via pupil dilation, which is known to be a cognitive load measure [28, 29]. For instance, Guo et al. [30] identified the significant impact of time pressure, latency, and task specificity on mental workload and emphasized considering such factors when designing assistive devices. Aside from basic pupil diameter measurement, gaze data have played a critical role as a crucial ingredient in measuring cognitive load and mental workload. Moreover, researchers have expanded their research to study the relationship between power and frequency at mean frequency in an attempt to advance their knowledge of cognitive load [31]. This testifies to the power of eye-tracking and pupil dilation data not only as a measure of user attention but as a predictor for enhancing more natural

and adaptive assistive technologies.

Gaze-controlled assistive technologies are now valuable tools for supporting individuals with severe physical disabilities [32, 33, 34]. Pupillary reactions and eye tracking, in general, have been accorded a high level of interest from disciplines and applications in everyday life—education [35], psychology [36, 37], marketing [38], and communication [39]. Among the results to be replicated across these disciplines is that pupil size is larger with higher cognitive load [40]. Additionally, pupil size changes have also been linked to subjective task difficulty [41], and pupil dilation can therefore serve as a useful measure of mental effort. The fact that the pupil responds rapidly and involuntarily to neural activity also contributes to its worth as an online, non-invasive assessment of establishing the state of mind of a user. This makes it extremely appropriate to the adaptive system design, which appropriately reacts to the cognitive or affective needs of the user.

A growing body of research has shown that pupil dilation tends to increase during effortful decision-making [42, 43]. This highlights a clear link between cognitive load and the decision-making process. Since cognitive load can greatly impact user performance [44] and design systems that help reduce this load is essential—especially in the context of assistive technologies [45]. For many individuals who depend on assistive devices as their primary mode of interaction or communication, particularly those dealing with long-term health conditions, the system's usability and mental demand can directly affect their quality of life. While there have been notable advancements in the field of Human-Computer Interaction (HCI), adaptive systems that respond to user workload remain underdeveloped—especially in assistive contexts, where such capabilities could make a profound difference.

Although extensive research on autonomous assistive technologies, their widespread adoption among the target user groups remains limited. Part of the most important challenge facing the improvement of their usability lies in comprehending dynamic changes in users' cognitive and emotional states during interactions with these technologies. Exploration of the way assistive systems can be adjusted to adapt to changes in users' cognitive and emotional states has

the promise to greatly enhance their responsiveness and effectiveness. Through adjusting these systems to respond more to the users' needs and attitudes at the moment, more active user participation can be fostered, greater satisfaction can be achieved, and ultimately the overall user experience can be improved [46].

Pupil diameter is strongly correlated with all types of mental activity, with pupil dilation having been seen in experiments as a common byproduct of higher cognitive load [47] and pupil narrowing when fatigue is felt [48]. These automatic physiological responses to mind states have thus made pupil diameter a valuable measure to distinguish among different cognitive processes, such as decision-making and sustained concentration. Therefore, pupil diameter is a valuable metric of user interaction and cognitive states that provides insight into the way people read information and apply mental effort [5]. Having such a feature in monitoring and analyzing pupil size changes has important implications in making assistive technologies more adaptive and responsive to suit users' requirements.

While reviewing the literature and exploring existing products, it became evident that although numerous studies and publications address specific aspects of individual user needs, there is a lack of integrated solutions that combine all dimensions in a single, accessible product. Furthermore, there has been limited research investigating the adaptability and user acceptability of such comprehensive approaches and presented a clear opportunity for further exploration. This study was therefore motivated by the need to investigate the feasibility of developing an affordable, adaptive assistive solution. Although custom-made systems tailored to individual users do exist, they are often prohibitively expensive and inaccessible to the wider public, which runs counter to the aims of promoting cost-effectiveness and broad availability.

1.1 Motivation

The motivation and inspiration for this project originated years ago during my experience of caring for my grandmothers. Witnessing their struggles with daily activities, despite the availability of assistive devices, was both frustrating and heartbreaking. A key issue I observed was their difficulty with adapting to new technologies and the ongoing challenges posed by frequent changes, such as updates or new versions of their assistive devices, phones, televisions, and other tools.

Assistive technology users often rely heavily on their devices for daily tasks, spending significant portions of their time using them. It is essential to ensure that these devices are not only safe and comfortable to use but also capable of adapting to the user's changing needs and conditions throughout the day.

For instance, a person may feel rushed at one point during the day or overwhelmed at another. A fixed setup for speed, the duration a user must fixate their gaze to trigger a selection (commonly known as dwell time in eye-tracking based systems), or the number of available options may not be appropriate in such situations. Therefore, the adjustability of the system can enhance the user experience by accommodating these changing conditions.

Another concern for many elderly and disabled individuals is the cost of care associated with their conditions. While services in the UK, such as the NHS, provide some support and offer products to help disabled individuals maintain their independence, such services are not available in many other countries.

Full-time care can also be financially demanding, and although certain support schemes may be available, the self-funded cost can represent a significant burden. According to the NHS, the cost of a full-time carer can range from £800 to £1,600 per week [49]. Therefore, it may be crucial for individuals to invest in assistive technologies that can reduce the level of care required while simultaneously enhancing independence and overall quality of life.

To purchase an assistive device such as a wheelchair, in the UK, the NHS may provide wheelchairs for short-term use and, in some cases, offer vouchers to eligible individuals based on their specific circumstances to support the purchase of a wheelchair [50]. Additional support may be available through a personal health budget, which can offer greater flexibility in choosing a wheelchair [51]. However, access to such resources depends on a professional assessment, an established care plan, and the individual's personal needs and conditions.

On the other hand, the waiting time to obtain a wheelchair through the NHS can range from 3 months to over 12 months [52], which may not be practical or suitable for individuals with urgent or evolving mobility needs.

Therefore, providing affordable assistive solutions to individuals can be highly beneficial and crucial. Access to cost-effective assistive technologies that empower users and promote independence is essential for improving quality of life and reducing reliance on full-time care.

Furthermore, beyond these personal and practical considerations, a review of the scientific literature reveals specific technological gaps that form the core research motivation for this thesis. While gaze-based interfaces are well-established, their development is often constrained by several key challenges that this work aims to address directly.

First, the predominant method for command activation in existing gaze-based systems is a standardized, fixed-duration dwell time. This approach is scientifically suboptimal as it fails to adapt to the user's cognitive state. There exists a clear dichotomy between the dynamic nature of human decision-making processes and the static nature of the interface, which can result in interactions that are either inefficient or susceptible to unintended activations. This presents a clear research need for more intelligent and adaptive activation mechanisms.

Second, while a significant body of research in psychophysiology has established pupil dilation as a reliable indicator of cognitive load, its application as a real-time, implicit control signal in assistive human-machine interfaces remains an under-explored area. A key motivation for this research, therefore, is to bridge this translational gap—to move pupillometry from a passive

measurement tool to an active component of a dynamic control system, thereby creating a more symbiotic and intuitive user experience.

Finally, a significant disconnect persists between the advanced, custom-built systems often presented in academic literature and the practical need for affordable and accessible solutions. Many documented hands-free systems are prohibitively expensive or require invasive electronic modifications, which limits their replicability and potential for widespread deployment. Consequently, a central motivation for this work is to engineer and validate a non-invasive, low-cost, and easily replicable hardware solution that can make advanced gaze-based control a viable option for a much wider audience.

Therefore, this thesis is motivated by the need to synthesize these distinct research threads into a single, cohesive system—one that is not only adaptive and intuitive in its control paradigm but also genuinely accessible and practical in its design.

1.2 Aim and Objectives

The primary objective of this project has been to enhance the quality of life and independence of individuals with severe mobility challenges, specially upper-limb disabilities, by enabling a user-friendly and hands-free control of assistive technologies. By minimizing both the physical effort and cognitive demands required for system interaction, the project aims to improve accessibility and make assistive solutions easier and more practical to use in daily life.

To guide the direction of this work, the thesis investigates the following research questions:

1. Can a low-cost, 3D-printable mechanism effectively convert a conventional powered wheelchair into a gaze-controlled system, thereby enhancing accessibility and affordability?

2. To what extent can pupil diameter data be used to detect user intention, and can it serve as a viable alternative to traditional dwell-time methods for button activation?

3. Can the integration of object detection algorithms enhance the usability and effectiveness of assistive robotic arms in supporting activities of daily living for individuals with upper-limb impairments?

4. Are the proposed developments practical and user-friendly?

To address the aforementioned research questions, this thesis pursues the following objectives:

1. To investigate the efficacy of real-time pupillometry as an implicit input for adaptive system control, by training and validating a machine learning model capable of classifying a user's cognitive state (focus vs. decision-making) from their pupil dilation patterns.

2. To design and develop a novel, low-cost, and non-invasive robotic controller, utilizing 3D-printable components and mechanical actuation, to serve as a modular and accessible hardware solution for retrofitting conventional powered wheelchairs with gaze-based control.

3. To design and integrate an object-detection framework into the gaze-based Human-Machine Interface to enable high-level, semi-autonomous control of an assistive robotic arm, thereby reducing the effort and cognitive load associated with manual, joint-level manipulation.

4. To empirically evaluate the integrated assistive system's performance, usability, and user acceptability through a series of structured, user-centered studies in realistic navigation and manipulation tasks.

To address the aforementioned research questions and objectives, a comprehensive study was designed and conducted which will be described briefly in the following section.

1.3 Thesis Organization

This project brings us a step closer to more adaptive assistive devices with a user-centered design. Throughout the thesis, multiple versions of the system were designed, upgraded, and improved to achieve the next iteration.

Chapter 2 presents a comprehensive literature review of the relevant scientific fields. It covers assistive technologies, focusing on gaze-based control methods, human-computer interaction, and the established use of pupillometry as a measure of cognitive load. This chapter critically assesses the state-of-the-art and identifies the specific limitations in existing research that this thesis aims to address.

Chapter 3, presents the first step which involved developing an initial version of the gaze-based GUI, designed to control the movements of a mobile robot. To evaluate this system, a controlled experiment was conducted, where data has been collected from healthy participants as they performed a navigation task. The robot was controlled via participants' eye movements using the eye-tracking-based interface, which incorporated directional control buttons and a live video feed of the navigation environment.

The collected data were utilized to determine whether variations in user performance during a Human-Robot Interaction (HRI) task can be captured and quantified through changes in pupil diameter, serving as an indirect estimate of mental workload. Such insights could enable future HRI systems to adapt to the user's evolving mental state. Specifically, we investigate the relationship between pupil diameter variation and performance metrics, including lap completion time, the number of commands issued, and the average time required to select commands. Additionally, subjective assessments of user mental workload during the task, as well as system usability and acceptability, are evaluated using standardized scales. The observed changes in pupil diameter are analyzed in relation to these performance parameters, with a focus on providing a comprehensive evaluation of the system's effectiveness and user experience.

In Chapter 4, the previously collected pupil data were annotated and used to train a deep learning-based model aimed at detecting user intention by classifying between focus and decision-making states. The methodology and results of this classification approach are detailed in this chapter. The presented model was subsequently integrated into the next version of the GUI to enable an adaptive command selection mechanism.

In Chapter 5, describes the methodology to enable wheelchair control via the GUI, which includes a 3D-printable add-on mechanism. This mechanism allows the wheelchair to receive commands from the user interface. The GUI was also updated and enhanced for wheelchair use, incorporating feedback from participants in the previous experiment. Additionally, the adaptive command selection model was integrated into this version of the interface. To evaluate the design and its usability, a user study was conducted involving healthy participants. The methodology and results of this evaluation are presented in this chapter.

Chapter 6 details the extension of the system to incorporate the control of an assistive robotic arm. It describes the integration of an object-detection model to enable semi-autonomous, high-level control. The results of a final user study, which compares the usability of this object-based approach to traditional manual control, are presented and analyzed.

Chapter 7 provides a consolidated discussion of the research findings, synthesizing the results from all experimental stages. It reflects on the scientific contributions in the context of the literature, addresses the limitations of the current work, and outlines promising directions for future research and development.

Finally, Chapter 8 concludes the thesis by summarizing the key achievements of the project, reiterating the main scientific contributions, and offering final remarks on the overall impact of the work on the field of assistive technologies.

Chapter 2

Literature Review

Advancements in various disciplines and technologies have cumulatively resulted in the development of modern assistive technologies. Each discipline of knowledge, from artificial intelligence and robotics to human-computer interaction and biomedical engineering, has played a crucial role in the development of these technologies. Although each discipline has its own unique applications and benefits, it is the interplay of all these developments that has made modern assistive technologies possible. This multi-disciplinary research is continuing to determine what can be done with the result being increasingly smart, effective, and tailored assistive technology in the future.

This section provides a brief review of the existing literature on the major parts of this project. The chapter commences with a general overview of pertinent assistive devices and user interfaces in respect of their evolution, functionality capacity, and impact. Finally, it keeps making comments about research related to pupillary response and mental workload, their suitability for adaptive systems and usability.

2.1   Assistive technology

The World Health Organization (WHO) defines assistive technology as services and devices aimed at enabling users to enhance or preserve their functional capacities, including but not limited to cognitive, self-care, and mobility functions [53]. Hearing aids, eyeglasses, walking frames, stair lifts, mobility scooters, and wheelchairs are examples of assistive devices. Each of these technologies is separately designed to meet a particular requirement or simplify a task for the user. Ultimately, the ultimate goal of assistive technologies is to support users' quality of life and enhance their independence by enhancing their functional ability.

Additionally, according to the UK government website, assistive products that enable the user to perform daily living activities, although not necessarily directly related to a medical condition or diagnosis, are classified as "aids for daily living" [54]. These technologies are essential for the greater independence and quality of life of their users as they may be dependent on them for activities of daily living. The significance of such technologies extends beyond convenience, enabling individuals with various needs to remain independent and participate more actively in their daily lives.

2.1.1   Wheelchair

Wheelchairs are utilized by millions of people globally as a vital tool for mobility aid. The timeline of the wheelchair, or wheeled chairs, goes back to the sixth century, as attested by a stone slab inscription in ancient China [55]. The development of the modern wheelchair, advanced by design, material, and technological innovation, remains a key factor in enhancing independence and mobility for people worldwide. As society evolves, the need for further adaptive and user-centered wheelchair innovations remains an integral part of enhancing the quality of life for those who rely on them for daily mobility. Their facilitatory role in health care, access rights, and social interaction says much about how a modest invention, refined over the centuries, is still

transforming lives.

Wheelchairs have evolved immensely over the centuries to enhance significantly the mobility and independence of the disabled. One milestone innovation was made in 17th-century Germany when the self-propelled wheelchair was invented [55, 56]. The invention was a big breakthrough by enabling the user to move himself around without entirely relying on caregivers—a discovery that vastly improved their lifestyle. Despite such marvelous advances, however, wheelchair systems today remain wanting for individuals with limited hand mobility.

Besides the standard joystick controls of mass-produced wheelchairs, other controls have been developed that are based on chin, head, and tongue actions. Sip-n-puff control is yet another innovative system in which an individual can operate a wheelchair by inhaling and exhaling on an innovative device [57]. These options are particularly beneficial for people who have minimal or no hand movement and give them more independence and enhancing their lifestyle.

Most likely the most renowned example of assistive technology is Professor Stephen Hawking's wheelchair. Often described as his "mobile office," this remarkable machine not only facilitated physical mobility but included a highly developed voice synthesizer that served as his primary mode of communication. This innovative integration allowed Professor Hawking to articulate his groundbreaking ideas and maintain his influential presence in the scientific community despite his severe physical limitations [58, 59].

However, scientific literature indicates a much wider range of control modalities and interfaces than those conventionally observed in typical wheelchair design. Contemporary wheelchairs are not only augmented with capabilities such as stair-climbing and standing but are also equipped with novel control modes that accommodate a wide range of user needs and objectives. These developments signify a dynamic shift in assistive technology, which is designed to substantially enhance mobility and independence. In the following, some of these innovations have been covered to demonstrate how continued research and development are paving the way for more flexible and accessible assistive technologies.

2.1.1.1   Types and Functionalities

Stair-climbing functionality in wheelchairs usually comes in two prominent forms. There are wheelchairs with specially designed wheels or track systems that allow them to climb stairs independently. There are also add-on designs that can either provide a different mechanism that transports the user while seated or be integrated with the wheelchair itself to facilitate the movement of both the wheelchair and the user up the stairs [60].

Although advanced features like stair climbing are certainly impressive, they can be overly sophisticated and expensive for many users. specially when accessible facilities such as lifts, ramps, or other adaptive infrastructures can be available.

However, some activities—such as independent standing—have far fewer alternative approaches. Standing not only allows users the independence to reach items on higher shelves or utilize such devices as stoves, further enhancing their independence in activities of daily living. It also has health related benefits and can prevent the development of some conditions, specially for full-time wheelchair users [61, 62].

Stand-up wheelchairs have been developed in both manual [63] and electric versions [64, 65, 66], which were useful for users with varying requirements and physical capabilities. Shaikh-Mohammed et al. [63] introduced a low-cost manual stand-up wheelchair that allows users to transition from a sitting to a standing position. While users must engage the provided handles to lift themselves, the system utilizes gas springs to offer weight support, making the act of standing simpler and less physically demanding.

Besides the standard wheelchair use, standing wheelchairs have also been explored for rehabilitation. Ortiz et al. [67] integrated a standing wheelchair with an interactive Virtual Reality (VR)-based system and robotic assistance to simulate rehabilitation processes for users.

Lots of research has gone into the material, structural designs, and simulation of stress and force in wheelchairs under production [68], [69], [65]. This kind of researches have played a great part in making today's wheelchairs more durable, comfortable, and versatile.

However, the majority of wheelchairs are normally equipped with touchscreens and joystick as user interface. while they remain the most universal and user-preferred control schemes, they are not appropriate for users with severe upper-limb disabilities or hand impairments.

To address this limitation, researchers have explored other user-specific control interfaces based on users' mobility needs. Other research has considered novel control methodologies with incorporating EEG-based BCIs, detection of muscle activities through EMG, speech commands, and tongue-operated control. Such technologies aim at enhancing accessibility and independence for those who cannot apply standard wheelchair control methods.

2.1.2 Controller Interfaces

Struijk et al. [70] developed an inductive sensor-based wireless interface to enable individuals with severe physical disabilities to control a computer. The system consists of an activation unit positioned on the tongue and a set of inductive sensors embedded in a Printed Circuit Board (PCB) board, along with the necessary electronic components, all housed on a custom-fitted appliance placed on the roof of the mouth. This new device behaves like a trackpad that allows users to navigate a cursor with tongue movement. It also includes dedicated key areas that can be used for making selections, mimicking mouse or keyboard behavior.

This product requires the user to hold all electronic components, along with the battery, inside their mouth. Further, the activation unit must be placed directly on the tongue. While this design offers novel advantages, e.g., stealthy use and hands-free functionality, it may not be suitable for everyone. It can be uncomfortable for some users due to the constant presence of foreign bodies in the mouth, potential interference with speech or eating, or the sensation of the activation unit on the tongue.

Poirier et al. [71] developed a prototype voice-controlled interface to control the movement of a robotic arm. In this interface, the user provides voice commands to select the direction of motion, and the movement is triggered by pressing a button. This approach combines the sim-

plicity of voice recognition and the definiteness of manual triggering to achieve precise control and prevent accidental motion. Although the system presents a promising assistive solution for people with mobility impairments, the system's success may depend on speech clarity, environmental noise, and the ability of the user to control the supporting button.

The results of the literature review indicate that BCI and EEG signal-based methods have been explored more than the other control interfaces discussed above. This suggests a growing interest in employing neural signals for assistive technology, particularly for individuals with severe mobility impairments who may struggle to utilize traditional input methods. The increasing utilization of BCI and EEG-based systems is feasible because both can use hands-free, intuitive operation to enable customers to interact with devices using brain signals only. Despite these advantages, these systems do have downsides, which include signal noise, extended calibrations needing to be run, and adapt users, and are in need of support via more development and research that will provide them even more usage within practice because of more solidified reliability.

In order to record EEG signals, electrodes perform the most critical role in capturing electrical brain activity. They are commonly integrated into various head-mounted devices, such as EEG caps, headbands, or even discreet wearable designs, depending on the application. The number of electrodes can be as high as needed or as few as a handful for minimal monitoring to high-density systems for advanced neural analysis [72]. EEG electrodes could be generally divided into two groups: wet and dry. Wet electrodes utilize a conductive gel to reduce impedance and improve the quality of the signal. Although more precise, they are plagued by problems of preparation time, maintenance, and inconvenience to the user. Dry electrodes, on the other hand, eliminate the utilization of gel and are user-friendly, portable, and convenient. But dry electrodes are to be expected to experience signal consistency and quality problems because they are more susceptible to noise and movement artifacts.

In research focused on movement control, EEG electrodes are typically positioned over brain

regions closely associated with motor functions, particularly the sensorimotor cortex. This area plays a crucial role in motor imagery and movement planning, making it a key target for BCI applications aimed at assistive technologies. Additionally, the number of electrodes, the placement and the channel selections will effect the usability and system peprformance [73, 74, 75].

Swee et al. [76] also designed an EEG-controlled wheelchair and established the possibility of brain-signal-based assistive mobility. A custom-built, scooter-motor-driven wheelchair under remote control was utilized. It was a workable and adaptive platform for using BCI technology in assistive mobility aids in individuals with severe motor disability. To obtain EEG signals, they employed the Emotiv EPOC headset, a widely used non-invasive brainwave-sensing headband. The system was set up to recognize and translate four basic movement commands—forward, backward, left, and right—so that the user could navigate their environment solely on the basis of their brain activity. One of the major shortcomings of this study was that no other types of user feedback were present. Unlike some of the latest BCI-driven assistive devices that use other multi-modal inputs such as haptic feedback, EMG, or eye-tracking, this utilized only EEG signals for operation. Although this simplified the design feature, it raised concerns about the aspects of user fatigue, precision, and reliability, much like in the majority of EEG-based control systems.

Li et al. [77] developed an EEG-controlled wheelchair system using a 14-channel EEG cap to capture brain signals. Their system was set to recognize and process three main movement commands: move forward, right turn, and left turn, which allowed users to instruct their movement in the environment through the use of BCI technology. A primary characteristic of this system was that it was coupled with a GUI. The interface was created to improve usability by allowing caregivers to configure system settings and individualize controls according to the user's specific needs and wants. With the incorporation of variable parameters, the system sought to enhance wheelchair operation comfort and efficiency where some common issues included calibration problems, signal integrity, and adaptation by users.

Xiong et al. [78] created a semi-autonomous wheelchair control system by integrating EEG, EMG, and Electrocardiogram (ECG) signals as a more intelligent and adaptive means of wheelchair control. Their system has three main modes of operation: autopilot, controlled movement, and complete stop. To make independent movement possible, the wheelchair is equipped with location and ultrasonic sensors to allow it to detect obstructions and travel through spaces in a safe manner. The EEG signals, received from the sensorimotor cortex, are used to determine whether the user wishes to turn left or right so that intuitive control of directional motion is achieved. Besides EEG control, the system also utilizes EMG activity of jaw muscles to pick up jaw clenching, which is used as a switch for changing control modes. One of the novel features of this study is the utilization of ECG monitoring. Electrocardiogram signals are recorded from the wrist to track stress changes in the heart so that the system can identify stress on the user. The system can notify a caregiver if higher than normal stress is registered, providing an extra layer of protection and early intervention if required.

Glavaš et al. [79] developed a novel brain-eye hybrid control system for wheelchair control based on EEG and EOG signals. It improves the accessibility of people with severe motor impairment by using multi-modal biosignals for easier and more flexible control system. The recording of the neural activity is made using an Emotiv Epoc EEG headset, for left and right turns in this example. Autopilot, instead of needing ongoing input from the user to change direction, now takes over once the system is initialized to facilitate forward motion of the wheelchair automatically. Stress associated with thinking and physical activity is reduced for the user, as well as driving becoming easier and less labor-intensive. To provide a simple and effective way of starting and stopping movement, the researchers incorporated EOG sensors to detect eyebrow raises. The system interprets an eyebrow raise from the user as a signal to initiate or halt movement. This is a straightforward and non-invasive way for the user to be in control without requiring complex motor functions or extended concentration.

Based on the previously cited literature and a broader review of studies on motor imagery-

based EEG systems, the range of different commands that can reliably be generated using EEG alone is small and comparatively limited. Although EEG-based control systems have demonstrated potential for hands-free and intuitive control, their application in daily control of complicated systems is still problematic because of the limitations of signal classification accuracy, user training time, and mental fatigue. In spite of these limitations, EEG-based control can nevertheless be extremely useful in certain applications, especially for severely motor-impaired users without many alternative control options. The ability to produce even a small number of accurate commands (e.g., simple direction-of-movement) can increase independence and mobility for such individuals. However, for applications that require more intricate and dynamic control, EEG alone may not be sufficient, and hybrid approaches—combining EEG with other input modalities such as EMG, EOG, or environmental sensors—may be necessary to facilitate more effective and efficient use.

Eye-tracking technology is another promising solution for people with severe disabilities. Eye-tracking has particular benefits compared to other assistive control methods, especially for users who have no control or extremely limited control over their hands and other bodily movements. One of the most significant advantages of eye-tracking is that it has the capability to enable natural and intuitive interaction since eye movement is not usually affected by neuromuscular system diseases that restrict voluntary movement. Eye-tracking systems can also offer a non-invasive and relatively easy way of giving commands and are, therefore, an efficient option compared to more physically invasive interfaces.

Eye-tracking studies primarily focus on providing users with a GUI and enabling them to interact through looking at items for selection. Unlike Motor Imagery (MI) BCI systems that usually are limited to few commands, eye-tracking interfaces can have significantly more complex sets of interactions. They enable users to scroll through menus, pick options, and even regulate assistive devices with greater flexibility and accuracy. The capability to identify continuous eye movement enables detailed and user-configurable controls to be realized, which provides an

edge over the conventional MI-BCI approaches, which at best have difficulty with small command sets and reduced accuracy. Thus, eye-tracking technology has been extensively researched in assistive applications to enable people with severe physical disabilities to possess an effective method of communication and environmental control. Eye-tracking can be realized by several modalities that all have their advantages and limitations. In the following subsection, the various methods will be discussed more in-depth on how they are constructed, function, and perform in practical applications.

2.1.3   Eye Tracking

one method of eye-tracking uses muscle sensors to pick up movement of the extraocular muscles. The human eye has six extraocular muscles that coordinate with each other to determine its direction and movement. By sensing the electrical activity of the muscles, sensors can monitor where the user is gazing and use their line of gaze as input to a control system. These portable devices, often in the form of headsets or glasses, employ strategically placed sensors to track fine eye movements. This approach offers an alternative to camera-based eye tracking, possibly a less obtrusive and privacy-respecting one but still an adequate response for assistive uses.

Electrooculogram (EOG) is widely used method for detecting eye movements. This technique involves placing electrodes on the skin around the eyes to measure the electrical potential differences generated by eye activity. Since the cornea (front of the eye) carries a positive charge while the retina (back of the eye) has a negative charge, any movement of the eye creates a measurable change in electrical signals.

EOG has been extensively explored in the literature as a means to control wheelchairs, both on its own and in combination with other biosignals such as EEG and EMG.

Huang et al. [80] proposed a novel system using a vertical EOG channel for blink detection as a control. The system has 13 buttons that are presented in a series, and each button flashes separately in a predefined sequence. The user chooses his/her desired command by blinking in

synchronization with the flashing button. It is an easy and efficient method for people with low mobility to interact with the system. The study specifically focused on participants with spinal cord injury, and the results were promising. The system was capable of achieving an overall accuracy rate of 91.7%, which proves its potential as a valid assistive technology.

In another publication, Huang et al. [81] extended their previous EOG-based control system for integration with a robotic arm mounted on a wheelchair. The GUI of this version had a two-level control hierarchy. The users controlled the system by synchronizing blinking with flashing buttons on the screen. The system chose a button based on detected blinking and visually highlighted the button in the GUI. Users could confirm the selection by eyebrow raising, which provided an additional verification step for higher accuracy and intent. In order to move the robotic arm, the users first chose an object in the GUI. The movement path was planned automatically by the system with a shared control architecture. Two cameras were used by the system—one to identify the position of the object and another to identify the position of the user's mouth, to accurately release the object.

Rusydi et al. [82] proposed a wheelchair control system utilizing a fusion of blinking and two-channel EOG gaze detection. Hands-free mobility is achieved with the system through interpreting voluntary eye movement as control commands. Voluntary blinking in this system serves as an activation switch, and one can switch the system on and off by simple blinking. Upon activation, movement is controlled by direction of gaze. The wheelchair turns left or right when the user looks left or right. The wheelchair moves forward when the user looks upwards and in the backward direction when the user looks downwards. The study demonstrates how EOG-based interfaces can be applied practically to enhance assistive mobility aids to facilitate independent navigation at reduced cost.

Another category of eye-tracking equipment uses camera-based technology to sense and measure eye movement. These systems operate by taking images of the eye in real-time and processing fine movement changes to sense gaze direction [83]. The majority of eye-tracking

devices available in the market employ a method called corneal reflection for accurate tracking[83, 84]. Figure.2.1 shows the eye's structure and parts names.

The cornea, the transparent front of the eye that protects the pupil and iris, is used to to detect the eye movements. When light is shone onto the eye, a bit of it is naturally reflected back, creating what is called the corneal reflection. By analyzing this reflection, the system can accurately determine where the user is gazing [83, 85]. These camera-based eye-trackers have general applications across a broad variety of applications, from assistive technology and human-computer interaction to psychology studies and even to games.

Infrared illuminators in eye-tracking systems emit light towards the eye. By recording how infrared is reflected off the cornea and the pupil, these types of systems can estimate precisely where one is looking [83, 84]. One of the most important benefits of this approach is that it also enables the measurement of pupil diameter precisely, from which cognitive load, emotional reactions, and visual attention can be inferred.

Eye-tracking devices come in various forms based on their application. Some come in the form of wearable glasses, like the Tobii Pro Glasses 3, that allow natural movement and real-world behavior and can thus be used for a wide range of applications, from behavioral research to usability studies and cognition research. Screen-based eye trackers, on the contrary, like the Tobii Pro Nano and Tobii Pro Fusion, are usually mounted on a screen and utilized for GUI-based applications, where precise tracking of a user's gaze on a screen is essential.

Subramanian et al. [86] proposed an eye-gaze semi-autonomous wheelchair to enable people to move around in their environment more comfortably. Unlike the majority of gaze-controlled applications, this work does not offer a GUI to directly control the movement in front of the user specifically. Rather, the system determines the intended destination by explicit gaze fixations, allowing for more natural and intuitive interaction. The scientists used a Tobii EyeX eye tracker to monitor the user's eye movements so that the system can identify where they are focusing. Other than that, the wheelchair is also fitted with a 2D LiDAR, 3D LiDAR, and an RGB-Depth
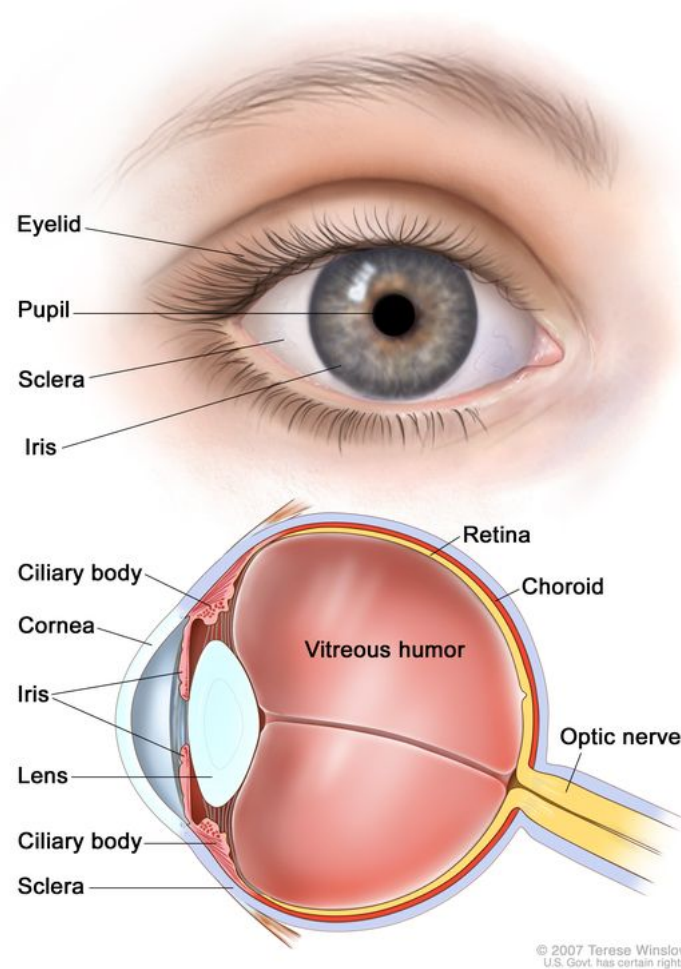
Figure 2.1: The image showing the different parts of the eye including the iris, pupil, and cornea. Image courtesy: [https://www.cancer.gov/publications/dictionaries/cancer-terms/def/cornea][1]

camera, which collectively assist in path planning and avoiding obstacles. Equipped with all these sensors, the system can take the user autonomously to where they want to go or towards the objects that they wish to interact with.

Sunny et al. [87] designed a gaze-controlled robotic system that combines a robotic arm mounted on a wheelchair with an eye-tracking interface. The system uses a Tobii PCEye5 eye tracker to detect the user's gaze to navigate a custom-designed GUI to drive the wheelchair and the robotic arm. There are two control levels in the interface. The first one is employed for the

control of the wheelchair with four direction buttons to go forward, backward, left, and right. The second one is employed for the detailed control of the 6-Degree of Freedom (DoF) robot arm to let users control each joint or move the arm in x, y, z directions for more advanced tasks. To assess the effectiveness of the system, the subjects were required to carry out activities of daily living, including picking and placing objects from the floor or a shelf.

Eye-tracking has also been investigated with camera-based arrangements and advanced image processing. Viswanatha et al. [88] developed an innovative wheelchair controlled by eye movements. The system makes use of computer vision methods including Haar Cascade classifiers, image processing, and eye tracking in order to determine the eye movement of the user in a suitable manner. Using these methods, the system can interpret the direction of the user's sight and translate it into motion of the wheelchair. The user can manually control the wheelchair to move forward, or to turn to the left or to the right, by simply altering their vision in the corresponding direction. Furthermore, the system can also sense blinking, being a command to brake the wheelchair, and yield a natural and comfortable way of braking without needing additional physical input.

Table 2.2 presents a summarized overview of some of the aforementioned studies.

2.1.4   Affordability and Costs

Apart from functionality and usability of the systems, affordability is a key factor in the accessibility of the devices and technology. Table 2.1 presents brief examples of assistive devices and control interfaces available on the market, outlining their key specifications and associated costs.

The price range for powered wheelchairs varies considerably depending on their functionalities and technical specifications. In contrast, assistive robotic arms tend to be consistently expensive, often placing them out of reach for many users.

Among control interfaces, sip-and-puff devices are relatively affordable; however, they are limited in terms of functionality and the number of available commands. For instance, the DX

Table 2.1: Price and specifications of some commercially available assistive devices and controllers.

The system	Name	Price	Functionalities
Sip-Puff controller	Original Instrument Sip-Puff switch with headset [89]	£350	4 main directions, Speed functions
Head Controller	Switch-it-Vigo [90]	$5,537 [91]	Wireless wearable headset, App for setting control
Head Controller	Permobil Total Control Head Array [92]	$4,968	Total head control, swing-away sensor placement, sensors won't touch the head
Assistive Arm	Knova Jaco Gen2[93]	$35,000 [94]	Mounted and stand-alone, Three finger, Manual control using joystick, 1.6 Kg payload 4 or 6 DoF [95]
Assistive Arm	Assistive Innovations i ARM [96]	Not publicly available	Two finger, Can be added to the wheelchair joystick controller, Mounted on wheelchair, Manual control using joystick or phone
Head Controlled Wheelchair	2021 Permobil F3 Power Chair with Head Array [97]	£54,045 (sale: £13,125)	Tilt, Recline, Power Legs, Seat Elevate, Head array, Front wheel drive
Powered Wheelchair	Ottobock Juvo B5 [98]	£4,475	Rear wheel drive, Joystick controlled
Powered Wheelchair	Permobil F3 Compact Corpus [99]	£8,495	Front wheel drive, Electric lift, Electric tilt, Joystick control
Powered Wheelchair	Permobil F5 VS Standing Power Chair [100]	£24,500	Standing, Tilt, Lift, adjustable for adults and children
Powered Wheelchair	MobilityPlus Ultra-Light Instant Folding Electric Wheelchair [101]	£769.99	Folding wheelchair, Light weight, Rear wheel drive, Joystick controlled

sip-and-puff controller enables only four primary directional commands [102]. Additional settings, such as speed control or the option to select between variable and fixed speeds, must be configured by the manufacturer's professional installation team.

The Tobii Pro Nano eye tracker, which was used in this project, cost £2800 at the time of procurement. While eye-tracking systems may involve higher initial costs, they offer significantly greater control flexibility and a wider range of interaction options. These interfaces can be enriched with multiple functionalities to accommodate diverse tasks and user needs, potentially

making them more cost-effective in the long term.

2.1.5   Summary

The literature on assistive technology demonstrates a clear progression from conventional manual controls towards more sophisticated human-machine interfaces, including BCI and advanced gaze-tracking systems. These innovations offer significant potential for enhancing the autonomy of individuals with severe motor impairments.

Despite these advancements, a critical review reveals several persistent limitations that hinder real-world deployment. Firstly, biosignal-driven modalities, particularly those based on EEG, often suffer from high cognitive overhead, extensive calibration requirements, and limited command bandwidth, making them challenging for reliable daily use. Secondly, while camera-based eye-tracking presents a more robust alternative, the majority of implementations rely on a static, fixed-duration dwell time for command activation. This standardized approach lacks the flexibility to adapt to the user's dynamic cognitive state, often resulting in an interaction that is either inefficient or fatiguing. Finally, a significant and overarching challenge is the issue of accessibility; the most capable systems described in the literature are frequently associated with prohibitive costs and require invasive electronic modifications, placing them outside the reach of most users.

This thesis directly confronts these deficiencies. The development of a novel, adaptive control system that moves beyond static dwell-time by interpreting pupil dilation as an indicator of user intent will be detailed in Chapter 4. Furthermore, the engineering of a low-cost, non-invasive, and 3D-printable controller designed to make advanced gaze-based navigation widely accessible is presented in Chapter 5.

2.2 Mental load

One of the first experiments, Hess et al. [41], examined the relationship between cognitive load and pupil size using observations of how pupils respond during a simple multiplication problem-solving task. The findings were that pupil dilation is proportional to mental activity and that the amount of dilation is proportional to the complexity of the problem being solved. Briefly, cognitive load is proportional to pupil size, and both are quantifiable physiological indicators of cognitive effort. The present study laid a basis for indicating the possible applications of pupillometry, or the science of pupil dynamics. The variation in pupils provides an objective and non-intrusive approach of quantifying activity within the brain, and the measurement is useful for tracking utilization of the mind faculties, attention, as well as challenging processes in general application in many such areas as human-computer interaction, neuroscience, and rehabilitation technology.

2.2.1 Mental load and cognitive load in Eye-tracking studies

The use of pupil dilation measurement as a measure of mental load in Assistive device application is rare in the literature.

Carlson et al. [103, 104] designed a wheelchair navigation experiment with an innovative combination of eye-tracking head-mounted, joystick, and tablet. The system combined both the inbuilt joystick of the wheelchair and an externally mounted additional joystick for facilitating user control in the navigation tasks. The primary objective of the study was to propel the wheelchair along two routes: a loop route [103] and a cluttered maze-like route [104], which had obstacles such as doorways and hallways. The wheelchair was operated along these routes primarily by the wheelchair joystick. A secondary task was introduced in the experiment, however. This task required subjects to match a direction on the screen with the direction shown by the other joystick. This added complexity tested both the ability to navigate and the cognitive

flexibility of the subjects. One of the best features of this study was that it involved a collaborative control system, which was something that could be activated to assist the user while working on the tasks. This was what allowed a more dynamic interaction and provided more flexibility for the user as well as potentially better ease of use. The collaborative control was put in place to enhance user control and minimize physical and cognitive effort required for the navigation of wheelchairs.

Safety of navigation has been a primary area of focus in such experiments, particularly in evaluating how secondary tasks might affect the attention and overall performance of participants. Secondary tasks, although useful in evaluating cognitive flexibility, have the potential to distract users when they are navigating as well. However, the researches discovered that participants navigated safer with fewer collisions when the collaborative control system was engaged. This means that the system helped people deal with both navigation and secondary tasks more effectively. In addition, the study determined that the subjects were able to respond quicker to the secondary task when there was collaborative control. This indicates that aside from improving safety, by introducing a supporting layer, the system also facilitated the subjects to handle multitasking more effectively.

2.2.2   Summary

To summarise, existing research offers substantial support for the use of pupil dilation as a non-invasive and reliable physiological indicator of cognitive and mental workload. The field of pupillometry has been extensively validated across various domains, establishing it as an objective measure of task-related cognitive demand.

Despite this, a closer examination of the literature reveals a notable gap in translating these findings into real-time applications—particularly within assistive technology. Pupillometry is predominantly employed in retrospective analyses to assess user workload after interaction. Its potential as a dynamic input for real-time, adaptive human-machine interfaces remains insuffi-

ciently explored. Although prior studies acknowledge the relationship between task complexity and pupil size, few have leveraged this relationship to actively inform or adapt system behaviour during interaction. Furthermore, in the limited number of assistive applications involving eye-tracking—such as gaze-controlled wheelchairs—pupil dynamics have rarely been central to the system's control architecture.

This thesis seeks to bridge that gap by investigating the feasibility of using real-time pupil data to infer user intent through machine learning. The development and validation of this approach are discussed in Chapter 4, followed by an empirical evaluation of its impact on user performance and cognitive effort in Chapter 5.

2.3   Synthesis of Literature

This chapter has provided a critical review of the literature on assistive technologies and the principles of mental load assessment. The survey of control modalities, synthesized in Table 2.2, highlights a clear technological progression from conventional controls towards intelligent, biosignal-driven interfaces. While promising, a closer examination reveals that even advanced methods like BCI are often constrained by practical challenges such as user fatigue and calibration overhead. Gaze-tracking emerges as a more robust and intuitive alternative, yet its full potential is unrealized due to persistent limitations in its application.

From this comprehensive review, three principal research gaps have been identified that directly form the justification for the present work:

- A Reliance on Static Control Paradigms: The majority of existing gaze-based systems employ a fixed-duration dwell time for command activation. This non-adaptive method fails to account for the user's dynamic cognitive state, creating an interaction that is scientifically suboptimal and can impair usability.

- A Translational Gap in the Application of Pupillometry: The literature in psychophysiology

robustly confirms that pupil dilation is a strong correlate of cognitive load. However, in assistive technology, its use is largely restricted to post-hoc analysis rather than as a real-time, implicit control signal for an adaptive interface.

- A Disconnect Between Technological Novelty and Practical Accessibility: A significant portion of advanced assistive systems described in the literature remain high-cost, proprietary, or require invasive modifications, limiting their potential for real-world deployment and creating a need for affordable, non-invasive solutions.

These identified gaps directly motivate the research questions and objectives established in Chapter 1. The challenge of static control paradigms and the underutilization of pupillometry are directly addressed by Research Question 2 and Objective 1, which focus on investigating and developing an adaptive, intention-based control system using pupil dilation. The critical need for accessible hardware is the driving force behind Research Question 1 and Objective 2, which center on the design and development of a low-cost, non-invasive, 3D-printable wheelchair controller. Finally, the high cognitive burden of assistive manipulation is tackled by Research Question 3 and Objective 3, with the overarching goal of validating these solutions through the empirical evaluation outlined in Objective 4.

Therefore, this thesis is positioned at the intersection of these challenges, aiming to deliver a cohesive and validated system that is not only technologically innovative but also fundamentally accessible and user-centered.

Table 2.2: Categorized Summary of Assistive Technology Control Methods (Landscape)

Reference	Method	Advantage	Disadvantage	Data Type	Device Type	Commands
Brain-Computer Interface (BCI)						
Swee et al. [76]	EEG (Emotiv EPOC)	Hands-free, intuitive	User fatigue, limited feedback	EEG signals	EEG headset	4
Li et al. [77]	EEG (14-channel cap)	Customizable GUI	Calibration issues	EEG signals	EEG cap	3
Xiong et al. [78]	EEG + EMG + ECG	Semi-autonomous, stress detection	Complex integration	Multi-modal	Integrated sensors	3 modes
Glava's et al. [79]	EEG + EOG	Reduces mental effort	Limited command diversity	EEG + EOG	EEG + EOG sensors	4
Eye Tracker						
Huang et al. [80]	EOG (blink detection)	High accuracy (91.7%)	Sequential button selection	EOG signals	EOG sensors	13
Huang et al. [81]	EOG + GUI	Two-level hierarchy	Requires synchronization	EOG signals	Cameras + sensors	N/A
Continued on next page						

Table 2.2 – Continued from previous page

Reference	Method	Advantage	Disadvantage	Data Type	Device Type	Commands
Rusydi et al. [82]	EOG (gaze + blink)	Hands-free navigation	Limited directions	EOG signals	EOG sensors	5
Subramanian et al. [86]	Eye-gaze (Tobii EyeX)	Natural interaction	Requires gaze fixation	Gaze data	Tobii EyeX	1
Sunny et al. [87]	Eye-tracking (Tobii PCEye5)	Dual control (wheelchair + arm)	Complex interface	Gaze data	Tobii PCEye5	10
Viswanatha et al. [88]	Computer vision (eye direction)	Non-invasive, blink-to-stop	Limited precision	Image data	Camera	4
Others						
Struijk et al. [70]	Inductive tongue sensor	Stealthy, hands-free	Oral discomfort	Inductive	Mouth appliance	3
Poirier et al. [71]	Voice + button	Precise control	Noise-dependent	Voice + button	Microphone + button	N/A

Chapter 3

TurtleBot Navigation: System Development and Experiment

The original aim of this project was to develop a hand-free navigation method for wheel chair travel using eye-tracking technology. However, with the complexity and safety issues involved in testing such a system on a actual wheel chair in early development stages, a mobile robot was selected to simulate realistic navigation in an experimentally controlled environment. To this end, a robot platform that could be easily integrated into other external systems with opportunities for rapid prototyping was needed.

Beyond serving as a practical testbed, this chapter details the foundational experimental work of this thesis and makes several key scientific contributions. First, it provides the first empirical validation of the proposed gaze-based Human-Machine Interface in a dynamic and continuous assistive navigation task. Second, it systematically investigates the relationship between real-time pupil dilation and user performance metrics (such as task completion time and command frequency). This work serves to quantify the link between cognitive load and interaction efficiency in this specific context, providing evidence for the viability of using pupillometry as an input for adaptive control. Finally, this experiment establishes the foundational dataset that is

essential for the training and validation of the machine learning model presented in Chapter 4.

To this end, a Turtlebot was utilized as the mobile robot platform because it supports the Robot Operating System (ROS), open-source community, and ease of integration with external devices such as eye trackers. It provided a suitable testbed for illustrating the feasibility of gaze-based navigation before it could be translated to a full wheelchair system.

This chapter provides a summary of the eye-tracker and the Turtlebot, GUI design, and integrating relevant ROS packages. It also provides the experimental design whereby participants used the gaze-based interface to move the Turtlebot along specified routes. The objective of this experiment was to validate the system's design, acquire user feedback, and record pupil data for future analysis.

3.1 Systems and Requirements

The system incorporates a Tobii Pro Nano eye tracker, which serves as the primary device for data acquisition and gaze tracking. In addition, a TurtleBot Burger was used as the mobile robot platform to simulate wheelchair navigation. The development of the system was accomplished using Python, PyQt5 for the graphical interface, the Tobii Software Development Kit (SDK) for eye-tracking integration, and the ROS for robot communication and control. The following section provides a detailed description of the system components and the overall design.

3.1.1 Eye-Tracker

Eye-tracking technology plays a vital role in the identification of user attention, behavior, and interaction through observing and recording eye-gaze patterns. A Tobii Pro Nano eye tracker, as shown in Fig.3.1, was used in this research to acquire accurate eye-tracking information. As shown in Fig.3.2, this equipment is a compact, monitor-mounted setup and is designed with high precision to record gaze behavior. With a sample rate of as much as 60 Hz, Tobii Pro Nano

supports binocular eye tracking and is able to record the two eyes simultaneously. This provides increased precision and accuracy in measurements and thus finds applicability in uses requiring high-fidelity gaze analysis [105].

Figure 3.1: The image of the Tobii Pro Nano eyetracker (Image from [2]).

The data output generated by the Tobii eye tracker includes several key parameters that provide detailed information about eye-tracking measurements. These outputs are as follows:

- Timestamp: Represents the precise time at which the data is recorded.

- Gaze Origin: Describes the location of the origin of the gaze vector in the user's coordinate system, offering insight into the spatial starting point of the gaze [106].

- Gaze Point: Refers to the normalized coordinates of the gaze location on the screen which indicates where the user is looking.

- Pupil Diameter: Reports the dilation of the pupil, measured in millimeters [107].

- Validity Code: Outputs a binary value (0 or 1) to indicate whether the eye is detected during tracking.

These parameters are essential for analyzing gaze behavior and ensuring the reliability and accuracy of the collected data.

The Gaze Origin is the human physical position of the eye of the user and is utilized solely for the sake of initial setup and alignment so the face would be in proper distance from the eye tracker. This parameter is internally managed by the Tobii System Manager software during

Figure 3.2: Image of a user seated in front of a monitor with the Tobii Pro Nano eye tracker mounted beneath it. The monitor displays the Eye Tracker Manager.

setup and calibration to ensure correct eye tracking. Since these actions fall outside the scope of interface, information about the gaze origin was not incorporated into GUI development.

The parameters are measured during experiments as system timestamp, gaze point, pupil diameter, and validity code for the left and right eyes. They are crucial to the interpretation of gaze behavior as well as ensuring data reliability. A sample output measured during an experiment is demonstrated in Table 3.1 with respect to structure and type of information measured.

Table 3.1: A sample of data collected during the experiment

Time Stamp	3310699393
Left Eye validity	1
Left Pupil diameter	3.2055969238
Left gaze location	(0.6587189435958862, 0.4673101603984833)
Right eye validity	1
Right pupil diameter	2.9732360840
Right gaze location	(0.7544812560081482, 0.4861457645893097)

The eye tracker is mounted stably on a small metal fixture by a magnetic mount and then double-sided adhesive tape mounts the fixture to the bottom center of the monitor. The eye tracker is set up with the EyeTracker Manager application, which also serves as a major utility to operate and calibrate the device. The software provides particular instructions for correct positioning of the eye tracker, as shown in Fig.3.3, in order to achieve optimum performance. The software requests the user's entry of the position of the eye tracker in relation to the display when the user first employs a monitor and an eye tracker. This configuration guarantees accurate alignment of the eye tracker and the monitor, which is essential for acquiring trustworthy gaze data.

Secondly, the system must be calibrated before each use to account for variations in the user's posture and positioning with respect to the screen. This is done to obtain reliable data by fine-tuning the parameters of the eye-tracker to the user's personal alignment in each session. The step-by-step process of performing calibration and utilizing the system is explained in the sub-section 3.1.1.1, providing a detailed guide to achieving precision and consistency across experiments.

3.1.1.1 Usage

It is strongly recommended to calibrate the system before use, particularly if switching users or after it has not been used for an extended period of time. Changes in posture, seat height changes, monitor readjustments, and other extraneous variables will have a large impact on the validity
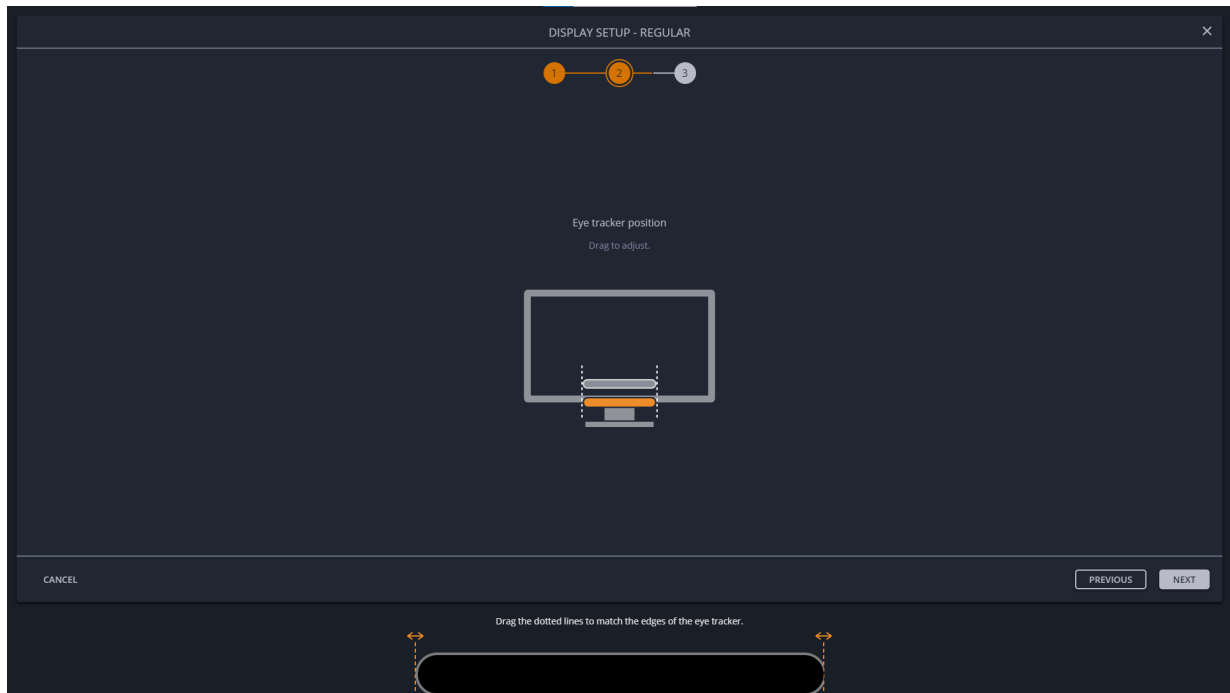
Figure 3.3: This image shows the eye-tracker manager software's eyetracker Placement guide.

of eye-tracking data. Regular calibration maintains such variables to the extent as ensuring data collection reliability and fidelity by the system.

It is also recommended to use an adjustable chair and monitor while operating the eye tracker on a standard computer. This keeps the user's face in the operating region of the eye tracker, which is important for accurate gathering of gaze information. Adjustability assists in putting both the device and the user in the proper position, hence enhancing the eye-tracking measurement reliability.

To calibrate the system, the user should first sit comfortably in the chair and ensure a relaxed and stable posture. Using the EyeTracker Manager software, the user should then verify that their face is properly aligned within the eye tracker's operating space. The software will guide the calibration process. This software confirms that the system is functioning correctly and that the gaze data will be accurately captured.

Figure 3.4 is an example of the position guide in the EyeTracker Manager software. In the

picture, both eyes are being tracked by the eye tracker, and the user's face is within the green region, which means that it is within the suggested region for optimal tracking. The purple circle represents the point of gaze on the screen and is dynamic with the user's gaze movement.

To ensure the eye tracker is functioning properly, it is essential for the system to detect the user's face within the designated zone, which will be highlighted in green. If the face is within the zone but the tracking quality is suboptimal, it will be marked in orange. While the system is still capable of recording data within this range, readjustment of position is advised to have better results. Red alert signifies that adjustment of the system is required to ensure correct detection of the face. Moreover, in case of glasses-wearing participants, particularly due to light reflection, ensuring that two eyes are clearly visible on the tracking display is of prime importance. If the screen shows one eye closed, then it indicates that the system was unable to recognize that eye, and adjustments may need to be made.
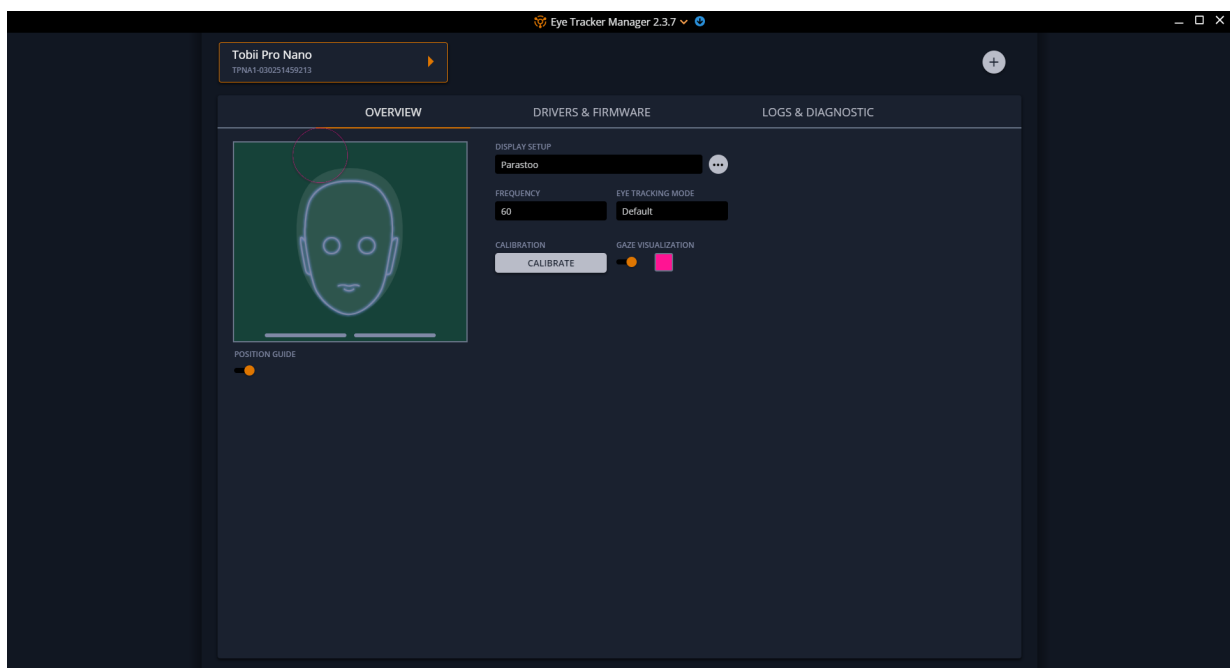
Figure 3.4: This image shows the eye-tracker manager software's position guide.

The next step in the process is to calibrate the eye tracker for the individual user, which is done using the EyeTracker Manager software. A 9-point calibration procedure is performed for

each user before the first use of the system. The calibration process involves displaying nine points on the screen, with eight located at the edges and one at the center. For each point, a dot will appear on the screen, and the user is instructed to focus on that location for a few seconds. The dot will animate and then explode once the gaze is detected which is signaling the completion of that point. After the dot explodes, a new dot will appear at the next location and continue until all nine points have been completed.

Once the calibration is finished, the system will display the readings on the screen. For each point, a plus sign indicates the actual location of the point, while two dots represent the previous calibration values for each eye. Another two dots will appear showing the updated calibration values, and a dashed circle will indicate the average calibration value for both eyes at that point.

Following 9-point calibration completion, the reading at every point is to be checked to ascertain whether the eye tracker could detect the gaze for every position successfully and whether the values are not substantially different from the actual points. Preview of gaze location will be provided to allow the user to assess the quality of calibration. The user must look around the screen to confirm that the eye tracking is correct and calibrated to his target points.

If the calibration is proven to be accurate and the points are accepted, the user can accept the calibration by choosing to use the new values. However, if some problems are discovered—such as there being significant differences between the points of gaze or the system failing to properly detect some points—the calibration process should be repeated in an attempt to deliver the optimal performance.

Figure 3.5 illustrates an example of calibration with different data readings. The yellow dots represent the left eye's readings, while the blue dot corresponds to the right eye. The average of these points, which will be used to control the gaze locator, is shown with a dashed circle. This image serves as a clear example of when recalibration is necessary. In this case, there is no reading near the upper-right corner point, and the other points on the right side are inaccurate, with one eye missing in each. As a result, the average circle is also absent. In the center of
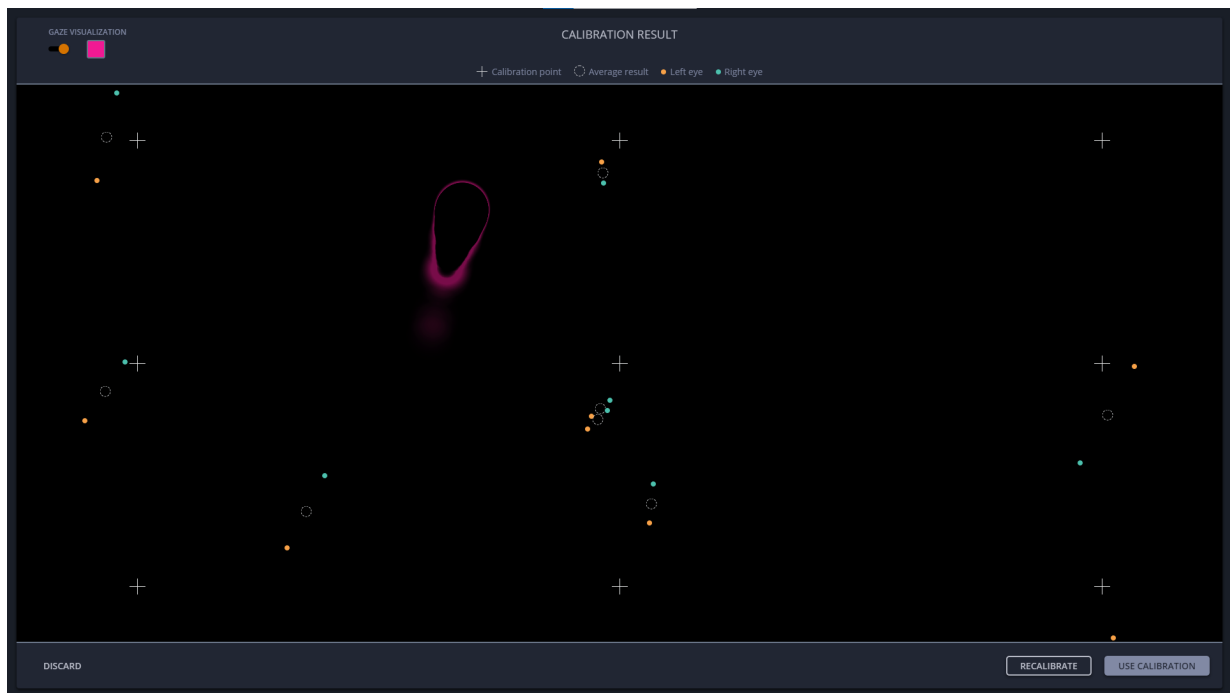
Figure 3.5: Example of a completed calibration. The plus signs represent the calibration points where the user is instructed to look. Blue dots indicate readings from the right eye, while yellow dots represent readings from the left eye. The dotted circle shows the average position of the eye readings. The user's real-time gaze location is depicted by the purple circle.

the screen, there are two readings close to each other, which suggests the user might have been looking at the middle of the screen while the upper-right point was being displayed, as it is the only one missing. The upper-middle point represents an ideal example of proper calibration. Ideally, for a good calibration, all points should display similar accuracy and alignment.

Once the system is calibrated and functioning correctly, the EyeTracker Manager software is no longer needed. The software is only required for the initial setup, guide, and calibration process. After calibration, data is captured directly from the interface, which has been combined with the EyeTracker SDK. This enables capturing data smoothly without the need to use the EyeTracker Manager and enables the system to capture eye-tracking data in real-time while the experiment is running.

3.1.2   User interface

The interface has played an important role in this project and has ensured the ease of achieving the target goals. Here in this section, the development process and enhancement in the interface made during the project are described.

A GUI was developed to create a user-friendly and accessible platform for operating the gaze-based human-machine system. Special attention was given to addressing the needs of older and disabled users, acknowledging that they may not feel comfortable or familiar with advanced technology. By keeping the visible options minimal and limiting them to only the necessary buttons, the aim was to avoid overwhelming users at first glance.

The primary goal was to design an accessible system that minimizes cognitive load, enabling users to operate it effectively without being hindered by its features or complexity. The interface was intended to support ease of use while remaining accessible to individuals with varying levels of technological literacy.

One of the great features about the designed interface is the display of live video, which overlays the user's environment onto the screen in real-time. Providing the essential view which might be more limited due to the monitors, is especially relevant for users with severe disabilities and limited head or body movement. The system enables these users to build a sense of engagement and be effective interactants without disengaging from a concentration set.

3.1.2.1   TurtleBot Navigation GUI

This is the initial completed version of the interface, employed during the TurtleBot experiment. Here, the eye tracker is utilized to monitor the position of the gaze and shift the cursor to the same position as the gaze. The system also saves all the relevant data, as mentined in Table.3.1, which are received from the eye tracker into a file for further analysis at the same time. Also, the interface can remotely transmit the commands that are produced by button clicks to the TurtleBot that provides gaze-based real-time control.

Figure 3.6 illustrates the first completed version of the interface. This version features a simple layout consisting of five main buttons and a camera view. Four of these buttons are designated for movement control that help the user to navigate and send commands to the TurtleBot. The fifth button, labeled "Save and Exit," is used to save the recorded data and close the program.
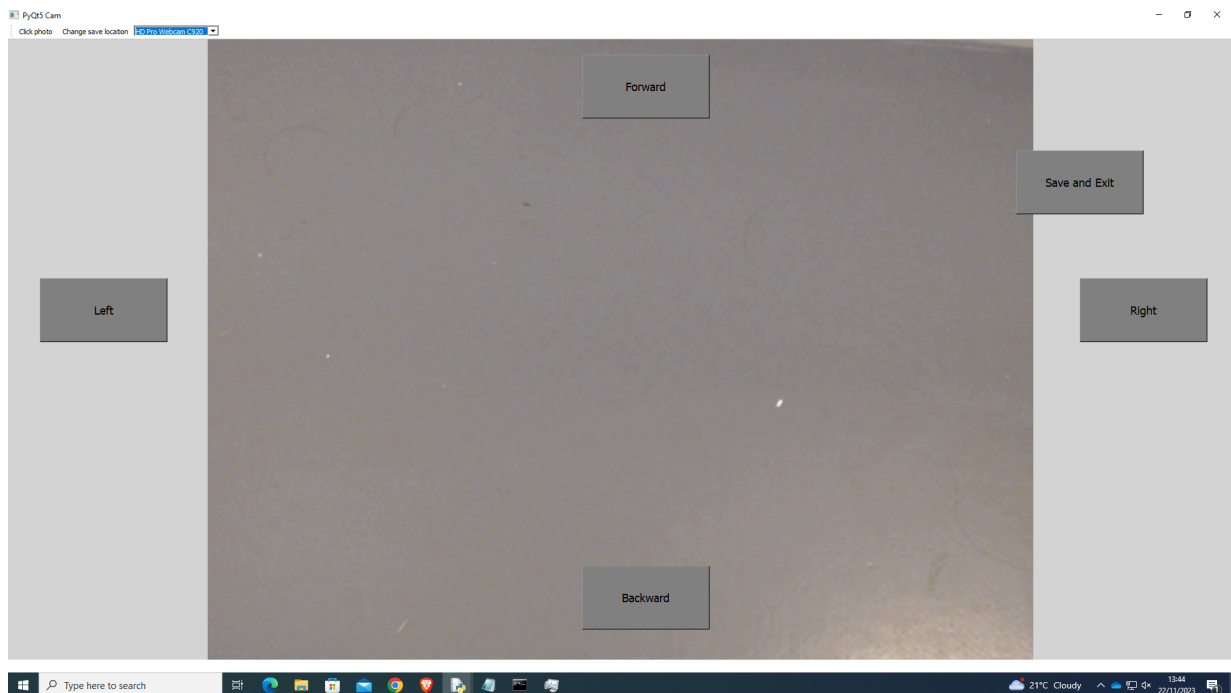
Figure 3.6: The first version of the interface featuring a live camera view and four directional control buttons. A 'Save and Exit' button is included to ensure safe program closure and proper file saving.

Regarding data saving, the recorded data is running is a separate thread and will automatically saved to a file every 30 seconds. This action is able to ensure that periodic backups are created throughout the experiment. Any additional data generated between these intervals is appended to the file as it becomes available. Once the experiment is complete and the "Save and Exit" button is selected, the system adds the remaining data, from the last backup until the moment the button is pressed, to the recording file.

In addition to recording the data, the received eye tracker data is used actively within the interface. The normalized gaze locations from both eyes are used to determine the position of
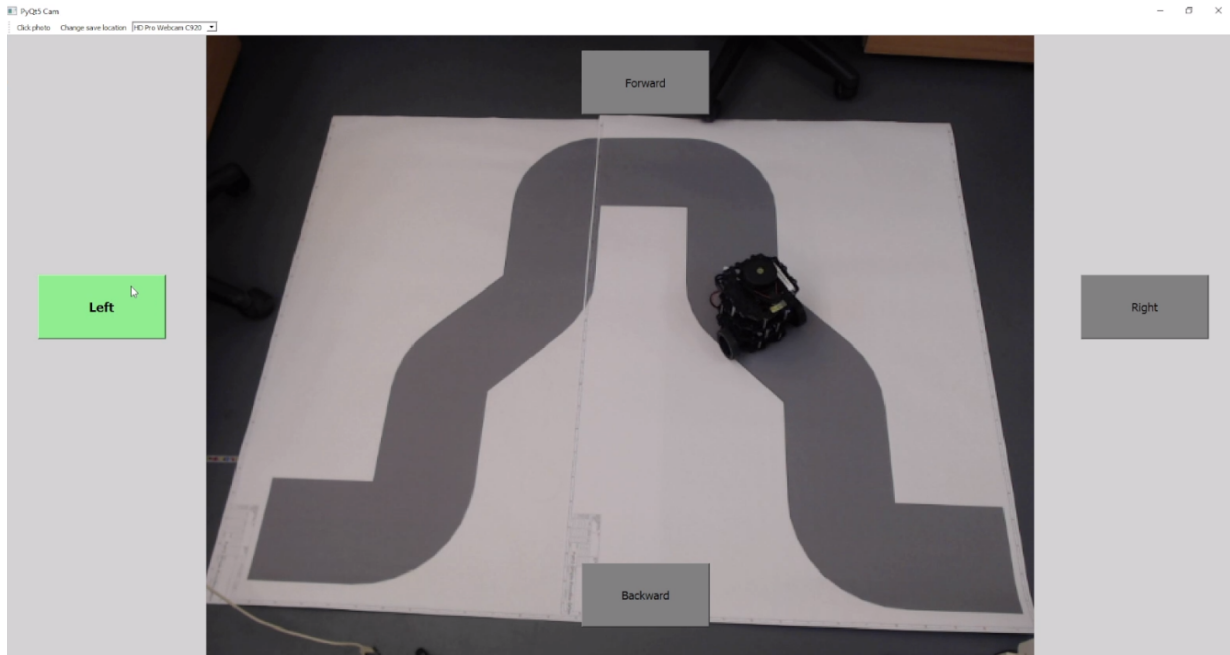
Figure 3.7: The Turtlebot user interface displaying a live video feed of the robot navigating Path One, while the user's gaze is focused on the left directional button.

the gaze on the screen and move the cursor accordingly. In this system implementation, one cursor position of the mouse is calculated from a constant counting duration of 30 time intervals.

During this intervals, the positions of the gaze of both eyes are saved. The system calculates the averaged positions of the gaze of both eyes after every period and then utilizes the averaged total to determine the cursor position. This operation enables the cursor to refresh within less than 0.5 seconds, providing the user with a smooth and responsive feedback to their visual input.

This was carried out primarily to restrict the graphical processing task of the program because frequent updates were causing performance delays as a consequence slowed down the program. Secondly, averaging the readings also helps to attenuate the impact of blinking and invalid (NaN) readings by ignoring non-valid data during calculation.

A timing system is used for activating buttons in the interface. When a cursor is placed over a button, the timer starts, and if the cursor remains on the button for two consecutive seconds, an automatic click occured. If the cursor is removed from the button before the timer ends, however,

the timer is left behind. To provide visual feedback, the button becomes green when the cursor passes over it. It indicates that it is active, and becomes gray when not in use. This timer-based action, which is refered to as "Dwell time" method, is implemented for all GUI buttons, including the "Save and Exit" button. The logic has been illustrated in the Algorithm 1.

Algorithm 1: Timer-based Button Activation Logic

Input : Cursor hovering over a button
Output: Button click triggered after 2 seconds or reset if cursor leaves

1 **if** *Cursor is hovering over a button* **then**
2   Start Timer for 2 seconds;
3   Change Button Color to Green;
4 **if** *Cursor is still over the button for 2 seconds* **then**
5   Trigger Button Click;
6   Restart the timer for 2 seconds;
7 **if** *Cursor leaves the button before 2 seconds* **then**
8   Cancel Timer;
9   Change Button Colour to Gray;

The two-second dwell time was made consistent to correspond to the robot's time spent in executing one step of movement. This guarantees that every command has enough time to be executed before a new command is issued. Choosing this time prevents the system from sending conflicting or overlapping commands in the event of continuous navigation. It also enhances control reliability by offering seamless transition from sequential commands, especially when the users need to enter multiple same directional inputs in a sequence.

Additionally, the two-second interval is not long enough to cause excessive boredom or frustration. It allows for a minimum of four cursor movements and sufficient gaze location readings, giving the user time to confirm or revise their selection and improving both accuracy and overall satisfaction. It also allows the robot to complete the previously generated command.

Upon button press, the corresponding command is transmitted to the robot. This command is entered as an alphabet letter within a shared file in a networked drive shared between the robot and the user interface.

Besides, the command, together with its time stamp, is also written in another file dedicated to maintaining records of commands received in the past. This is so that all interactions will be fully recorded and available for subsequent analysis and debugging. The flow of the GUI end-to-end process is indicated in Fig. 3.8.
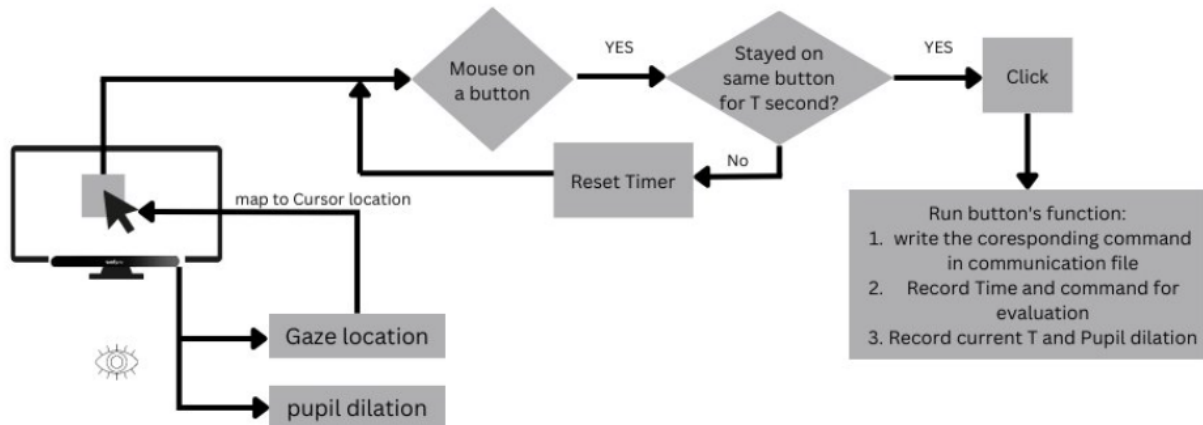
Figure 3.8: The GUI architecture and processing steps. The Picture is illustrating the flow from eye-tracker data acquisition and interpretation to command generation for the robot.

3.1.3 Turtlebot

The robot utilized in this version is the TurtleBot Burger [108], a compact and general-purpose robot well suited for a wide range of applications. It can perform a number of functions and operate with the ROS which makes it particularly well adapted to research and development.

Figure 3.9 illustrates the TurtleBot Burger robot used in this project. The robot's front and the direction of forward movement is marked for ease of users. It is equipped with two motors which are at the front of the robot. turtlebot has precise movement and maneuverability, which are essential for executing the navigation commands generated through the interface.

The TurtleBot Burger is programmed to acts incrementally and executes instructions for a short span of time followed by a halt, thereby producing motion in a specific distance. Each movement was broken down into steps to make tasks uniform in form across trials, as illustrated
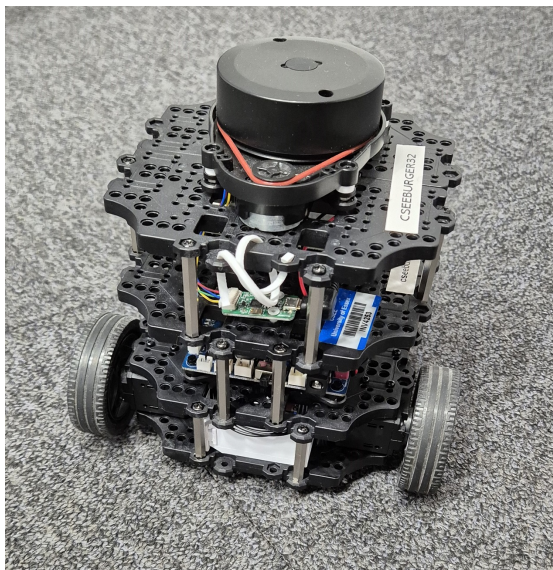
(a) front view
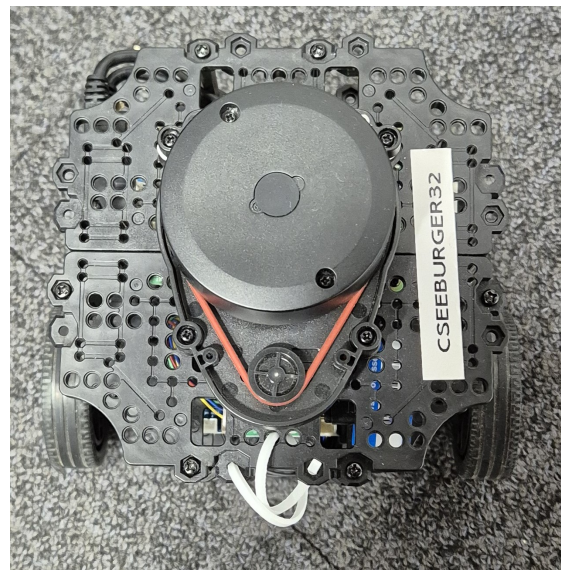
(b) top view

Figure 3.9: Images taken of the Turtlebot Burger used for this project.

Table 3.2: Steps for each movement

Step	Description
Lateral rotation	$45°$ per action using the left and right buttons
Linear movement	10 cm per action using the forward and backward buttons

by Table 3.2. During this phase, the robot travels around 10 cm along any forward or backward command. Similarly, rotate commands turn the robot around a range of about 45 degrees. This step-by-step movement cause facilitate control.

The robot operates using ROS, which provides a framework for its functionalities. Two primary nodes, a talker and a listener, are continuously running on the system. The talker node monitors the dedicated shared file on the shared drive between PC and robot over network for new commands. When a new command is detected, the talker processes it, translates it into the appropriate instructions for the listener node, and then removes the command from the shared file to prevent redundancy. Instead of directly transmitting commands, the listener node receives velocity instructions from the talker and publishes these to the motors till ensures precise and

smooth execution of movements.

On the receiving end, the listener node continuously monitors and processes inputs or communications published by the talker node. Upon receiving velocity commands, the listener node transmits these instructions directly to the motors that enable the robot's movement.
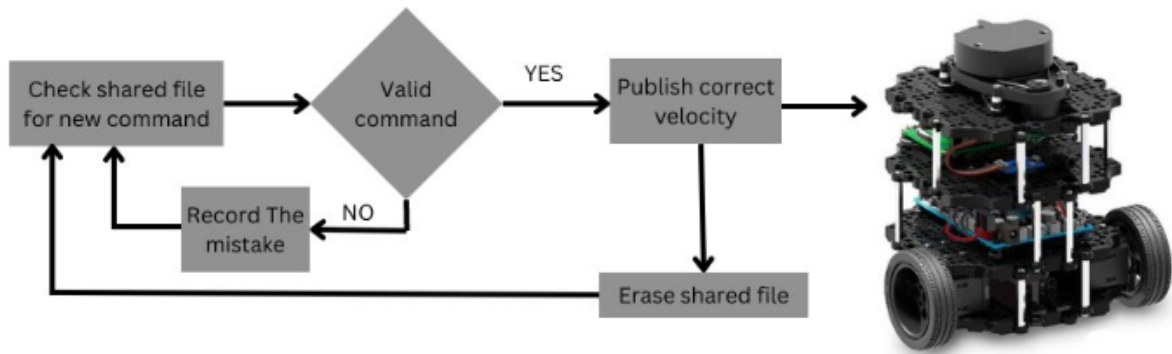
Figure 3.10: The overview of the robot's command execution flow, illustrating the sequential steps from monitoring the shared file to reading the command character and publishing the corresponding velocity message to initiate movement.

Figure 3.10 provides an overview of the robot's operational flow. The implementation details are further elaborated in the following section.

3.1.3.1 Technical and implementation

The development of the program involved the integration of several software packages and tools, as detailed below:

- tobii_research: This Python package is specifically designed for interfacing with Tobii eye trackers. At the time of development, it supported only Python 3.8 and was implemented on a Windows 10 system. While newer versions now support Windows 11 and Python 3.10, the specific eye-tracker model used in this project has been discontinued [109].

- pyautogui: This package was employed for cursor movement and implementing click functionalities. This package enables seamless interaction between the eye tracker and the GUI.

- PyQt5: This framework was utilized for designing the GUI. It facilitated the development of key features, including button integration, camera selection, and the display of the live video feed.

These tools collectively provided the necessary functionality for implementing the system and achieving the project's objectives.

The GUI is sending the commands to the turtlebot over the network using a shared file. The GUI part will write the respective command on the file and then the ROS package is used to read the file continuously and apply the command on the robot and then empty the file.

The ROS package is contains of three main programs/nodes which are written in python. One of the files is the "Setup" program which defines the requirement packages and the path for all the members of the package's codes. There are two main nodes in the package, one listener and one talker.

Algorithm 2 is showing the pseudocode of the listener node of the Turtlebot ROS package. It uses an spin function which is a infinitive loop to read the messages sent on topic and print them on the terminal.

Algorithm 2: Listener Node for ROS

Data: Receives messages on topic
Result: Prints Received messages

1 **Function** `main (`*args=None*`)`**:**
2   Initialize ROS node;
3   Create subscriber to `topic` using `String` message;
4   Set callback function to process incoming messages;
5   Keep node running using `spin()`;
6   Destroy node and shutdown ROS;

7 **Function** *listener_callback(msg)***:**
8   Print "I heard: msg.data";

Algorithm 3 describes the talker node. It has two publishers. This program is monitoring the shared file constantly. Once a new entry is written in the file, the message is published to the

topic which will then be received and printed by the listener. The message is also sent to another function which will determine the appropriate velocity for robot's motors trough `/cmd_vel` topic. Once the velocities are published, the robot will move for 1 second and then the speeds would set to zero to stop the robot. The velocities are designed in a way which make the robot to move for one step at a time.

To use the package, three terminal prompts are required. The terminals will run the following:

1. TurtleBot Bringup: This command will bring up and enable the turtlebot's systems and sensor. It initializes the internal systems of the TurtleBot and ensures that all necessary packages and services are ready for operation. It has various topics which are either subscribing to receive inputs or they are publishing data such as sensor readings or feedbacks. One of the topics is the `/cmd_vel`which will receive velocities as input.

2. Talker Terminal: This terminal runs the talker node, which monitors the shared file on the shared network drive, processes the commands and sends the corresponding velocity data to the motors, and publish the command to the topic for listener.

3. Listener Terminal: This terminal runs the listener node, which listens for incoming commands on the topic from the talker. This is mainly to insure that the package is working fine and then commands are received successfully.

All terminals need to be connected from the host Personal Computer (PC) (typically the experiment PC) to the TurtleBot, with the same username on both devices to ensure access to the personal shared drive on the university's network.

3.2   Experiment Design

Using the systems and configurations outlined in this chapter, the initial experiment was conducted with the TurtleBot. This section provides a detailed explanation of the experimental setup,

---

Algorithm 3: Talker Node for ROS

Data: Reads commands from a file and publishes velocity commands
Result: Controls movement of a robot

1 **Function** `main(`*args=None*`)`:
2   Initialize ROS node;
3   Create publisher for `String` messages on `topic`;
4   Create publisher for `Twist` messages on `/cmd_vel`;
5   Set timer to periodically check file and publish messages;
6   Keep node running using `spin()`;
7   Destroy node and shutdown ROS;

8 **Function** *timer_callback()*:
9   Open `command.txt`;
10   Read command from file;
11   If command is not empty;
12   **begin**
13   Create message with command data;
14   Call `publishVel(command)`;
15   Publish message;

16 **Function** *publishVel(command)*:
17   **if** *command == 'F'* **then**
18   Set linear velocity = 0.1, angular velocity = 0.0, Print "Going Forward";
19   **else**
20   **if** *command == 'B'* **then**
21   Set linear velocity = -0.1, angular velocity = 0.0, Print "Going Backward";
22   **else**
23   **if** *command == 'R'* **then**
24   Set angular velocity = -0.75, linear velocity = 0.0, Print "Turning Right";
25   **else**
26   **if** *command == 'L'* **then**
27   Set angular velocity = 0.75, linear velocity = 0.0, Print "Turning Left";
28   **else**
29   Set linear and angular velocity to 0.0 (STOP);

30   Publish `Twist` message;
31   Start a timer to call `STOP()` after 1 second;

32 **Function** *STOP()*:
33   Set all velocities in `Twist` message to 0;
34   Publish `Twist` message;

---

the procedures followed, and the data collected during the first trial. The purpose of this trial was to test the integration of the eye-tracking system with the TurtleBot's navigation capabilities, assess the functionality of the user interface, and evaluate the overall system's performance in real-world conditions. Data collected during this experiment include eye-tracking measurements, robot commands, and system performance metrics, which were used to analyze the effectiveness of the gaze-based control system in controlling the robot's movement.

The TurtleBot was used for navigation with the first version of the user interface. In this experiment, participants were tasked with completing navigation on two different paths. Each path was designed to assess the participants' ability to control the robot's movement using the gaze-based system. The path designs has been explained in Section. 3.2.1.

The following section describes the experiment protocol and the event. Then the chapter continues with the description of the collected data, performance and the feedbacks.

3.2.1 Path design

Two routes with opposing paths were created to help the participants navigate. The first route was a small and balanced layout, which contained an equal number of left and right turns. The balanced layout ensured that it did not have potential direction preference-biased routes and forced the participants to exercise balanced navigation decisions. Participants were instructed to navigate this path twice to facilitate investigation of variation in pupil responses with respect to familiarity and repeated exposure.

The paths were meant as general guidelines, not strict directions. Participants were instructed to drive the specified paths as closely as possible as a means of making an honest effort at staying on track. However, minor detours or shortcuts through turns were not penalized.

Figure 3.11 illustrates the layout of the first path, which was printed on two A0 pages and laid on the floor to enable navigation. This provided the opportunity for the TurtleBot to track the path accurately as well as having a standardized and uniform experimental setup for all the

participants. The large format and clear markings of the path minimized ambiguity, so, reliable data collection during the trials is been promoted.

The design of this path is founded on a balance between simplicity and complexity. The initial section, where the robot moves away from the camera, was kept simple to allow users to familiarize themselves with the system. However, the second half of the path becomes progressively more complex as the robot moves back toward the camera. This change in perspective effectively inverts the visual orientation, requiring participants to mentally re-map directional commands (e.g., left appears as right) as the robot approaches. This deliberate reversal was intended to increase cognitive load by challenging spatial reasoning and decision-making.

To try out the effect of fatigue on performance, a more complex and longer route, referred to as Path 2, was created. Figure 3.12 illustrates the general layout of the path. It was printed on five A0-sized sheets, slightly overlapping since the sheets were assembled in sequence.

The stationary location of the camera during the experiment compelled participants to orient themselves in relation to the front of the robot, rather than relying on an external landmark. To assist participants, the front of the robot was labeled with a sticker and an arrow.

3.2.2 Experimental Protocol

The initial experimental protocol utilized the first version of the user interface to allow for incorporating a fixed 2-second dwell time for button activation and the TurtleBot for navigation. Participants were tasked with completing two distinct paths: a shorter path, which they navigated twice, and a longer path, which was completed once. This protocol was designed to evaluate both system usability and user performance under varying task conditions.

Ethical approval for the study was obtained from the University of Essex Ethics Subcommittee 3 (Reference: ETH2223-2300) which ensured compliance with institutional guidelines and ethical standards. Participants provided written informed consent prior to the experiment. This informed consent confirms their understanding of the procedures and their voluntary participa-

Figure 3.11: Layout of Path 1 used in the TurtleBot navigation experiment. This path was designed to be directionally balanced, containing equal left and right turns, to avoid directional bias and assess baseline navigation performance. The layout also introduced increasing cognitive complexity in the latter half, as the robot moved back toward the user, reversing the visual perspective. This reversal required participants to mentally re-map directional commands (e.g., left becomes right), thereby increasing attentional demand and decision-making effort.

tion.

The completion of Path 1 for two times was designed to assess the influence of familiarity on participant performance. By navigating the shorter, symmetrical path twice, it was possible to observe how repeated exposure affected gaze behavior, pupil responses, and decision-making. This initial task served as a baseline for understanding system interaction under relatively simple conditions. Transitioning to the longer, more complex Path 2 introduced additional challenges,

Figure 3.12: Layout of Path 2 used in the TurtleBot navigation experiment. This longer and more complex path was designed to evaluate the impact of increased task duration and potential fatigue. It included more turns and extended segments, requiring sustained control. The path was printed on five A0 sheets and laid out sequentially. A directional marker on the robot assisted user orientation, as the fixed camera position required participants to interpret movement relative to the robot itself.

including increased sample collection and with more continues turns, which required more effortful decision-making. The longer path also aimed to simulate real-world navigation scenarios as a mean of demanding sustained attention and cognitive effort. As Path 2 was conducted at the end of the experiment, it provided an opportunity to examine the potential effects of fatigue on participant performance, such as slower responses or changes in pupil dilation patterns. These combined factors offered valuable insights into the impact of familiarity, task complexity, and tiredness on system interaction.

Upon arriving at the robot arena, the designated venue for this experiment, participants were provided with a Participant Information Sheet and a Consent Form. The information sheet outlined the purpose of the study, the procedures involved, and the potential risks and benefits and ensures participants were fully informed. The consent form formalized their agreement to participate and served as a record of their understanding of the study's requirements. Participants were then given detailed instructions about the system and the experiment. This briefing included an overview of how the TurtleBot operates, the functionality of the gaze-based interface, and the

paths they would navigate. To ensure clarity and comfort, participants were encouraged to ask questions at any stage of the process. It allowed them to resolve any uncertainties before beginning the experiment. This approach aimed to foster a supportive environment, in order to ensure participants were well-prepared and confident in using the system.

Once participants provided both verbal and written consent which means they confirmed their understanding of their rights and the experiment, they were directed to the PC station.

An adjustable monitor and chair were provided to accommodate individual preferences and ensure comfort during the experiment. The Eye-Tracker Manager software was opened on the PC in order to guides participants through the setup process. They were instructed to adjust their seating position to ensure a comfortable posture while making sure their face was correctly detected by the eye-tracker. The software displayed a live preview and allows participants to verify that their face was within the recommended range for accurate tracking.

Participants then completed the calibration process. This step involved focusing on a sequence of nine points displayed on the screen. IT ensures that the system accurately mapped their gaze movements. The calibration process was carefully monitored, and any adjustments required were promptly addressed to maintain data integrity and ensure participant comfort.

Calibration was performed before the first use and any subsequent times if participants moved away from the system. Participants who chose to complete all rounds continuously skipped additional calibrations unless requested. If participants opted to rest between rounds, felt the system was not functioning optimally, or believed they had moved significantly and required recalibration, the system was recalibrated before starting the next round. This ensured accurate tracking and consistent data collection throughout the experiment while accommodating participant needs for breaks or adjustments.

The experiment began with the TurtleBot placed at the left-hand side of Path 1. Participants were tasked with navigating the robot through the path to the right-hand side end. A camera, mounted on a tripod and positioned in the middle of the path, provided a complete view of Path

1. Participants completed Path 1 once, and upon finishing, exited the interface to save the data for that round. Afterward, they were asked if they were ready to continue or if they needed a short break. Once the participant confirmed their readiness, the TurtleBot was repositioned at the starting point, and they proceeded to complete the second round.

After completing the previous steps, participants were directed to navigate Path 2. Due to its length, the camera was manually repositioned four times during the experiment to ensure the entire path and the TurtleBot remained visible at all times. Figure 3.13 provides a visual representation of the experimental setup, including the arena, the paths, and the camera placement. This setup ensured consistent monitoring and data collection throughout the longer navigation task.
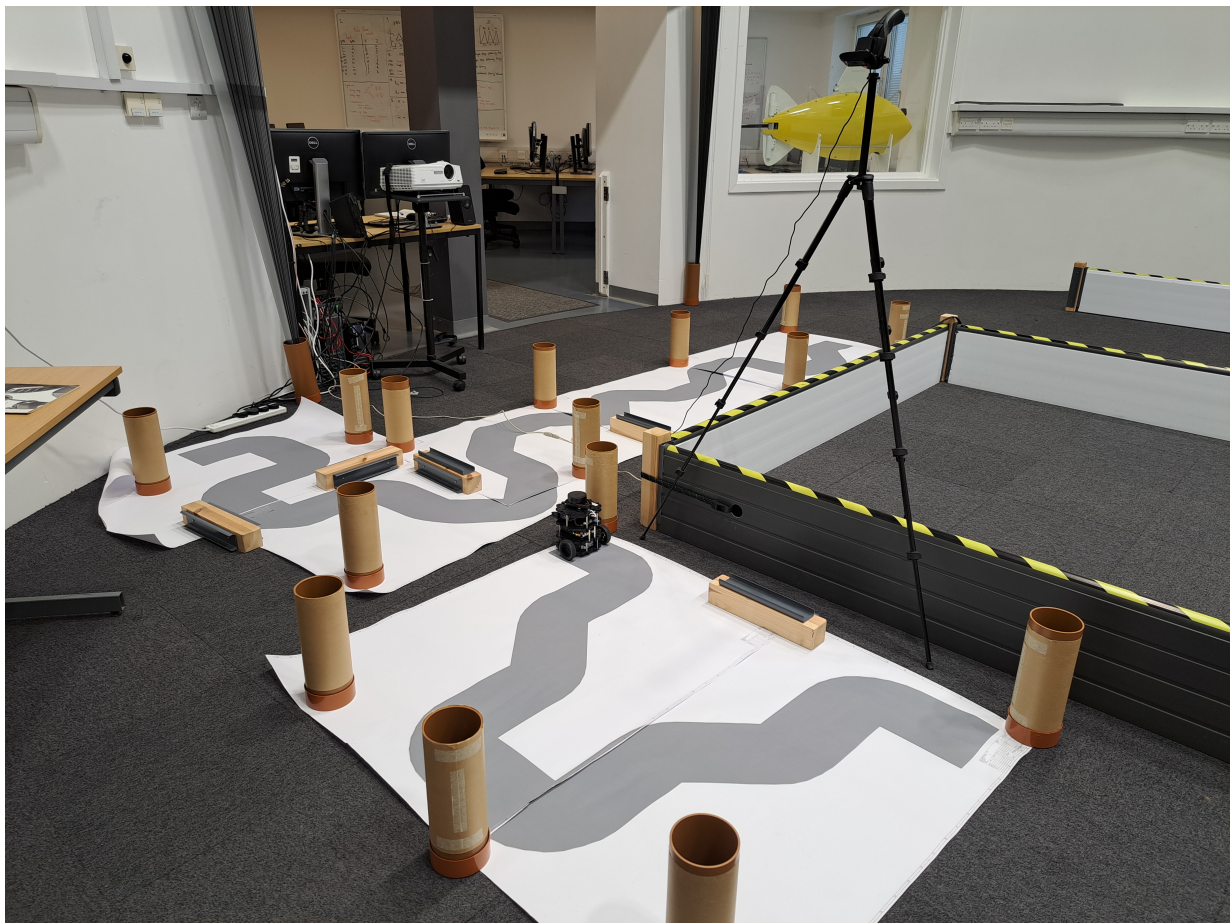
Figure 3.13: Picture of the robot arena with the experiment setup.

After completing all navigation rounds, participants were asked to fill out questionnaires designed to capture their experiences and feedback. These questionnaires aimed to evaluate user satisfaction, ease of use, and any difficulties encountered during the experiment. Additionally, participants were encouraged to share their opinions about the system and highlighed any concerns or offering suggestions for improvement. This feedback was crucial for refining the system and ensuring it met user needs effectively.

3.3 Turtlebot Navigation Experiment

In this study, we used an eye-tracking-based interface-controlled mobile robot to test its usability and effect on pupil response. We also quantified self-reported user experience via standardized questionnaires such as NASA-Task Load Index (TLX) and Quebec User Evaluation of Satisfaction with Assistive Technology (QUEST) 2.0. The details of the questions and the questionnaires has been provided in the Appendix.A.

3.3.1 Participant recruitment

Nineteen participants volunteered for this experiment, each of whom signed a written informed consent form prior to participating. This process ensured that participants understood fully the goals of the study, methodology, and potential risks associated with the experiment. The University of Essex Ethics Committee provided ethical approval for the experiment based on the institution's policy guidelines for conducting research with human subjects. This compliance indicates the study's dedication to ethical practices and the well-being of participants.

Table 3.3 provides details of the nineteen participants who volunteered for this experiment, forming a cohort designed to represent a variety of user characteristics. The sample included participants from a wide age range, with a focus on also involving older adults. This allowed an initial exploration of how age-related factors, such as familiarity with technology and cognitive

Table 3.3: Participant Data Table. U50: Under 50, O50: over 50, M: Male, F: Female, Y: Yes, N: No

ID	Age	Gender	Glasses	Path 1	Path 2	Survey
P01	U50	M	Y	2	1	Yes
P02	U50	F	N	2	1	Yes
P03	O50	M	Y	2	x	Yes
P04	U50	F	Y	2	x	No
P05	U50	F	Y	2	1	Yes
P06	O50	M	Y	2	1	Yes
P07	U50	M	N	2	1	Yes
P08	U50	M	N	2	1	Yes
P09	U50	M	N	2	1	Yes
P10	U50	M	Y	2	1	Yes
P11	O50	F	Y	2	1	Yes
P12	O50	M	N	2	1	Yes
P13	U50	M	N	2	1	Yes
P14	U50	F	N	2	1	Yes
P15	U50	M	N	2	1	Yes
P16	U50	M	N	2	1	Yes
P17	U50	M	N	2	1	Yes
P18	U50	M	Y	2	1	Yes
P19	U50	M	N	2	1	Yes

processing, might affect how the system is used. The group also included several participants who wore corrective eyewear (8 out of 19), which was important for testing how well the eye-tracking system performed under real-world visual conditions, such as light reflections or lens interference. Additionally, the sample size of 19 participants allowed for the collection of a substantial amount of data across multiple trials per user. This provided a robust dataset for training and evaluating the machine learning model introduced in Chapter 4, supporting the development of a system that can generalize across different user characteristics and usage scenarios.

3.3.2   Data analysis

The summary of key details of the experimental setup is shown in Table 3.4.

During the experiment, data was recorded at a rate of 60 Hz, capturing the following parameters:

- Timestamp of the System: Each data entry includes a precise system timestamp to maintain temporal alignment across all recorded variables.

- Left/Right Eye Validity: This binary value indicates whether the eye-tracker successfully detected the left and right eyes (1 for detection, 0 for no detection).

- Left/Right Pupil Diameter: The diameter of each pupil was recorded in centimeters.

- Left/Right On-Screen Gaze Location: The normalized x and y coordinates of the gaze location on the screen which represented where the participant was looking at a given time.

This dataset serves as a foundation for analyzing user interaction and system performance that includes gaze patterns and participant decision-making during the navigation tasks.

Table 3.4: Summary of Experimental Setup, Devices, and Data Collection Methods

Category	Details
Device	**Eye-Tracking System:** Tobii Pro Nano (60 Hz sampling rate)
	Robot: Turtlebot Burger 3
Questionnaires	**NASA TLX:** Measures mental and physical demand of tasks
	Quest 2.0**:** Measures user experience, comfort, and usability of the system
	System Feedback: Questions related to participant feedback on the system
Paths	**Path** 1 **(P1):** Short path, repeated twice (P1R1, P1R2) for familiarization with the interface. Challenge in the second half—requires concentration for right/left direction.
	Path 2 **(P2):** Longer path, designed to increase fatigue with various turn angles and longer distance.
Task Details	**Navigation Task:** Participants were asked to guide the robot from a starting point to a designated endpoint, staying on track.
	Data Collected: Performance data (time taken, error rate) and gaze tracking data (60 Hz rate) during real-time task execution.
Participant Demographics	**Total Participants:** 19 healthy adults
	Exclusion Criteria: Participants with uncorrected vision problems.
Groups for Analysis	**Age Group:** Under 50 years old, Over 50 years old.
	Vision Correction Group: Participants who wore glasses or corrective lenses, and those who did not.
Calibration Process	**Eye Tracker Calibration:** 9-point setup before each trial to ensure accurate gaze tracking.
Actions/Tasks	**Command Selection:** Participants guided the robot by fixing their gaze on specific buttons for 2 seconds to issue commands.
	Turn Limitations: Robot movement aligned with 45° rotation step.

Table 3.5: A sample of data collected during the experiment

Time Stamp	3310699393
Left Eye validity	1
Left Pupil diameter	3.2055969238
Left gaze location	(0.6587189435958862, 0.4673101603984833)
Right eye validity	1
Right pupil diameter	2.9732360840
Right gaze location	(0.7544812560081482, 0.4861457645893097)

3.3.3   Pupil response and performance

For comparing the results, the following performance measures have been suggested:

1. Lap Completion Time: This measure represents the total time taken by participants to complete the navigation rounds. Lap completion time is calculated from the time the first command is sent until the time the last command is executed.

2. Command Selection Time: This is the time elapsed between the execution of each command. The average command selection time is an important performance measure since it demonstrates how quickly participants can make decisions and respond to the navigation commands. It relies on the decision process, interface familiarity, and comfort with selecting the buttons. The minimum selection time of the command is set at 2 seconds due to the constant dwell time, which is also common among all participants.

3. Average Number of Commands: This is the count of commands that were given in the experiment. This informs us about the level of correction or change as they traverse along the path. Increased commands may imply more change of direction or behavior by the

participants, and decreased values may be indicative of more fluid movement along the path with less correction.

These performance measures allow information and data regarding both user activity as well as the effectiveness of the system to be closely analyzed. By employing an analysis of lap completion time, command selection time, and commands, usability and effectiveness of the gaze-based interface can be quantified.
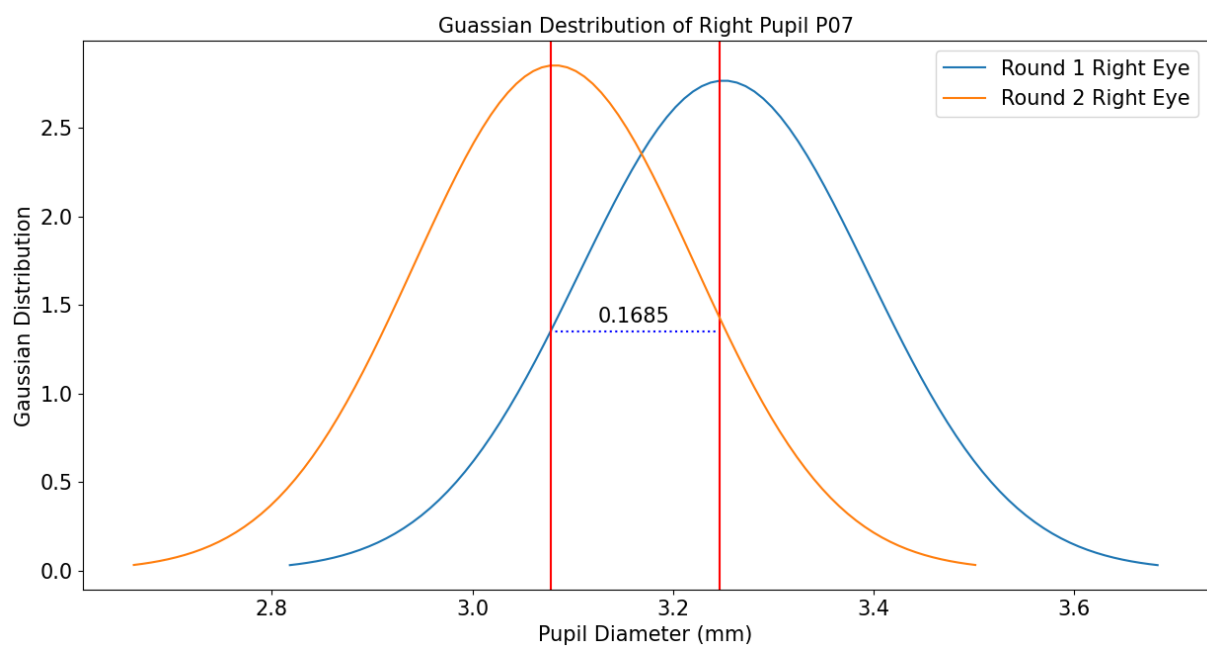
Figure 3.14: The comparison of Guassian distribution of right pupil data in participant 07 [3].

In order to gain a thorough understanding of the interaction and its outcomes, this study focuses on analyzing the overall changes and patterns in pupil dilation, alongside the corresponding performance metrics for each participant. Additionally, the results from the questionnaire are being examined.

The Gaussian distribution analysis indicates that 50% of participants exhibit greater dilation in the left pupil compared to the right, while approximately 37% demonstrate dilation in the right pupil during the recordings. Furthermore, there were cases where participants exhibited similar or overlapping pupil diameters.
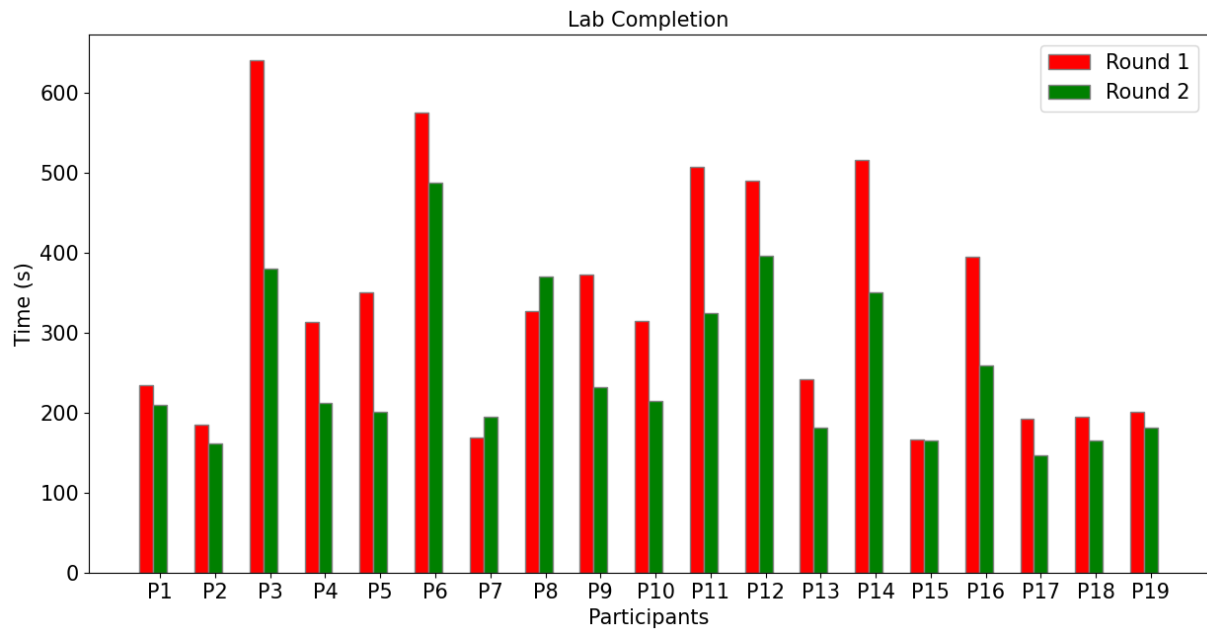
Figure 3.15: The bar chart of the lap completion time for participants [3].
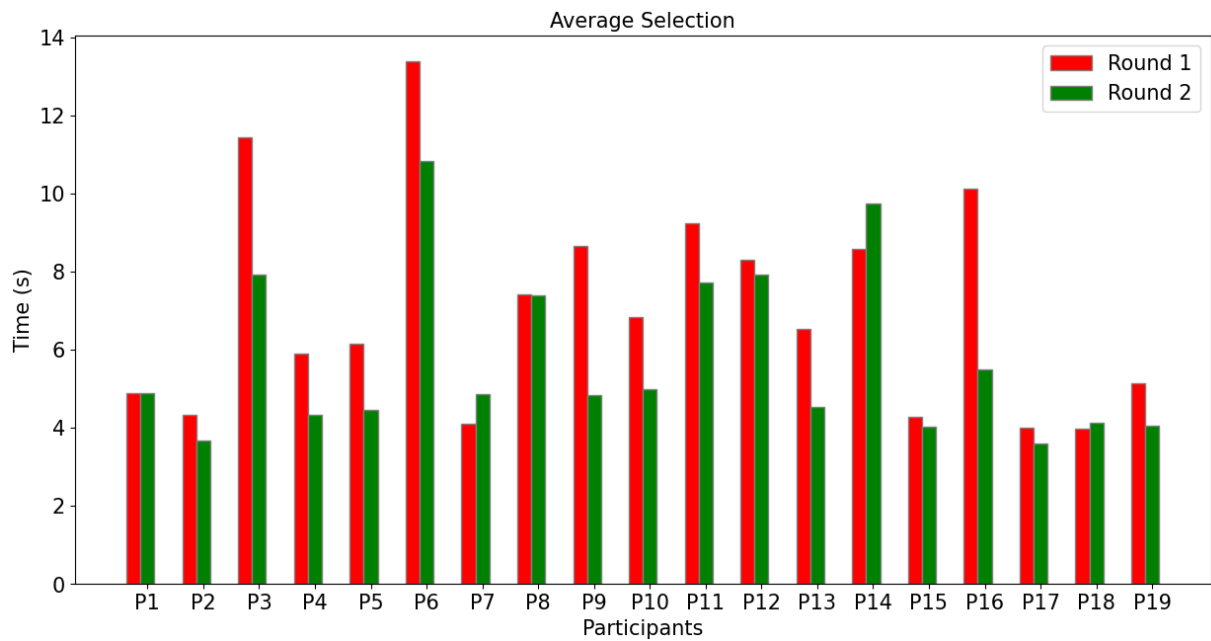
Figure 3.16: The bar chart of the average command selection time for participants [3].

Table 3.6 offers a comprehensive summary of the data collected throughout the experiment. The 'Minimum' column presents the lowest pupil value recorded across participants, while the
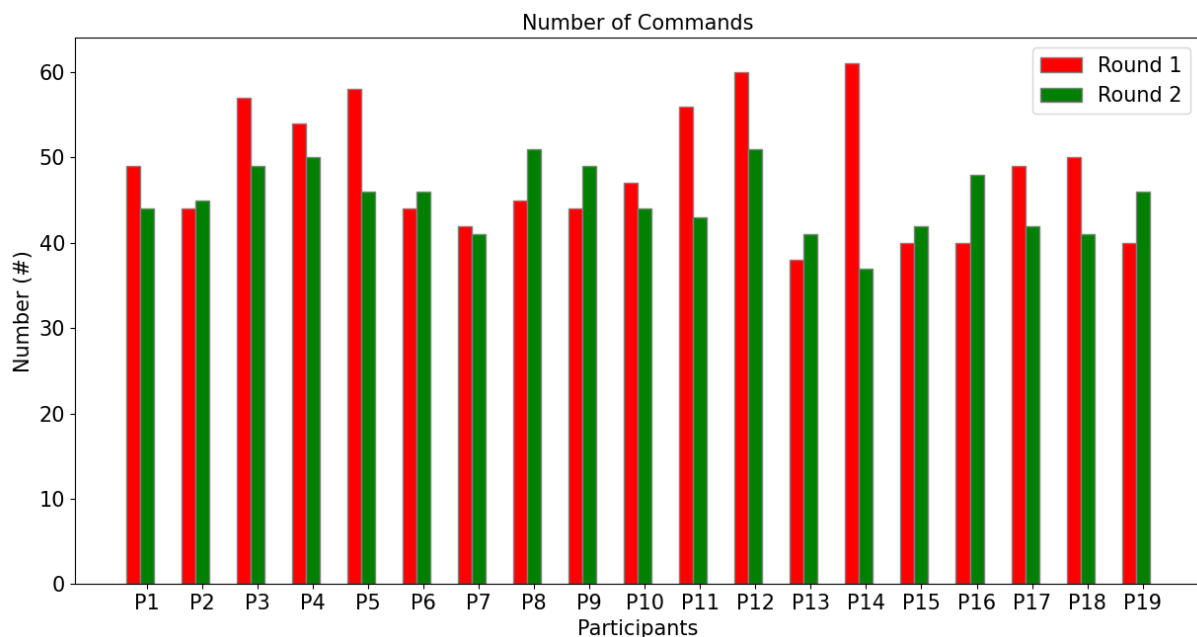
Figure 3.17: The bar chart of the number of commands generated for participants [3].

'Maximum' column indicates the highest value observed. The 'Mean' columns report the average pupil diameter for each eye during the rounds, and the 'Standard Deviation' column reflects the mean standard deviations.

Table 3.6: Minimum and Maximum pupil in the data, along with Average Mean and average Standard deviation of each pupil in the rounds [3].

	Minimum	Maximum	Mean	Standard deviation
Round 1 Left Pupil	0.8998	5.0078	3.2477	0.1808
Round 1 Right Pupil	0.9412	5.2929	3.1883	0.1871
Round 2 Left Pupil	0.9951	5.0728	3.2	0.1748
Round 2 Right Pupil	0.8621	5.2542	3.1533	0.1799

Figure 3.18 illustrates key performance metrics under varying rounds, including lap completion time, number of commands, and average selection time per case. Box plots provide the distribution and range within a round, which provides a sense of trend or inconsistency in per-

formance over the course of rounds. A comparison among these measures reveals differences in user efficiency and responsiveness, with implications for potential improvement or suggestions of fatigue that can compromise task performance over time. Following the first round, subjects registered significant improvement on all of the primary measures of performance—completion time per lap, number of commands utilized, and average time per selection—an adaptation period during which users became more familiar with the operation of the system. This learning effect indicates that the initial round of experience with the interface enables the users to understand the syntax of commands and sequence of interactions internally, and hence, their performance on the task improves later, lap times decrease, there are fewer inputs of commands, and less decision time. This trend shows how intuitive the system is, how easy it is to use, and how easy-to-use its interface is because the users had learned it so fast in just a few rounds.
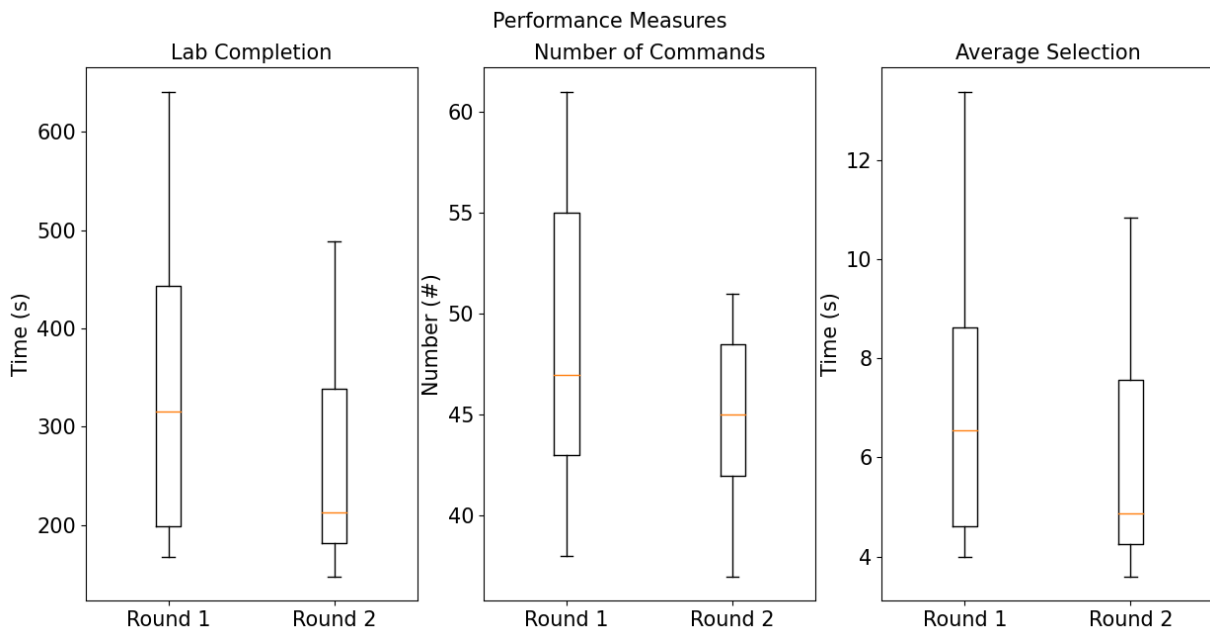
Figure 3.18: Box plots representing the distribution of three key performance measures across two experimental rounds: lap completion time (left), total number of commands issued (middle), and average selection time per command (right). Each pair of box plots compares the performance for Round 1 and Round 2. The boxes represent the interquartile range (IQR), with the horizontal line inside each box indicating the median value. The whiskers extend to the minimum and maximum values [3].

Figure 3.16 presents the average selection time for each participant across the different rounds. The time differences between rounds, used as a performance measure, are displayed in Fig. 3.21. As shown in Fig. 3.18, performance metrics demonstrate a general improvement in Round 2. It undergoes an abrupt decrease in lap time, average selection time, and number of called commands.

But about 15% of the participants saw a slight increase in average selection time (Fig.3.16), and about 10% saw an increase in lap completion time (Fig.3.15). Further, about 42% of the participants saw a slight increase in the number of commands issued in Round 2, while the rest saw more improvement (as shown in Fig. 3.17).

Figure 3.17 illustrates the total number of commands issued by participants during the rounds. The difference between the values in Round 2 and Round 1 is used as an indicator of performance, as shown in Fig.3.19.

Fig.3.14 presents an example of the Gaussian distribution for the right pupil data of participant number 7. The red lines indicate the peaks of the Gaussian distribution (mean). The difference between these lines is utilized to calculate the mean difference, which is subsequently used in Figs. 3.19 to 3.20.

Fig. 3.20 illustrates positive linear trend for Round 1 to Round 2 right pupil diameter and Round 2 lap completion time. It can be inferred from the results that, on average, the people who have larger dilation of the right pupil will take longer to complete the second lap, which corresponds with the perceived correlation between pupillary response and task performance.

Similarly, a similar trend is observed in Fig. 3.19, where the difference in mean right pupil diameter is analyzed in relation to the average selection time between commands. The figure indicates that participants with increased right pupil dilation tend to have longer pauses between issuing commands. This finding may offer additional insights into the potential influence of pupillary dynamics on the temporal characteristics of user interactions with the system.

It is noteworthy that approximately 10% of participants showed an increase in lap completion
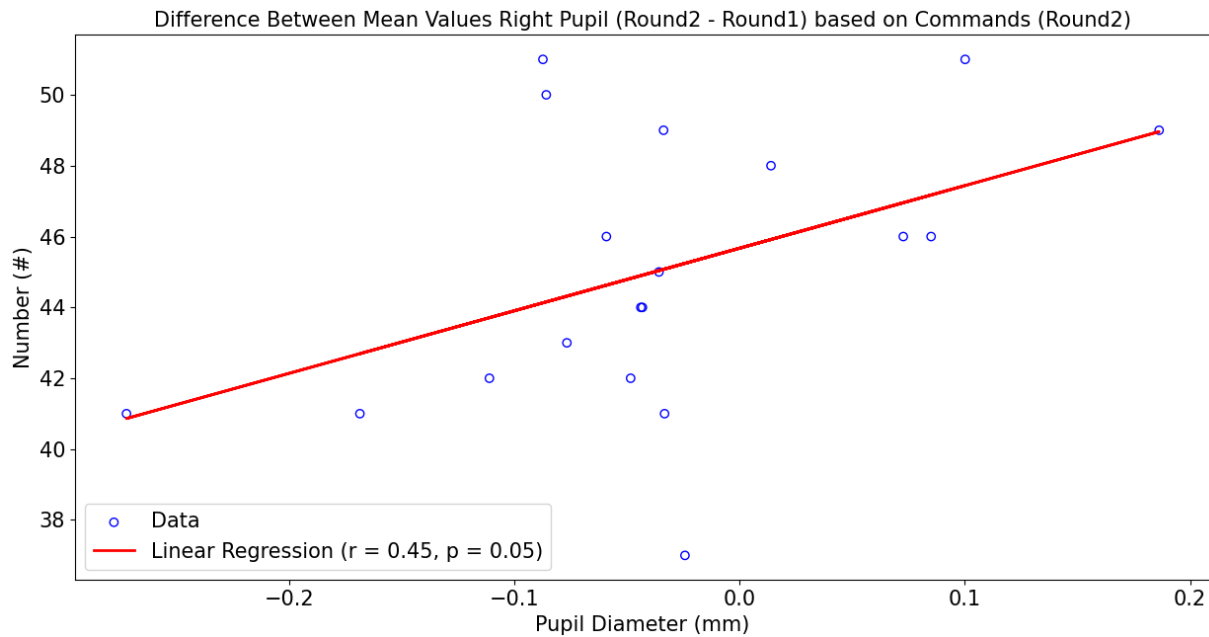
Figure 3.19: scatter plot and linear regression analysis will be conducted to examine the difference between the mean pupil sizes of Round 2 and Round 1, correlating these differences with number of commands selected in round 2 [3].

time during Round 2 compared to Round 1. Furthermore, around 21% of participants exhibited a longer average duration between commands in Round 2 compared to Round 1. These results highlight the heterogeneity of participants' performance, suggesting individual differences in adapting to the system or the requirements of the task.

Analysis of data of what was collected in each round reveals an interesting trend: participants whose lower mean pupil diameter take longer to complete the lap, whereas those whose higher mean pupil diameter complete the lap sooner. However, these participants did not report elevated levels of mental load or fatigue in the questionnaire responses.

Figure 3.21 illustrates the difference in the average time between each command and the variation in the total number of commands between Round 2 and Round 1. Interestingly, those who exhibited a slower pace in sending orders in Round 2 were also more likely to produce fewer orders compared to Round 1. This presents a potential link between generating rate for commands and the total number of commands sent, with the increased effort and precision utilized
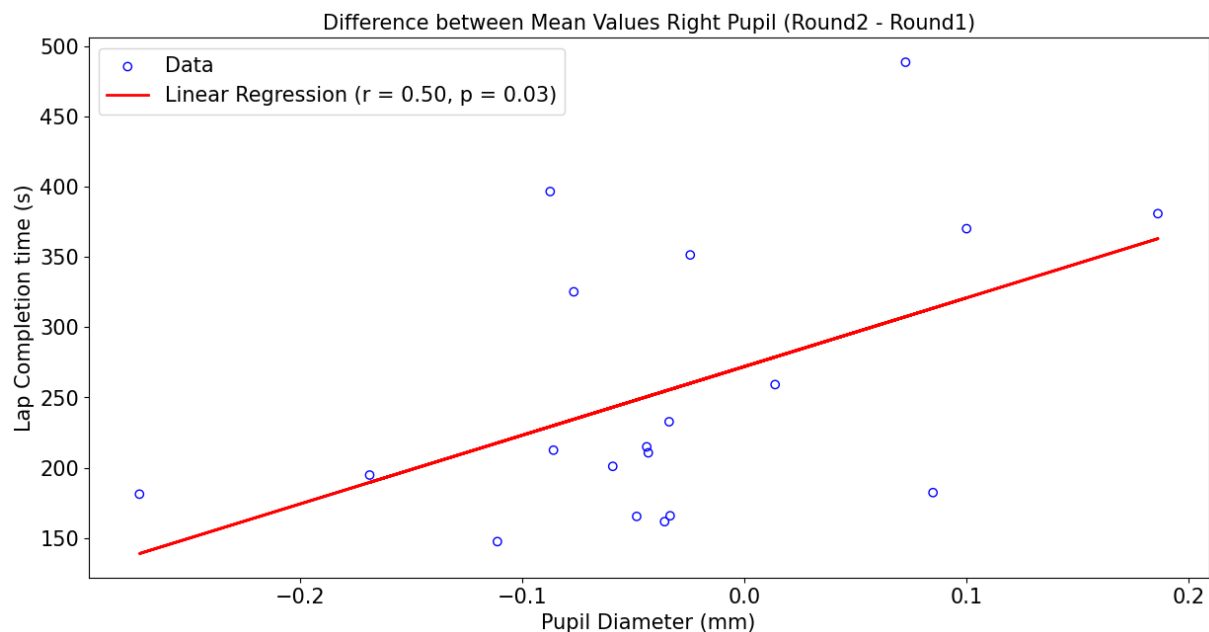
Figure 3.20: A scatter plot and linear regression analysis is conducted to examine the difference between the mean pupil sizes of Round 2 and Round 1, correlating these differences with Lap 2 completion time [3].

in decision-making in the second round.

3.4 Subjective Measures

After completing the experimental tasks, participants were asked to fill out a questionnaire to provide feedback on their experience. In addition to the written responses, participants also shared verbal feedback during and after the experiment.

While objective measures and pupil data offer valuable insights into system performance and user behavior, subjective feedback is equally important for evaluating the system's usability and acceptability. It provides a user-centered perspective on the system's practicality for real-life use and whether it meets user expectations.

The following subsections presents a summary of the participant feedback, followed by the results of the questionnaires.
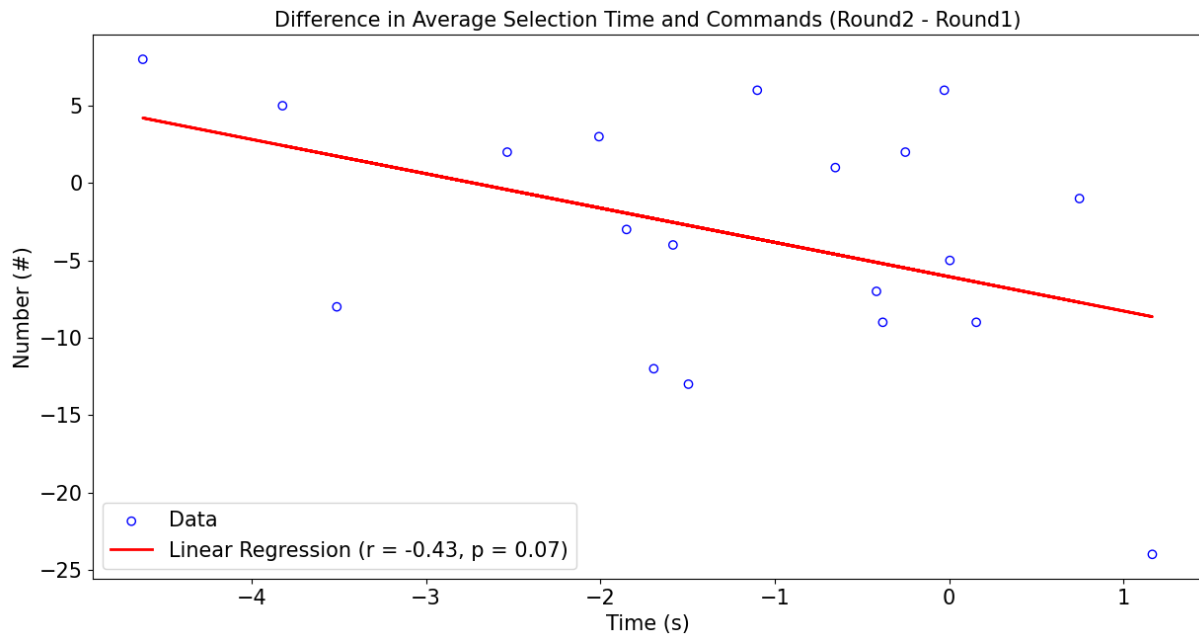
Figure 3.21: A scatter plot projecting the relation between The difference between the average selection time and the difference in the number of total commands generation during R2 and R1[3].

3.4.1   Subjective Feedbacks

In the area of participant feedback, one of the issues that were raised was pre-programmed robot movement steps and the use of a mobile robot instead of a real wheelchair. Some participants complained that the 2-second constant dwell time was too long, and this could have hampered their productivity in communicating with the system. Moreover, most of the users blinked less while focusing on the buttons, leading to eye strain and discomfort. The results show the possibility of making the system more responsive and the importance of taking the users' comfort into consideration in an effort to improve the overall interaction experience. Additional development may involve dwell time optimization and adding features to reduce eye strain, which can further enhance the usability and satisfaction of the system.

Although every aspect of demand—physical, mental, and temporal—was rated as low by the participants, most of them found the physical demand to be the most challenging. The most

common reasons for high physical demand were eye strain and maintaining a constant posture. Mental demand was particularly noted in relation to being unable to tell the direction of the robot throughout the activity. These results are crucial to future development, especially as we move away from the mobile robot paradigm and towards a powered wheelchair system with an adaptive HRI interface. Based on these results, we plan to include new adaptive settings directly addressing concerns of eye strain and posture discomfort, ultimately resulting in a better overall user experience and easier use for mobility-impaired individuals.

In reasoning the result, fatigue and increased mental demand lead to poor performance results. Another observation can be seen from results in Round 2 where reduced button choice time, reduced overall completion time, reduced commands, and reduced mean pupil diameter were noted. These trends suggest that participants may have become more familiar with the task and its requirements that it leads to a reduction in mental workload and an improvement in overall performance. The decrease in lap time and pupil diameter may reflect increased efficiency and lower cognitive effort in Round 2, likely due to a learning effect or enhanced task familiarity gained during Round 1. While tiredness and mental demand undoubtedly influence performance, the effect of participants' growing familiarity with the task should also be considered when interpreting the results.

Although it was observed and mentioned by participants that, due to tiredness and eye strain, they opted to perform shortcuts and did not commit to the full defined turns during the final part of Path 2, this suggests that user engagement was affected by fatigue and exhaustion.

In line with previous research, this experiment observed similar patterns in pupil diameter. During Round 1, when most participants interacted with the system for the first time, their pupil diameters were generally larger that is suggesting a higher cognitive load. By Round 2, the pupil diameter reduced, presumably with the reduction in the cognitive load brought about as subjects became accustomed to the system and possibly some fatigue. Perhaps unsurprisingly, the subjects showing superior performance metrics exhibited larger pupil diameters in following

rounds reflecting larger cognitive loads. On the other hand, those subjects subject to higher fatigue had smaller pupil diameters. This is a representation of lower levels of cognitive effort.

3.4.2 Questionnaire Results

Some of the notable outcomes of the questionnaire responses are described in this section.

As can be seen in Fig. 3.22, the familiarity with Path 1 yielded the most favorable results for lowering the completion time of the second round for the elderly, with a correlation coefficient of $r = 0.518$ and a statistically significant p-value of 0.028. This suggests that the recurrence of the shorter route helped older participants to perform the task better, perhaps due to higher comfort and familiarity with the interface, leading to quicker navigation times in the following trial. Such findings suggest the potential of performance facilitation by repetition of the task, particularly for users who may take longer to acclimatize with new control strategies.
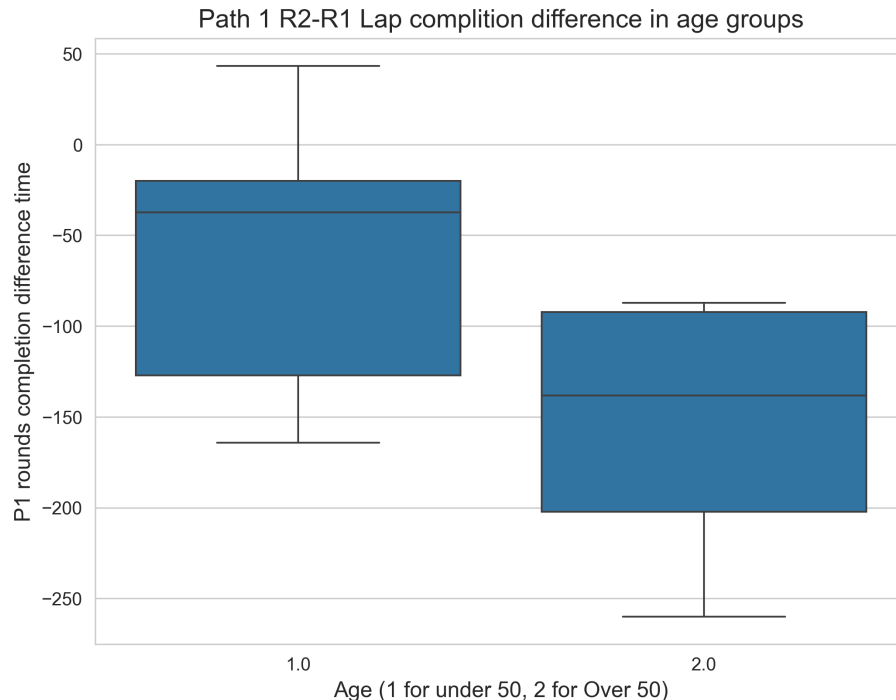
Figure 3.22: The box plot presenting the difference of lap completion time of round 2 and round 1 on the path 1 based on the age groups [4].

Figure 3.23 also shows a significant correlation between self-rated mental demand as measured with the NASA TLX questionnaire (Mental Demand vs. Lap Completion Time: $r = 0.609$, $p = 0.007$). The NASA TLX scale is between -10 and $+10$, where -10 indicates very low demand and $+10$ indicates very high demand. It suggests that it takes longer to complete each lap as participants subjectively report greater mental demand. This suggests that the more participants have reported mental demand, the more time they will take to complete each lap. The positive association between the completion time for a lap and the self-reported mental demand not only measures the mental load of driving the robot but also implies that higher mental demands can lead to longer times in completing the tasks.
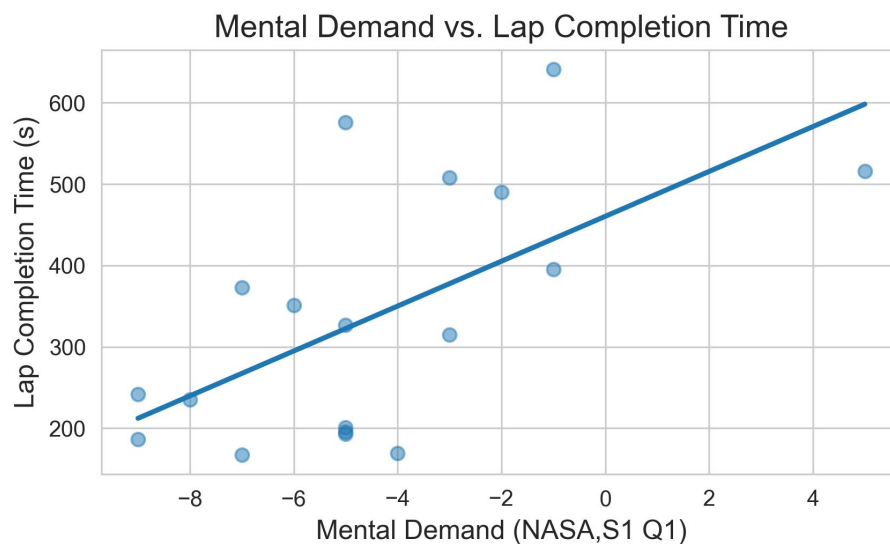
Figure 3.23: Lap completion times for Path 1 in Round 1, alongside participants' self-reported mental demand ratings [4].

On average, participants reported that the system did not induce much demand. The Average results from the NASA TLX questionnaire for all participants are shown on Table 3.7.

As indicated above, a lower rating, i.e., a value closer to -10, indicates that the task is less cognitively demanding. As can be seen in Table 3.7, the negative values here indicate that the task was not perceived by participants as being particularly demanding in mental and physical effort. The mental demand score of -4.44 shows that subjects did not find the task to be too mentally

Table 3.7: Average results from NASA TLX questionnaire for all participants [4]. The response scale ranges from -10 to +10, where -10 indicates very low demand and +10 indicates very high demand, with 0 representing a neutral response. For the performance dimension specifically, -10 indicates perfect performance and +10 represents complete failure. The negative values across all dimensions suggest that participants generally experienced low levels of demand and good performance.

Demand	Values (-10 to 10)
Mental Demand	-4.44
Physical Demand	-2.94
Temporal Demand	-4.28
Performance	-5.39
Effort	-1.22
Frustration	-6.89

demanding, while the physical demand score of -2.94 also shows that the gaze-controlled system was not physically demanding. The temporal demand score of -4.28 reveals that users did not feel rushed or under temporal pressure in completing the task. The performance score of -5.39 shows that, although participants found the system to be quite effective, there was still some scope for improvement in terms of optimal performance. Effort scored the highest at -1.22, which implies that although participants found the system to be effortful to use in some sense, the negative value of this measure is a positive indication for ease of use. However, frustration was rated the most negatively at -6.89, which means that possibly interaction problems or minor delays in command execution did not result in a lot of frustration.

Overall, while the results presented show that the system is highly intuitive and low in cognitive and physical demand, improvements can be made in the performance and frustration scales. Since users liked a system that was easy to use and imposed minimal demand on their effort, increasing the responsiveness of the system and providing users with more control could serve to enhance the user experience.

Out of the 12 components that comprised the Quest 2.0, subjects ranked 'Ease of Use,' 'Comfort,' and 'Effectiveness' as the most important characteristics in selecting an assistive device. The rankings suggest that users find devices not only tuned for performance but also highly comfortable and easy to use, which is most important for long-term satisfaction and usage.

The performance of participants was enhanced in both age groups (over 50 and under 50) along Path 1 in the second round, as their lap times decreased, a result which is evident in Fig. 3.24. For the under 50 participants, the total time spent by Path 1, Round 1 averaged approximately 230 seconds and dropped to approximately 200 seconds on Round 2. This shows that practice efficiency has been attained. However, for this group, Path 2 time of completion was around 500 seconds and identified a harder path due to its length and numerous turns. For the greater-than-50 group, Path 1, Round 1 was significantly longer with an average completion time of around 550 seconds. During Round 2, one could observe improvement as the time of completion decreased to around 400 seconds. Despite this improvement, the over-50 group was still far slower on Path 2, which is taking around 1150 seconds to complete the more complex path.

Figure 3.24 indicates that while both age groups learned and improved from Round 1 to Round 2 for Path 1, the older group had a harder time navigating the longer and more complex Path 2. This can be explained by a number of factors, including the higher cognitive or physical cost of navigating a more complex route, which would have been the cause of the higher completion times of the over-50 group. Nonetheless, the improvement between rounds indicates that both groups were able to adjust and become more efficient with the system over time.

Figure 3.25 shows the heatmap of correlations of the questions related to workload, satisfaction and acceptance of the proposed system. Darker colours presents stronger correlation between the questions. The details of the questions can be found in Appendix. A.

Lap Completion Time by Age Group and Path/Round
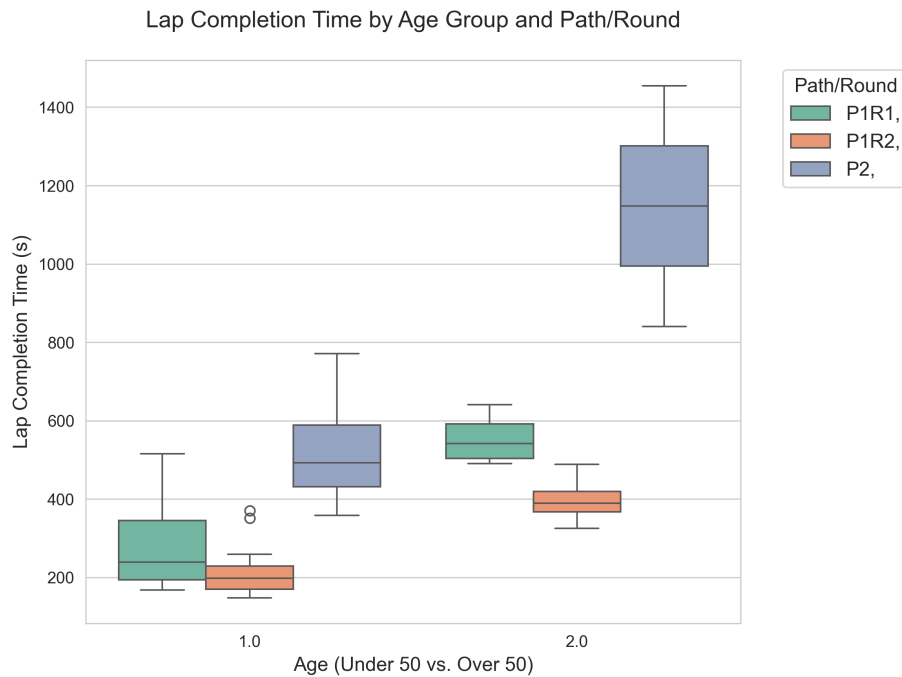
Figure 3.24: This plot illustrates lap completion times categorized by age group, where 1 represents participants under 50 years old and 2 represents participants over 50 years old [4].

3.5   Summary

This chapter presented the initial development and validation of the gaze-based assistive interface. The methodology involved a structured experiment where nineteen participants used the system to control a TurtleBot mobile robot through two predefined navigation paths. Throughout the experiment, key performance metrics, along with continuous pupil dilation and gaze data, were systematically recorded to evaluate the system's functionality and its effect on the user. The results demonstrated the system's high usability and intuitive design, evidenced by a significant learning effect where participants consistently improved their navigation performance over successive trials. Furthermore, the analysis revealed a quantifiable relationship between pupil dilation and task performance, providing strong empirical support for the potential of using pupillometry as an indicator of cognitive load in this assistive context. In conclusion, this foundational study successfully validated the core principles of the gaze-based interface and,
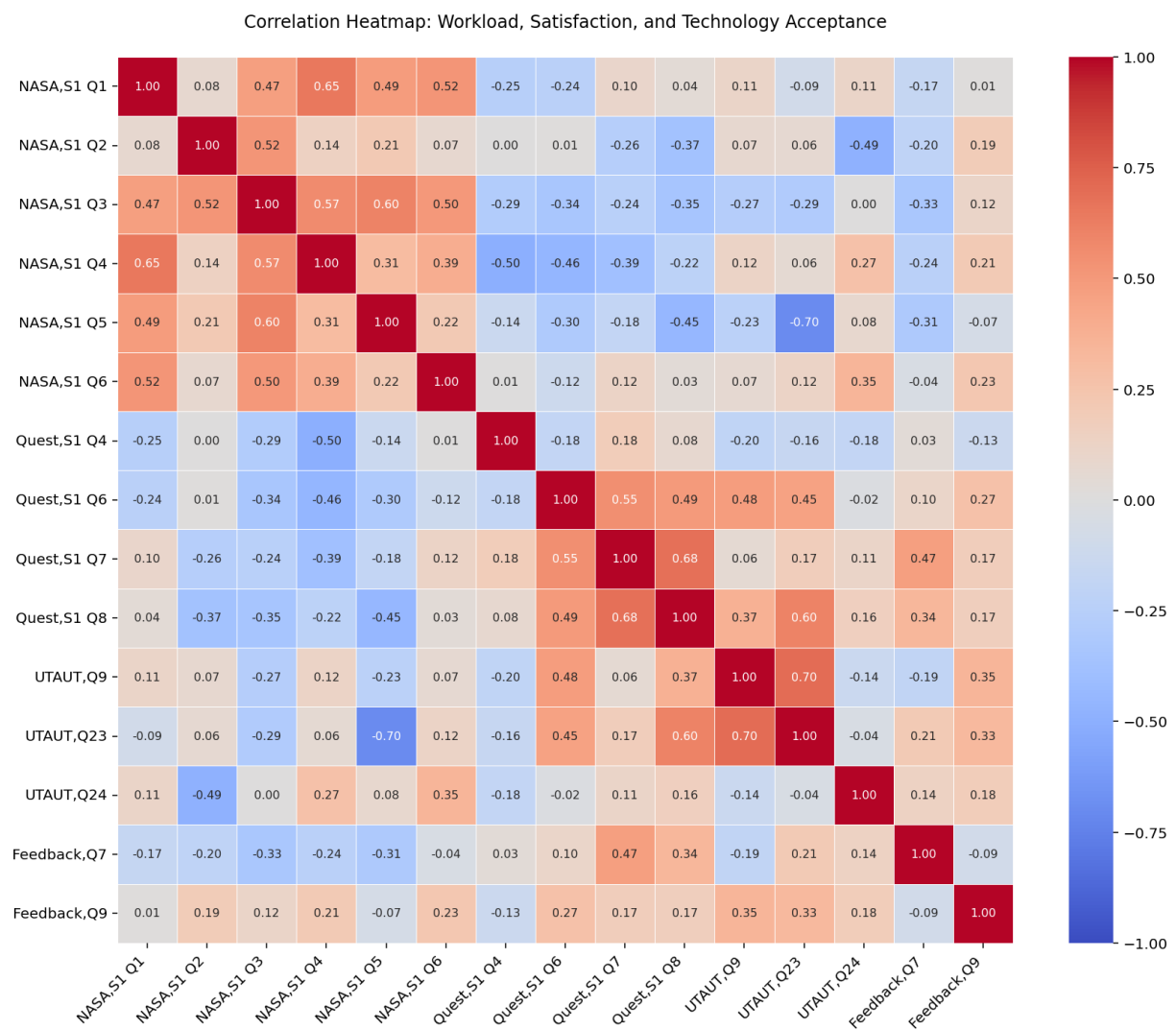
Figure 3.25: The heatmap of the correlations of the questions related to Workload, Satisfaction, and technology acceptance.

most critically, resulted in the collection of a robust dataset linking pupil dynamics to specific user actions. This dataset provides the essential empirical foundation for the next stage of the research. The following chapter will therefore leverage this data to design, train, and validate the machine learning model proposed as an adaptive alternative to the static dwell-time method.

The outcomes of this chapter provided a critical enabler for the work presented in the following chapters. The dataset of pupil and gaze data provides the essential input for the work in Chapter 4, which details the design and training of the machine learning model proposed as the solution to the static dwell-time problem. The feedback regarding the limited realism of the mobile robot directly motivates the transition to the powered wheelchair in Chapter 5, where the adaptive model will be tested in a more practical context. Furthermore, the core principles of the GUI validated here form the design basis for the assistive arm control interface in Chapter 6.

Chapter 4

Classification of Pupil Dilation for Pupil-Informed Activation

In this chapter, the machine learning algorithms employed to classify pupil diameter data for two cognitive events, decision-making and focus, are explained. For the classification task, two primary approaches were implemented and compared: Support Vector Machine (SVM) and a deep learning strategy. The pre-processing of the data was the beginning, which is a crucial first step to render the input data consistent and of high quality. After data preparation, both classification techniques are applied and compared. Finally, the performance of the two methods is compared in order to ascertain their relative performance and which of them is most appropriate to distinguish between the two cognitive events based on pupil diameter.

The selection of these two classification methodologies was deliberate, reflecting a specific research strategy for this novel application. The deep learning approach was investigated as the primary method due to its inherent strength in handling raw, sequential data. This provides an end-to-end learning framework that is feature-agnostic, allowing the model to learn discriminative patterns directly from the pupil dilation time-series without the need for manual feature extraction—a process that risks excluding subtle yet significant temporal patterns. To provide

a rigorous baseline for comparison, the Support Vector Machine (SVM) was also implemented. As a powerful and widely-used traditional classification algorithm, SVM serves as a critical benchmark to validate the performance of the deep learning model. As the results will show, this comparative approach demonstrates the efficacy of the feature-agnostic strategy.

This chapter presents a key scientific contribution of the thesis by detailing the development and validation of a machine learning model capable of classifying user intent from real-time pupil dilation data. It provides a systematic comparison between a classic machine learning approach (SVM) and a deep learning strategy to determine the most effective method for this novel application. The results demonstrate the high feasibility of using pupillometry as a robust signal for an adaptive interface, with classification accuracies exceeding 90%. The resulting trained model forms the core of the adaptive activation mechanism that is implemented and evaluated in the high-fidelity assistive systems in the following chapters.

4.1 Pre-processing Data

The pupil measurements were categorized into two primary labels: decision and focus. The focus duration refers to the pupil data recorded during the 2-second interval in which participants maintain their gaze on a button, as described in Section 3.2.2. Participants select a button by keeping the pointer over it for this 2-second period, termed the focus event. In contrast, the decision event is defined as the phase during which participants search for and identify the button they wish to activate. To process and analyze these events, the following steps were implemented:

- Handling NaN Values: Missing data, represented as NaN values, can occur when tracking devices fail to detect pupil activity due to blinking or head and body movements. To address this, NaN values were replaced by averaging the data points immediately before and after the missing values. This method ensures dataset continuity while minimizing the effects of missing information on the analysis.

- Determining Gaze Position: The gaze position was calculated as the average of the normalized coordinates of the left and right eyes at each time point. This approach identifies the point where participants direct their gaze using both eyes simultaneously.

- Identifying Exit Time: The exit time marks the moment when the participant's gaze leaves the previous button. This may occur under two conditions: (1) the participant glances at the robot's position before returning to the same button, or (2) the participant shifts their gaze to a different button. Determining this time is essential for delineating the decision event.

- Identifying Last Enter Time: The last enter time corresponds to the moment participants finalize their decision by shifting their gaze to the next button and maintaining focus. Minor eye movements can cause temporary gaze deviations. As noted in Section 3.2.2 and Table.3.4, button activation requires the pointer to remain over the button for two continuous seconds. If this condition is not met, the process resets. Consequently, the decision event spans from the first instance of gaze leaving the previous button to the final instance when the participant's gaze aligns with the new button and remains stable for the required duration.

These steps facilitate a systematic approach to processing and interpreting pupil data, enabling the effective distinction between focus and decision phases during participant interactions.

This preprocessing framework ensures that the collected data is clean, consistent, and accurately segmented into meaningful events, such as focus and decision. By addressing missing data, calculating precise gaze positions, and delineating event intervals, the dataset becomes well-suited for subsequent analysis. These preprocessing steps prepare the data for advanced classification methods, including deep learning techniques, which leverage complex patterns in the data, as well as traditional machine learning approaches such as SVM. This systematic preparation enhances the reliability and robustness of the dataset, facilitating the application of

various analytical models to extract insights and improve performance outcomes.

4.2 Classification Methods

Using machine learning models to label pupil diameter really enhances our approach, and can facilitate button choice in a more user-friendly and convenient manner. Through the evaluation of pupil dilation patterns, we aim to produce a more adaptable and user-centered system.

In this study, two classification approaches were applied to the dataset. The first is the application of a deep learning model, which can learn intricate relationships among the data. The second approach employs a Support Vector Machine (SVM) algorithm, which is a well-established classification method. Both approaches were utilized to classify the dataset into two classes: Decision – when the user is making a decision on some action during processing information. Focus – when the user has made the decision and is focusing on a button to select it.

These classifications have been derived using the data collected from the participants (as specified in Section 3.2.2). The application of these machine learning techniques makes it possible to have a comprehensive analysis of the data, and valuable information about the inherent trends and patterns is provided. This approach not only enhances system accuracy but also user experience by making the gaze-based decisions more responsive and dynamic to individual needs.

4.2.1 Deep Learning-based Classification

Deep models have now surfaced as powerful algorithms to handle time-series data [110] and hence are well suited for this research. Since the patterns of pupil dilation are successive, a deep model can thus learn temporal relations effectively and give important features.

In order to address the classification issue in our data, we employed a Convolutional Neural Network (CNN) architecture [111]. CNN architecture is particularly best for handling time-series

data by application of convolutional layers for feature extraction that can be used for participants' eye-pupil motion.

The model presented here has three one-dimensional convolutional layers sequentially extracting hierarchical features from input. Each convolutional layer was followed by a max-pooling layer to decrease dimensions but preserve important details and a dropout layer to prevent overfitting and improve model generalization. A fully connected layer subsequently, which combines the features extracted to make a decision. A classifier layer with the softmax activation function to calculate probabilities of various classes, ensuring strong classification.

This architecture allows the model to perceive subtle pupil dilation differences in diverse states of cognition, e.g., decision-making and focused attention. The typical deep learning model architecture described within this article is illustrated in Fig. 4.1, where data flow in different layers can be seen. By applying CNNs, we aim to maximize pupils-based classification accuracy and insensitivity to eventually create more adaptive and intelligent gaze-based interfaces.

Figure 4.1: The comparison of SVM and CNN algorithm for participants using average of left and right eye pupil data [5].

Model structure attempts to leverage the one-dimensional convolutional layers in order to identify localized patterns in the time series data. By applying filters across input sequences, these layers extract temporal dependencies and feature-extracting across different temporal scales. The first two convolutional layers employ F_1 and F_2 filters of kernel sizes K_1 and K_2, respect-

ively. With Rectified Linear Unit (ReLU) activation functions, the layers enable the network to delve into the temporal pattern of the data and extract efficiently a large range of localized features.

On this basis, the third layer of convolution increases the network's ability to refine and interpret the features that have been extracted. The third layer makes use of F_3 filters, which are double the number of filters used in the preceding layer, and a kernel of size K_3, enabling more sophisticated temporal features to be captured as well as improved understanding of the inherent patterns of the data.

Max-pooling layers follow each convolution for complementing convolutional layers. The layers actually perform downsampling, i.e., reduce the spatial dimensions of the features derived but keep the most prominent information. Aside from enhancing the model's focus on exceptional patterns, the process also reduces computational load. The sizes of the kernels of the max-pooling layers are M_1, M_1, and M_2 to correspond with each convolutional layer for greatest reduction in dimension in each stage of the network.

To deal with overfitting, a robust regularization scheme is implemented throughout the entire model. There exists kernel regularization in each convolutional layer using both the L_1 and the L_2 methods together with bias regularization and activity regularization using the L_2 method. Furthermore, Dropout layers are applied after each convolutional layer with dropout probabilities known as D_1, D_2, and D_3. This multi-regularization strategy enhances the capacity of the model to generalize because it reduces reliance on specific features or patterns and regularizes training and promotes good performance on unseen data.

Preceding the classification layer, a fully connected layer of N_1 neurons is employed to learn the ultimate temporal features that account for the intricate patterns identified by the convolutional layers. The classification layer with $softmax$ activation function generates probabilities for every class, and based on these, the time series data is classified into individual focus and decision classes. This carefully designed architecture effectively extracts the nuances of the input

data and thus enhances the accuracy and reliability of the classification process.

4.2.2 SVM-based Classification

In addition to deep learning models, this study involves SVM, a widely applied technique for biosignal classification. SVMs operate by identifying the optimal hyperplane that separates data points into classes, with a high capacity to recognize patterns in complex datasets having been demonstrated. This makes them extremely suitable for the analysis of pupil activity, which conveys information about cognitive processes, attentional states, and decision processes. For this study, the Radial Basis Function (RBF) kernel is employed since it is able to capture complex, non-linear relationships within the data. Furthermore, the regularization parameter, R_1, is carefully tuned to balance model complexity and generalization capability. With the tuning of parameters such as the kernel function and regularization parameter, the SVM is finely tailored to distinguish between subtle patterns in eye-pupil data, thereby informing cognitive and behavioral processes. The complete description of the parameters and settings utilized in this study are presented in Table 4.1.

4.3 Results: Classification on TurtleBot Experiment

As outlined in Section X, we employed two distinct classification models, deep learning and SVM, to classify focus and decision events. The performance of both models was evaluated based on their ability to classify pupil diameter data, with the objective of determining the most effective approach for this task. For the deep learning model configuration, binary cross-entropy was used as the loss function, paired with the Adam optimizer to facilitate efficient training. The model was trained over 250 epochs, utilizing a k-fold cross-validation approach with $K = 5$. This method provides a robust evaluation framework, improving the generalizability and reliability of the results. The effectiveness of both the deep learning model and SVM in classifying

Table 4.1: Parameters and setups used for training model [5].

	Parameter Name	Value
Data preparation	Normalization	Z-score algorithm
Deep Learning	F_1	16
	F_2	32
	F_3	64
	K_1	60
	K_1	30
	K_1	5
	Activations Functions	ReLU
	D_1	50%
	D_2	40%
	D_3	30%
	N_1	128
	Classifier	Softmax
	Loss	Binary Cross Entropy
	Optimizer	Adam
	Epochs	250
	Batch size	32
	K-fold	5
SVM	Kernel	Radial Basis Function
	R_1	1

focus and decision data will be assessed through various performance metrics, such as accuracy, precision, and recall, ensuring a comprehensive analysis of their capabilities.

This study employed both deep learning and SVM-based classification models to distinguish between focusing and decision-making events based on recorded pupil data. To evaluate the models' performance, accuracy was measured and compared across different input sets, including the right, left, and average pupil diameters for each participant during each round of the experiment. This approach enabled a comprehensive assessment of how different input features contribute to the classification task, providing insights into the models' ability to accurately discern focus and decision-making states from pupil diameter variations.

The initial analysis involved using pupil data from all three rounds of the experiment as separate inputs for both the SVM and deep learning models for each participant. Figure 4.4 shows the accuracies obtained by the SVM and deep learning models using the right-eye pupil data, while Fig. 4.3 illustrates the results for the left-eye data. For the results in Fig. 4.2, the average pupil diameter from both eyes was used as the input. The results indicate a substantial accuracy rate of approximately 90% for both the deep learning and SVM models. These findings highlight a clear distinction between the decision and focus labels, with the high accuracy rates underscoring the effectiveness of both algorithms in accurately distinguishing between cognitive states during the task.

Table 4.2 provides a comparison of the classification accuracies achieved by the SVM and deep learning models. Overall, the deep learning approach exhibits superior performance, achieving a maximum accuracy of 95.83% with right-eye data. However, it is important to note that the classification accuracies for both SVM and deep learning models vary depending on the input data and individual participants. In certain cases, SVM outperforms deep learning, while in others, the reverse is true. These discrepancies are also influenced by the specific input used. Nevertheless, across all input types, the overall accuracy for both algorithms remains relatively similar.
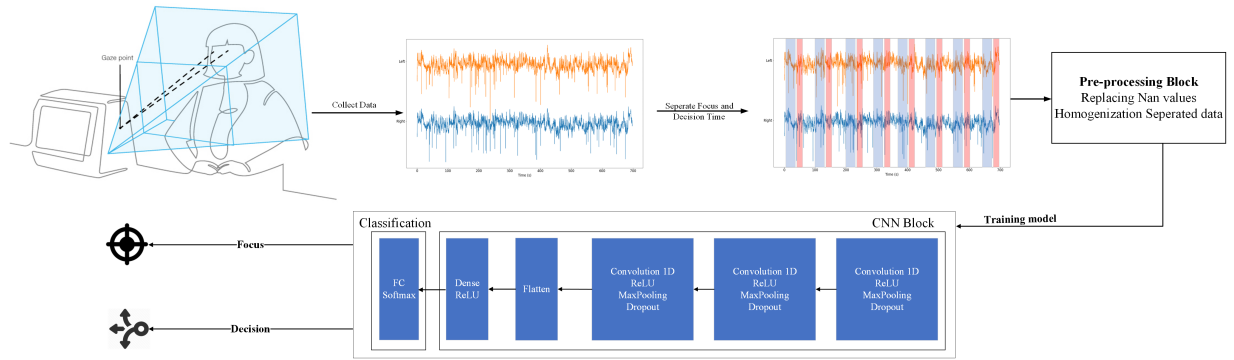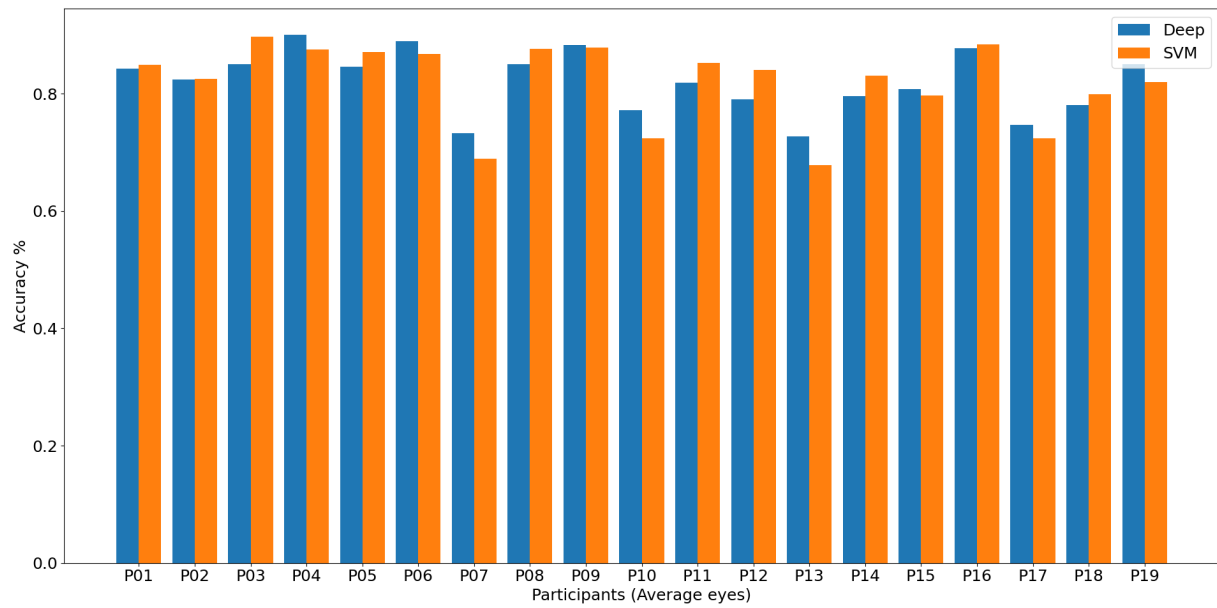
Figure 4.2: The comparison of SVM and CNN algorithm for participants using average of left and right eye pupil data [5].
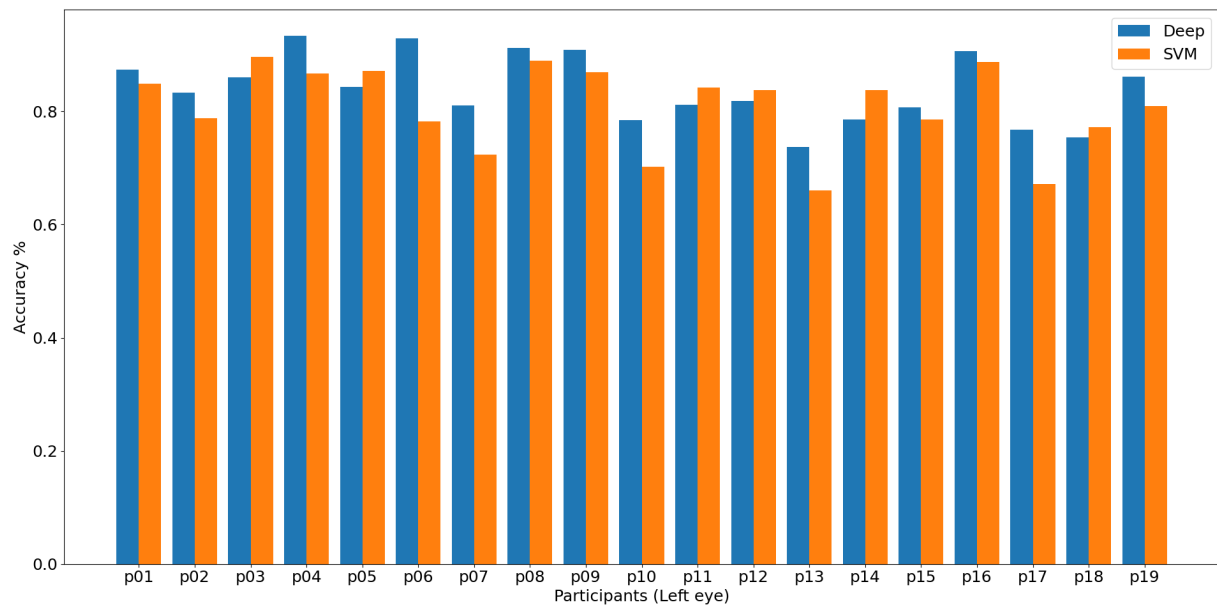
Figure 4.3: The comparison of SVM and CNN algorithm for participants using left eye pupil data [5].

Subsequent comparisons were performed using data from each round individually with the SVM model, as deep learning could not be utilized in some cases due to insufficient data for
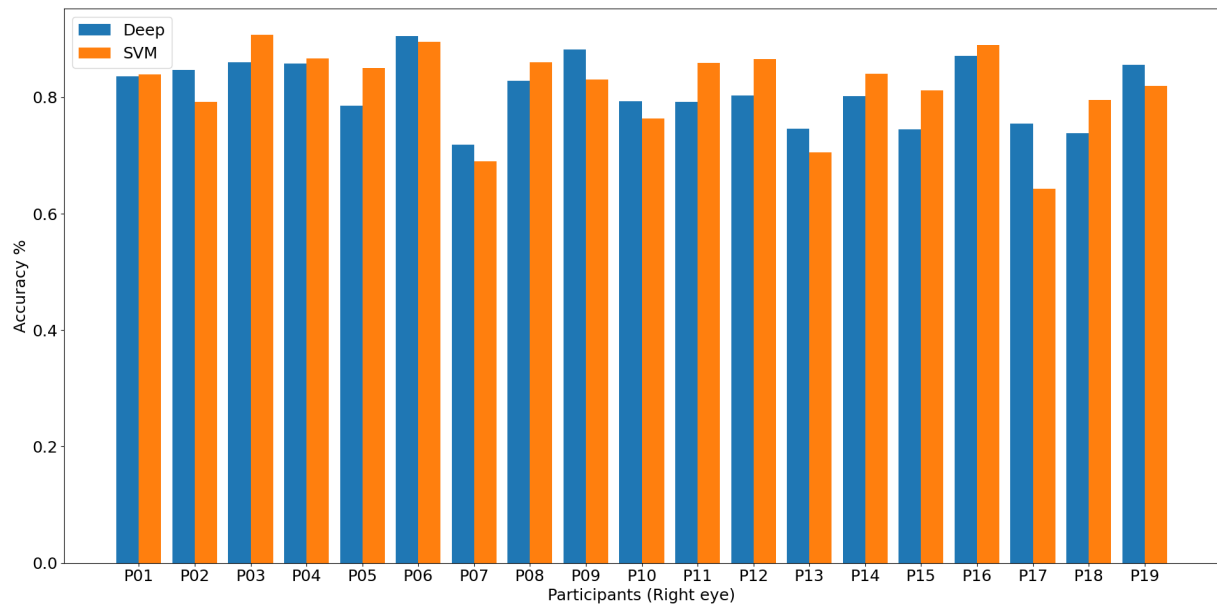
Figure 4.4: The comparison of SVM and CNN algorithm for participants using right eye pupil data [5].

Table 4.2: Deep Learning and SVM accuracy for each participants [5].

	Left			Right			Average		
	Max	Min	Average	Max	Min	Average	Max	Min	Average
DL	93.33%	73.66%	83.89%	95.83%	75.32%	84.24%	90%	72.76%	82.03%
SVM	89.68%	66.09%	80.75%	90.68%	65.62%	81.81%	89.71%	67.84%	82%

Table 4.3: SVM accuracy for each round [5].

	Left			Right			Average		
	Max	Min	Average	Max	Min	Average	Max	Min	Average
Round 1	91.61%	65.55%	79.56%	90.51%	54.22%	78.90%	96%	60.04%	78.97%
Round 2	89.64%	46.66%	73.71%	94.66%	47.50%	76.37%	91.21%	40.77%	75.91%
Round 3	90.24%	61.16%	77.83%	90.73%	65.38%	79.60%	90.75%	63.16%	78.85%

model training. Figure 4.5 shows the accuracy comparisons across different rounds using right-eye pupil data, while Fig. 4.6 displays the results for the left eye. Additionally, Fig. 4.7 presents the accuracies based on the average pupil data. A detailed comparison of the accuracies for each round is provided in Table 4.3.
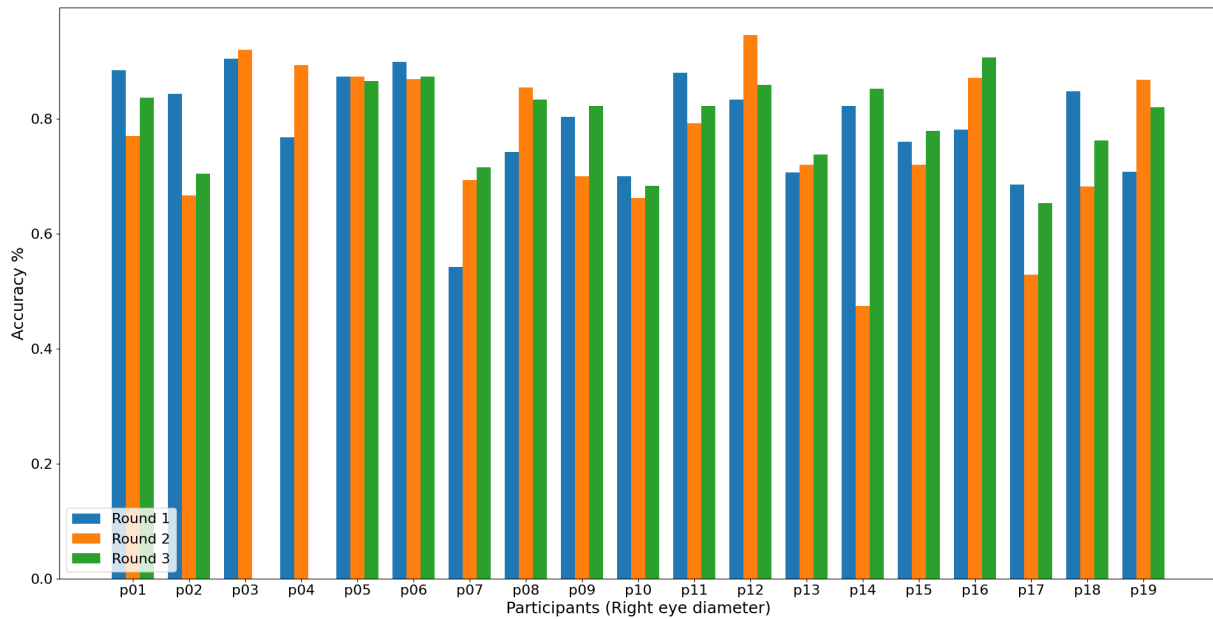
Figure 4.5: Right eye accuracy results using SVM for three rounds [5].

As previously noted, Rounds 1 and 2 are conducted on the same path, while Round 3 introduces a new, longer path. In some cases, participants exhibited lower accuracy in Round 2 compared to the other rounds. This could be attributed to reduced effort in decision-making due to increased familiarity with the path. Additionally, the consecutive execution of Rounds 1 and 2 may have induced fatigue among participants, potentially affecting their performance. Prolonged engagement in successive rounds likely led to both mental and physical exhaustion, which may have diminished their cognitive capacity and overall effectiveness in completing the task. It is also important to note that Participants 3 and 4 did not complete Round 3, resulting in missing data for these participants in the figures.

Although our proposed method directly utilizes raw data without feature extraction, Shannon
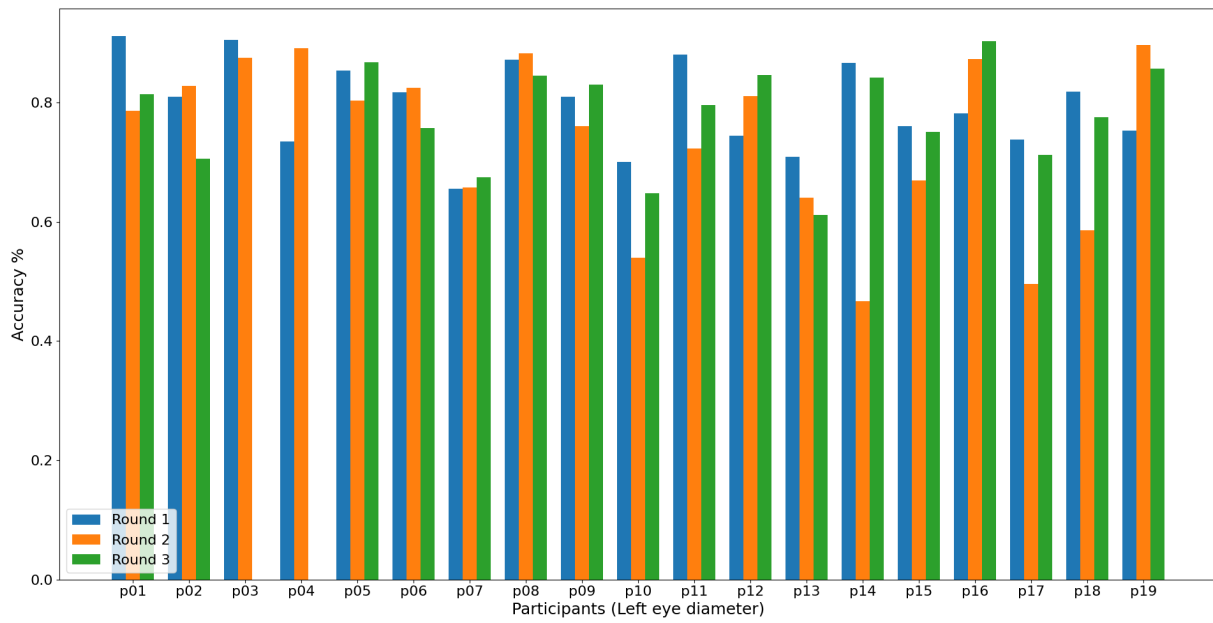
Figure 4.6: left eye accuracy results using SVM for three rounds [5].
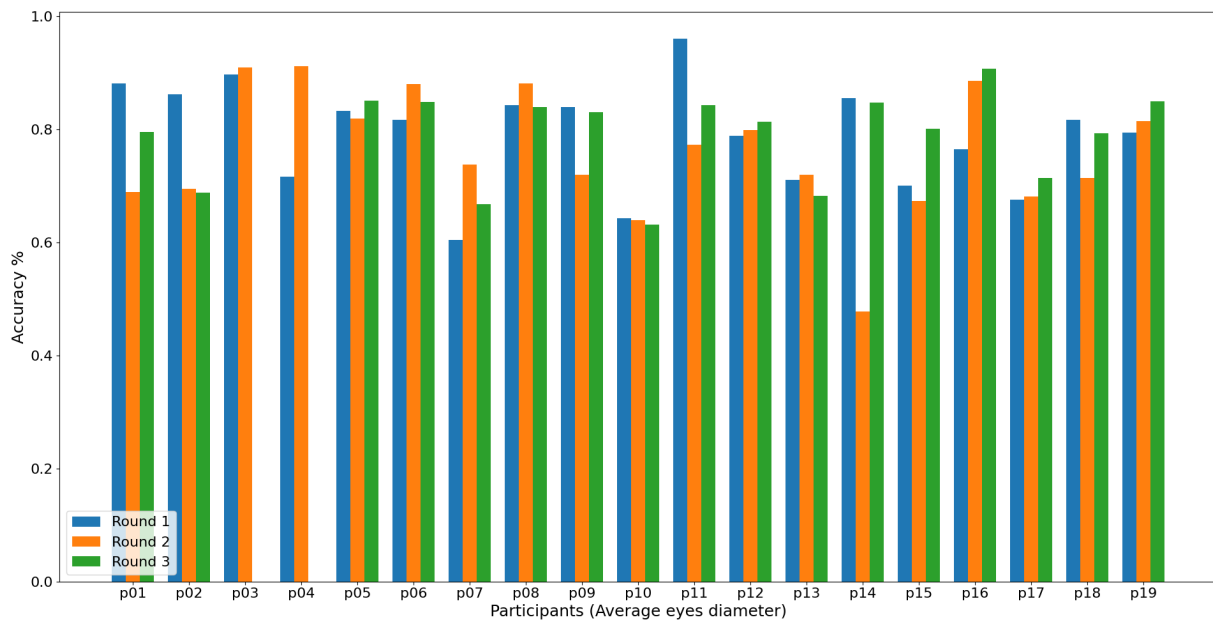
Figure 4.7: average of right and left eye pupil diameters accuracy result using SVM for three rounds [5].

entropy was employed for pupil dilation data in this study [112]. Table 4.4 presents the average

classification accuracies achieved by the SVM and Random Forest (RF) models, which were

applied to the features extracted using Shannon entropy from participants' pupil diameter data. These traditional classification models were used to assess the performance of our proposed approach. Remarkably, the deep learning-based method, which operates without explicit feature extraction, yielded higher classification accuracy. This finding suggests that utilizing raw data in conjunction with advanced neural network architectures can outperform conventional methods, providing more accurate and reliable results.

Table 4.4: Comparison of average accuracy between the traditional methods and proposed deep learning [5].

Classification Method	Feature	Left eye	Right eye	Average both eyes
SVM	Entropy	75.36%	73.38%	72.34%
RF	Entropy	79.51%	77.87%	76.89%
Proposed Deep Learning	-	**83.89%**	**84.24%**	**82.03%**

4.3.1 Discussion on Model Recommendation

The results indicate that both the SVM and the deep learning model achieve high classification accuracies, often exceeding 90% for individual participants and averaging over 82% overall. This demonstrates that both methods are effective at distinguishing between 'focus' and 'decision-making' states from pupil data. As shown in Table 4.4, the deep learning model, which operates directly on raw data, holds a performance advantage over traditional methods that require manual feature extraction, supporting the efficacy of its end-to-end, feature-agnostic approach. However, for a real-time assistive interface, accuracy is not the sole metric of performance; the practical feasibility of the model, particularly its prediction speed, is also critical. To address this, the average inference time for the deep learning model was measured. The inference time, which represents the latency required for the trained model to classify a new 1-second window of pupil

data, was found to be approximately 39.1 milliseconds. This rapid performance is well within the acceptable threshold for a real-time system, representing a latency that is imperceptible to the user and ensures a seamless and responsive interactive experience. While the SVM was implemented primarily as an offline benchmark for accuracy and was not optimized for real-time use, its function as a powerful baseline confirms the validity of the classification task. Based on this comprehensive evaluation of both accuracy and practical feasibility, the deep learning model is recommended for implementation in the assistive system. This recommendation is supported by three key points:

- Its superior accuracy when operating directly on raw data, as validated against feature-based methods.

- Its proven real-time performance, with an average inference time of under 40 milliseconds.

- Its end-to-end design, which makes it a more robust and scalable solution for a system that must generalize across diverse users.

Its end-to-end design, which makes it a more robust and scalable solution for a system that must generalize across diverse users.

4.4 Summary

This chapter detailed the methodological approach to classifying user cognitive states from pupil diameter data. The process involved the pre-processing of the dataset collected in the previous experiment, followed by the implementation and systematic comparison of two distinct classification strategies: a SVM and a deep learning model. The selection of these methods was deliberate, with the deep learning approach investigated for its end-to-end, feature-agnostic capabilities, and the SVM serving as a powerful, traditional benchmark to validate the classification task.

The results of the comparative analysis were highly successful. Both the SVM and the deep learning model demonstrated a strong ability to distinguish between 'decision-making' and 'focus' events, with classification accuracies for individual participants frequently exceeding 90%. Furthermore, the deep learning model's feature-agnostic approach was validated as superior to traditional methods that require manual feature extraction. The model's real-time feasibility was also discussed, confirming its suitability for a responsive user interface.

In conclusion, the key contribution of this chapter is the successful development and validation of a machine learning model that can robustly classify user intent from real-time pupil dilation data. This work provides an adaptive alternative to the static dwell-time methods common in the literature. The resulting trained model is not merely a theoretical outcome but the core functional component of the adaptive interface. Therefore, the next chapter will detail the implementation of this model in the GUI used for wheelchair control, where its practical performance will be evaluated in a real-world wheelchair navigation task.

Chapter 5

Wheelchair Controller: Design and Experiment

An electric wheelchair was bought for the purposes of this project so testing of the interface could be conducted in a more realistic and practical scenario. A picture of the wheelchair is included in Fig. 5.1.

The wheelchair has been equipped with anti-slip foot rest, seatbelt, horn, and control joystick with speed control setting. It has two motors controlling the two rear wheels independently, with two passive front wheels. It also has a neutral mode, which disengages the motors to allow the wheelchair to be pushed by another person.

This chapter outlines the rationale and motivation behind the design of the wheelchair control system, which includes a mechanical joystick actuation mechanism and a gaze-controlled GUI. It begins with an extensive description of the controller architecture, then describes the GUI used to operate the controller. GUI additions and adaptive features—namely those that represent an enhancement from the current TurtleBot navigation interface—are included as well. The chapter concludes with a discussion of the experimental setup and a showing of the results obtained.

Figure 5.1: The wheelchair used for this project(image from [6]).

5.0.1   Objective and Importance

Wheelchairs are the most common assistive mobility devices. Wheelchairs come in various types and may be personalized or configurable to individual user needs. Many wheelchairs are manufactured with individualized settings and may be equipped with additional devices such as ventilators or drug pumps. Therefore, wheelchairs most often are the initial mobility assistive device accepted by users with mobility impairments, and in cases of extreme disability, they may be the only viable mobility option. Apart from the fact that they are functional, wheelchairs also have an important function in increasing the independence of a user, and this can have a positive impact on their mental health.

However, for users with severe upper-limb impairments who cannot operate a standard joystick, advanced hands-free control remains a significant challenge. This chapter details the critical transition of this research from a low-fidelity prototype to a high-fidelity, real-world assistive system. To achieve this, the work presented in this chapter pursues three key scientific objectives:

1. To design and validate a novel, low-cost, and non-invasive robotic controller using 3D-printable components, providing an accessible hardware solution that addresses the high cost and complexity of existing systems.

2. To implement and evaluate the adaptive, intention-based control model developed in Chapter 4 in a real-world, dynamic navigation task. This serves as the first high-fidelity validation of the model's practical utility.

3. To empirically compare the performance and usability of the adaptive interface against a traditional fixed dwell-time system, in order to quantify the benefits of the novel approach in a more demanding and realistic assistive context.

Collectively, the significance of this chapter lies in its role as the central validation of the thesis. It demonstrates the successful integration of the core software and hardware contributions into a functional prototype and provides the empirical evidence for its superiority over conventional methods.

5.1 The controller Mechanism's design process

To control the wheelchair's movements, a mechanism has been designed to physically move the joystick. Since the joystick operates on a two-axis system, the mechanism must be capable of accommodating both axes of movement. Initially, the plan was to use two servos to manage the required motions and develop a mechanism that could accurately move the joystick in response

to these inputs. The first iteration of this design was outsourced to a mechanical designer. The initial outsourced design can be seen in Fig. 5.2.
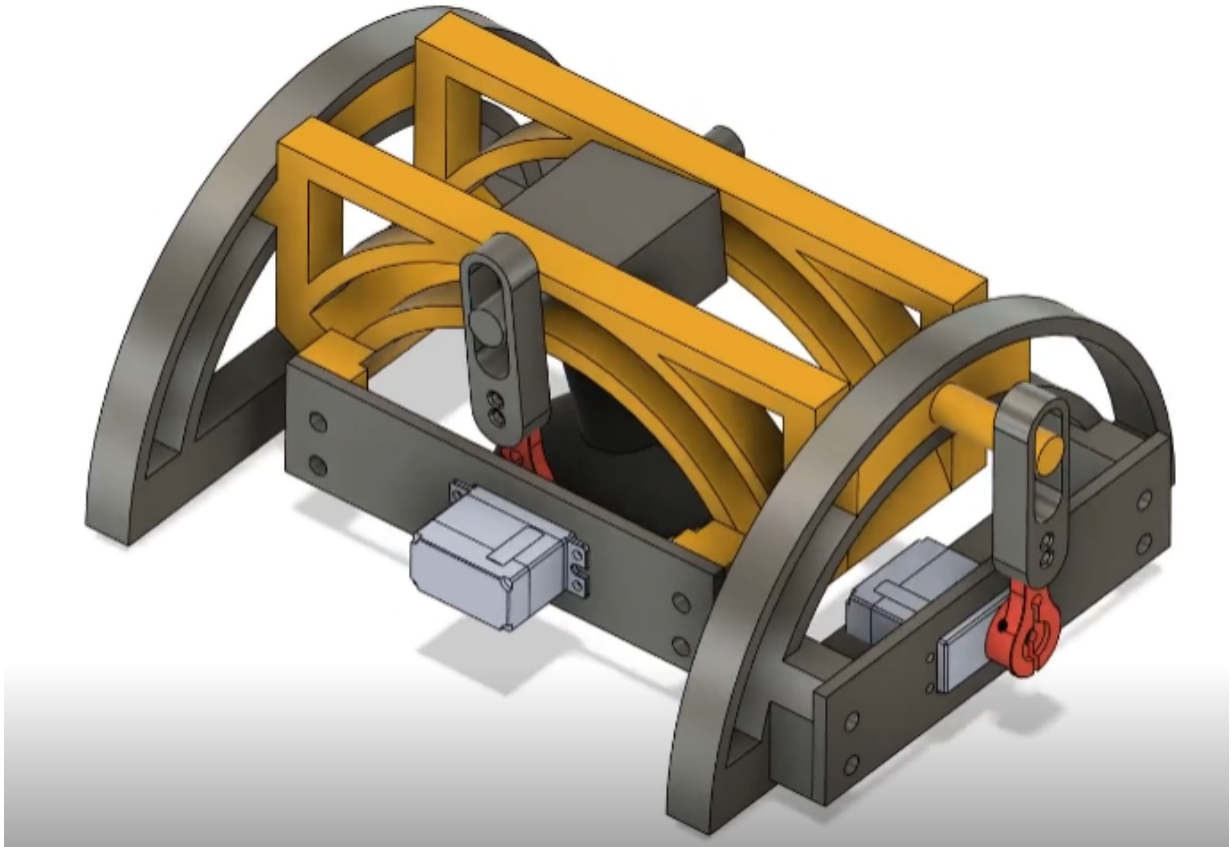
Figure 5.2: The first mechanism (outsourced design) to control the wheelchair's joystick.

This version of the design, however, did not align with the first idea and had several issues, so there was a need to come up with a superior design. The design was bulky and could not be mounted on the joystick in a suitable way. It was unstable, moving freely rather than attached to the framework of the controller. Furthermore, it lacked proper grip and stable control over the joystick. In addition, the tolerance between the inner components and the rails of the mechanism was too small, such that it sometimes got stuck in operation. The internal components were also heavier than they would have been and a single servo would not be able to move them properly, especially given the tight tolerances. Furthermore, the 3D printed components were not as smooth as their simulation CAD counterparts, and that made the mechanism behave differently

in real life compared to what was expected.

To address the issues highlighted in the last version and move closer to the original idea, the following version of the mechanism was developed. It focused on functionality and usability. One of its key strengths is that it is extremely universal and flexible, considering the similarities in wheelchair joysticks from different models. The system is made in such a way that it needs only slight changes when transferred to another wheelchair so that the joystick fits correctly with minimal modification and mainly to the base which is housing the entire joystick.

The parts related to the first working version can be seen in Fig. 5.3. This base design did not fully enclose the joystick controller and needed to be secured properly to avoid unwanted movements.
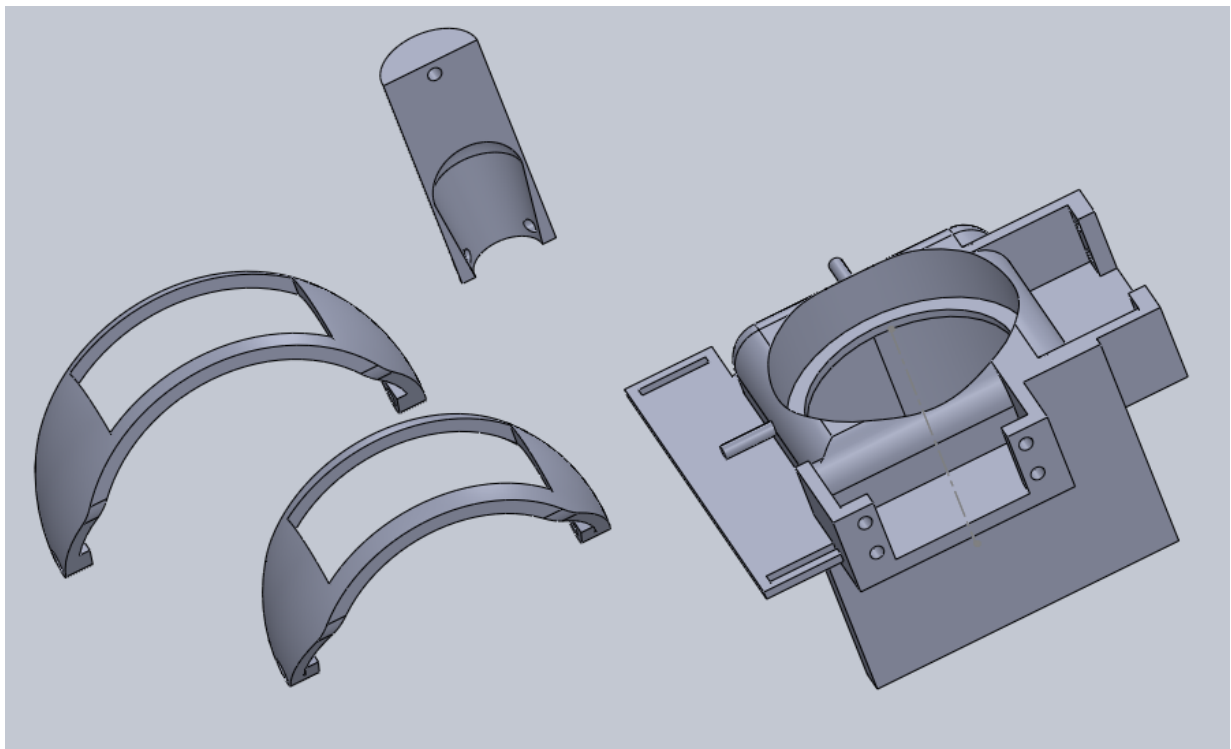
Figure 5.3: The first working version of the parts designed for the mechanism.

This mechanism consists of two servo motors, and each motor is attached to a curved link. The two links are manufactured as parts of spherical curves, therefore they are able to slide over

each other without collision. One link has a smaller curve radius, and the other one has a larger one. In order to have smooth movement and prevent resistance between the links, there is a gap of 4 mm between them. This design enables the links to travel freely without friction.

Each link is connected to a servo motor at one end, which is securely held to the base by four bolts and screws. The other end of the link runs through a support cylinder to keep the links stable. The base supports the motor weight and the entire mechanism, and it is bolted around the joystick controller. A circular opening at the center of the structure is where the joystick is mounted. To ensure stability in the structure and smooth movement, the design offers a small tolerance around the joystick controller to fit closely. Additionally, holes at the bottom allow it to be securely attached on the controller using zip ties and Velcro to also offer stability.

There is extender attached on the joystick to increase the height. This will allow the joystick to completely sit inside the links and also improves the accuracy with straightening the joystick's own curvy design. The extender can be seen in Fig. 5.4.

The joystick of the wheelchair is designed to be in the neutral position by default and once the pressure is lifted it will go back to the neutral position. Therefore, it is important to have good grip over the joystick so it doesn't slide back into the place or move in other directions.

In order to do this, a rectangular space is constructed in the middle of the links to house the joystick. This enables the joystick to be shoved by one of the servos through the window in the other link. By use of the window, the joystick is safely held in place so it doesn't drift over to the incorrect side.

For example, a servo will move the joystick forward, and the joystick will pass through the link's slot that deals with left-right movements. That servo, in this case, is immovable, so the joystick is only able to move forward. It is in a small slit, not allowing any other unwanted movement. This makes the movements of the wheelchair precise and accurate.

The joystick in the wheelchair is highly sensitive and can be controlled in various directions. For instance, if it is leaned to the right and left sides while pushing the wheelchair forward, it will
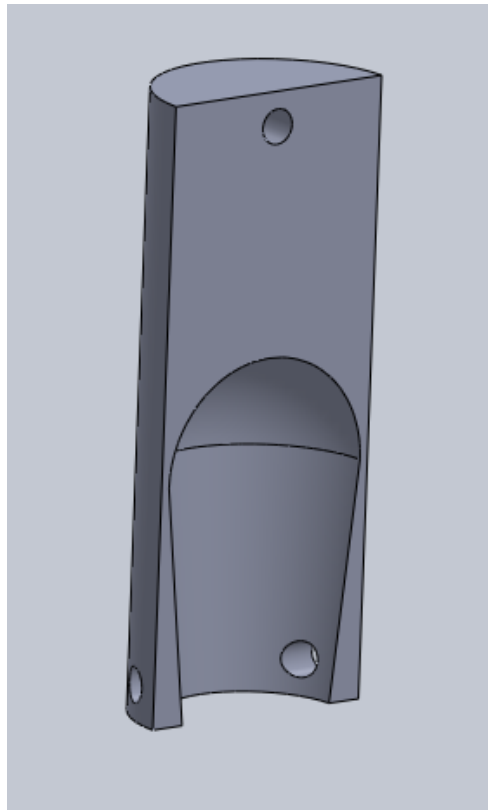
Figure 5.4: The half part of the joystick height extender. Two parts of the extender will be secured to the joystick via zip-ties.

steer the vehicle off course. Therefore, it is crucial to ensure that the joystick is maintained spot-on forward so that it maintains a straight line. This is where the link gap design comes in handy. These gaps help to maintain the joystick in direction, without any unwanted side movement and with the wheelchair traveling smoothly and directly in the wanted direction.

The base of the mechanism has been particularly designed to fit around the joystick in a manner that will provide precisely the movement desired with each movement. Any unnecessary movement or play within the mechanism would result in inaccuracies in the movement, affecting the overall function. The first base design was created to fully encase the joystick, curving around the only front part of the controller in a tight, controlled grip which needed to be secured using zipties and velcro.

Following testing of the first model of the mechanism on the wheelchair in actual conditions,

it was evident that the design needed to be improved in some ways. In the second model, the base covers the whole controller, unlike the front part in the first design. This modification provides a more stable and firmer fit, which improves the operation. As can be seen in Fig. 5.5, the new base design also includes a specially designed slot for the charging port of the wheelchair such that the device can be charged without the need to remove the robotic controller.

The new design also includes several entries for velcro straps, which ensure a more secure attachment of the mechanism to the joystick controller. These also serve as places for keeping the electronic board and battery pack in place securely, maintaining ease of access. The bottom has been specifically designed to hold controls such as the speed control, horn, and battery charge indicator in a way that they are easily accessible and functional even when the mechanism is in place. These thoughtful changes are to enhance the whole usability and practicality of the system for users.

In the redesigned layout, the servos' placement bracket has also been increased to fit the entire size of the joystick. This ensures that clearance so the links can be moved to their full range of motion without interfering. The servo position has also been reversed in this design to improve durability and safety.

One of the servos were also previously placed on the exterior of the wheelchair, where they were subject to damage. The placement on the exterior placed the servos in danger of damage, especially when transitioning through tight spaces or doorways where the servos might be struck. The outer placement also left the servos unprotected in case of an impact.

To resolve these issues, that servo is now positioned on the interior of the wheelchair so that they are better shielded from outer forces. The supporting cylinder has been shifted to the outside of the system in place of the servos. To further shield the system, the servo mounting bracket has been retained, acting to shield both the support cylinder as well as the link in the event that the system strikes an object. This change enhances the overall strength of the mechanism and reduces the vulnerability to damage caused by external shocks.
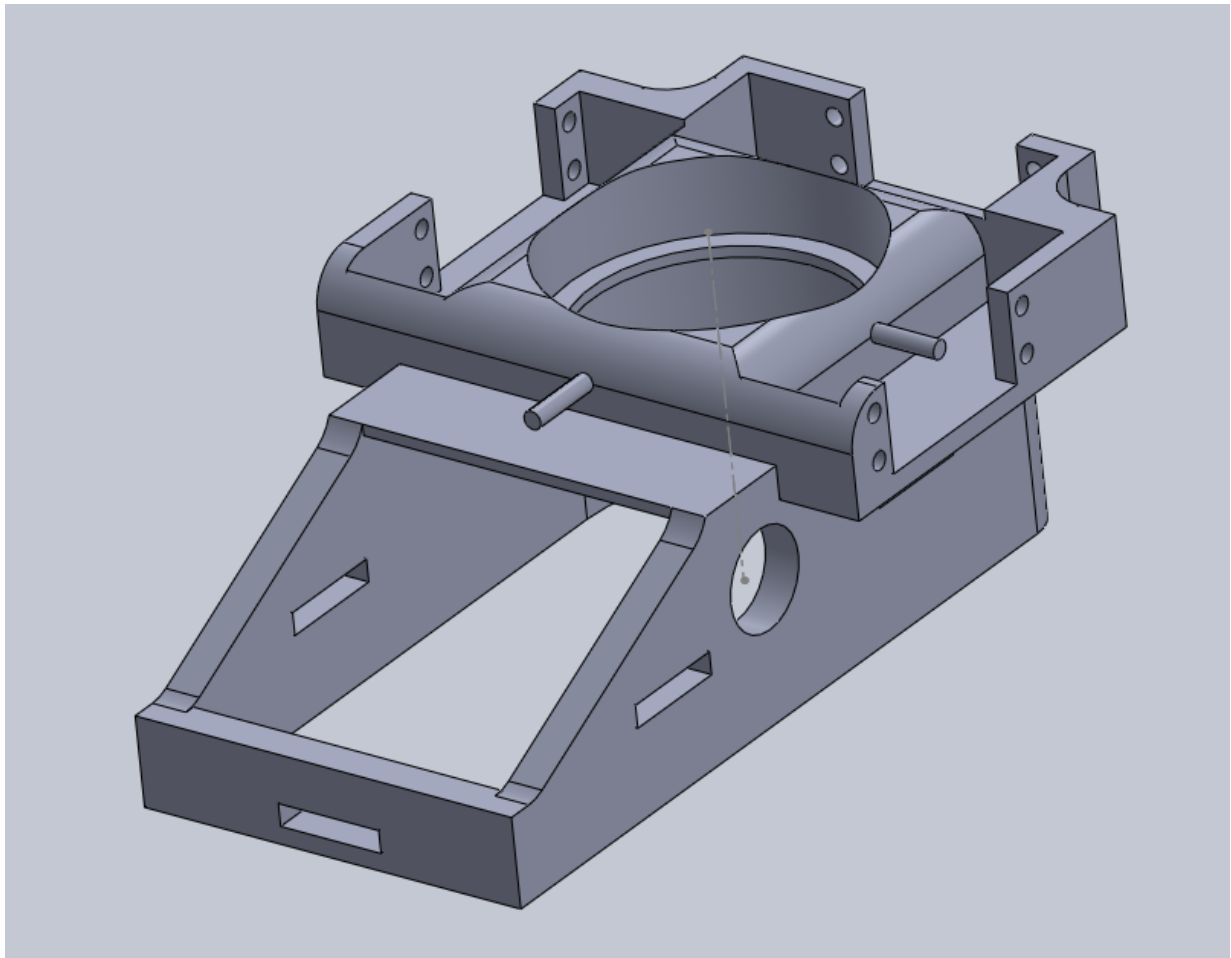
Figure 5.5: The improved base design which will contain the controller totally.

The new design includes new links, which can be viewed in Fig. 5.6. The new links were redesigned carefully to accommodate a round servo horn to be held firmly in place using four screws for a secure fit. This is to ensure the servos' movement is efficiently transferred to the links, providing smooth and precise movement.

The opening of the link has also been enlarged to allow for greater space for movement and to enable the joystick to be pressed to its full range of motion without limitation. This adjustment improves the overall functionality of the mechanism, as long as the joystick can travel smoothly and with precision in any direction. These adjustments create a more efficient and effective system, allowing the control of the wheelchair's movements to be made more effectively.
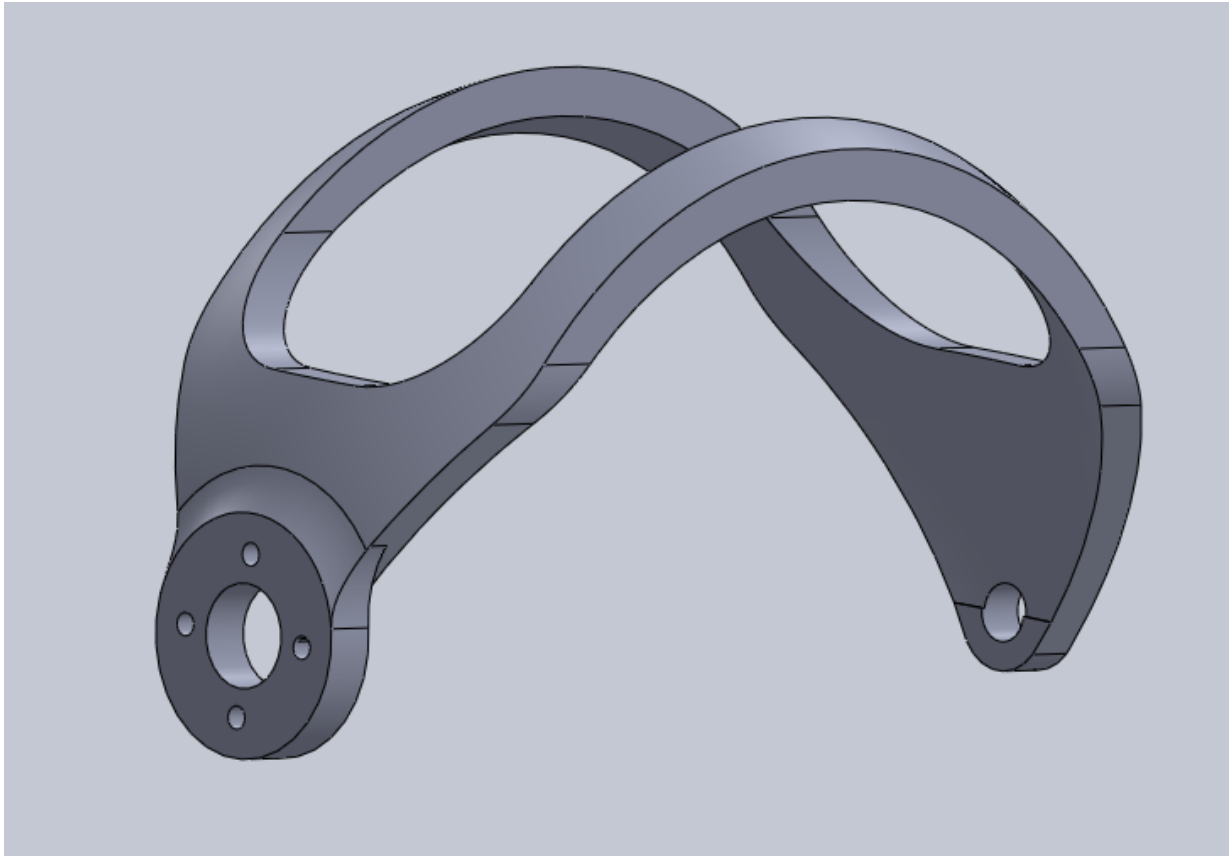
Figure 5.6: The improved version of the inner link for the mechanism.

Figure 5.7 provides a detailed view of the mechanism, showing different perspectives of the assembly, including the integrated electronics. The specifics of the electronic board and the program used to control the system are explained in the next section.

The design is structured in such a way that everything is housed within the base of the joystick controller, allowing for easy disassembly. By simply removing the base and removing the extender, the wheelchair can be returned to its standard configuration, ready for use with the standard joystick controller. Additionally, while the robotic mechanism is turned off, the servos can be back-drivable, eliminating the constant need to dismount the design.

Conversely, by reversing the parts and reattaching them, the wheelchair can be converted back to being a gaze-controlled version, offering a choice of hands-free control. This module-based system encourages flexibility and convenience because the user can switch between different

forms of control depending on what is needed.
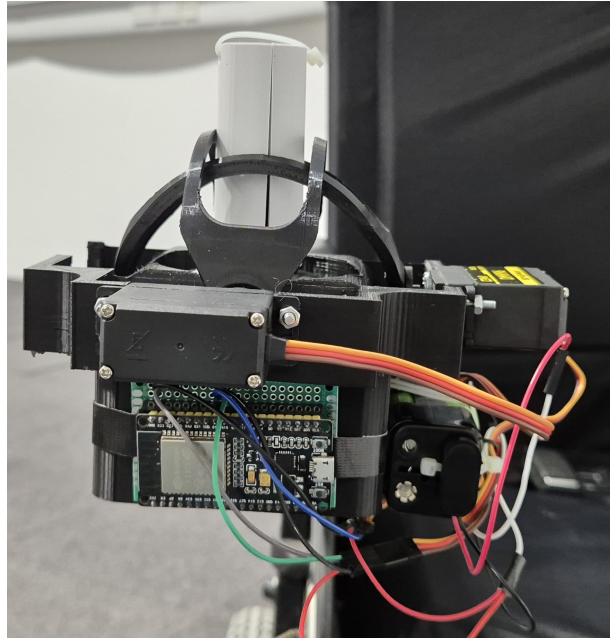
(a) The front view of the robotic controller with the ESP32 board attached.
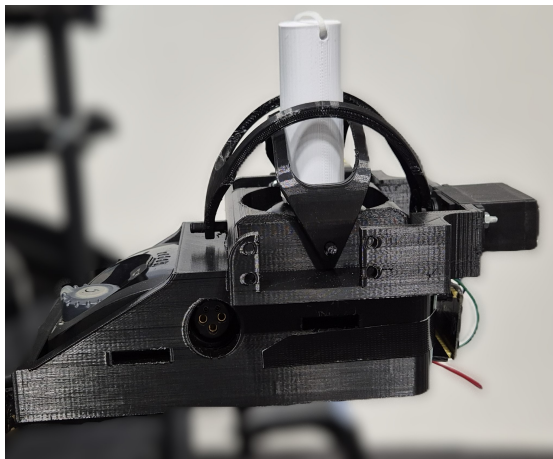
(b) The outer side view of the robotic controller showing the charging port.
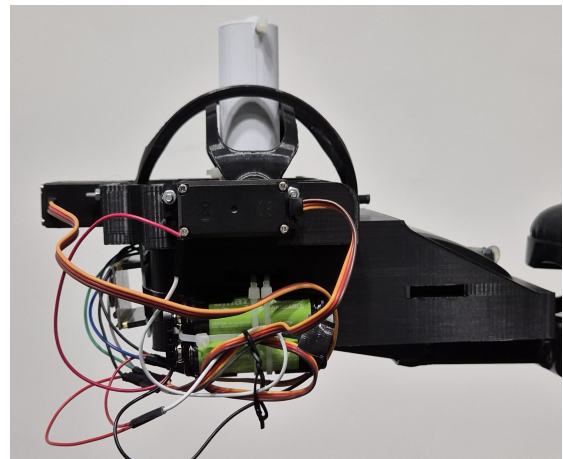
(c) The inner side of the robotic controller with the batteries attached.

Figure 5.7: The different views of the robotic controller.

5.1.1   Electronics of the controller

This robot controller utilizes two servo motors, each capable of revolving 180 degrees, thus allowing precise movement in joystick control. The operation voltage of these servos ranges between 4.8 V and 7.2 V, as specified in the maker's guide [113]. There are three wires in each servo: the red wire to power it, the brown wire for grounding, and the orange wire for the control data that drives the servos to respond to the commands of the control system.

The operation is controlled by an ESP32 board, which controls the two servo motors and facilitates communication with the computer or interface. The ESP32 board is highly versatile with onboard Wi-Fi and Bluetooth capability, making it ideal for wireless communication [114, 115]. It operates in a voltage range of 3 to 3.6 V.

In addition to its wireless feature, the ESP32 also offers various input/output functions, including a number of General-Purpose Input/Output (GPIO) pins and Pulse Width Modulation (PWM) pins, which are required in order to control the servos and other parts in the system.

Figure 5.8 illustrates the circuit design used in the robotic controller. In this circuit, the two servo motors are attached to pin GPIO 18 and 19 of the ESP32 board, which are utilized for the mobility of the joystick mechanism. The powering of the servos is achieved using a 6V battery pack, made up of four AA batteries, which gives the motor sufficient power for effective performance.

The board itself is powered through the micro USB port. The system communicates commands from the main PC or interface to it through Bluetooth, utilizing the onboard Bluetooth feature of the ESP32. This eliminates the use of additional modules or external wiring and simplifies the design and reduces the overall complexity of the setup. This also makes the robotic controller a stand-alone device that can be integrated with other interfaces, beyond the proposed GUI used in this study.

The Arduino Integrated Development Environment (IDE) has been used to program the ESP32 board. In the IDE, one must select the correct board type as "ESP32 Wrover Kit (all
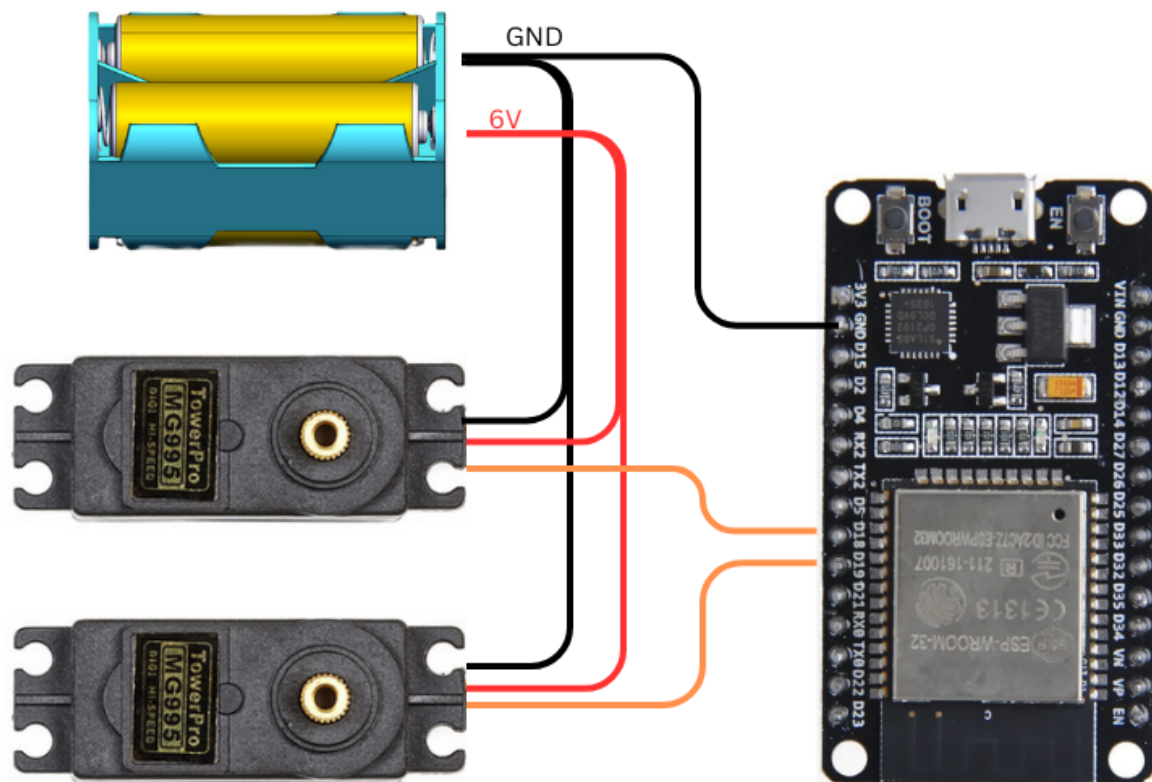
Figure 5.8: The circuit diagram of the electronic board used in the wheelchair mechanism.

versions)" so that it compiles and uploads properly into the board. The actual coding is written using the Arduino programming language, a simplified version of C++ which is optimized specifically for use on Arduino boards and other embedded platforms. This enables simple writing, compiling, and uploading the code onto the board, providing a straightforward development process for the robotic controller's operation.

The servo motors are received a certain degree of movement as an input and move to that position accordingly. The motors turn between 0 and 180 degrees. All the servo motors have a neutral position at 90 degrees, which is their starting or default position. For accurate correct and precise motion, the limitation for each motor is set in a way that it pushes the joystick to its limit so that it would place the joystick in its optimal point. It facilitates the joystick being operated

completely in the desired motion range so that it could be controlled optimally.

Every position of the mechanism is addressed by a specific letter, which is transmitted from the interface to the system. The program employs a switch/case mechanism to establish the correct degrees for each servo motor based on the received letter. Upon receiving a new command, the servos will go to the corresponding position and stay there for a brief period of two seconds. Next, following this time interval, the servos will go back to a neutral position where they are ready for the next instruction.

The pseudocode of the ESP32 program is provided below in Algorithm 4. In this implementation, specific letters are assigned to represent different movement directions. These letter-based commands are used to control the mechanism and correspond directly to the directional inputs illustrated in Fig. 5.12. Different positions of the mechanism along with their corresponding commands are illustrated in Fig. 5.9.

The controller board can receive commands from two places: the serial port on the PC when connected by USB, or via Bluetooth. With wireless communication, the interface uses Bluetooth. The system also offers the capability of operating the wheelchair through a smartphone. At present, the wheelchair may be operated through an Android application called "Serial Bluetooth Terminal." The smartphone and ESP32 board are paired with each other, and by sending specific command letters, the direction of the wheelchair can be controlled.

As a future work, an in-house mobile application can be designed to provide a more customized experience. There are also a number of other potential optimizations and features that can be implemented in this system, which will be discussed later in Section 8.2.2.

5.1.2 Other Mounted Components

The whole wheelchair setup is given in Fig. 5.10. Setup includes an adjustable laptop arm which has been well secured on the wheelchair, both for the laptop and the eye tracker. Mounting device was secured with utmost care using some of the mounting hardware provided with it, some zip

---

Algorithm 4: ESP32 Bluetooth Servo Controller Pseudocode

```
 1  Function setup:
 2      Initialize device_name = "ESP32-Servo-Controller";
 3      Create BluetoothSerial SerialBT;
 4      Initialize servo1, servo2 on pins 18, 19;
 5      Define movement angles: Forward = 55, Backward = 120, Right = 60, Left = 120;
 6      servo1.write(90), servo2.write(90);

 7  Function loop:
 8      currentMillis = millis();
 9      if Bluetooth data or Serial data is available then
10          if Bluetooth data available then
11              inputChar = Read Bluetooth from SerialBT;

12          switch inputChar do
13              case N do
14                  servo1.write(90), servo2.write(90);

15              case B do
16                  servo2.write(90), servo1.write(Backward);

17              case F do
18                  servo2.write(90), servo1.write(Forward);

19              case L do
20                  servo1.write(90), servo2.write(Left);

21              case R do
22                  servo1.write(90), servo2.write(Right);

23              case E do
24                  servo1.write(Forward), servo2.write(Right);

25              case W do
26                  servo1.write(Forward), servo2.write(Left);

27              case A do
28                  servo1.write(Backward), servo2.write(Left);

29              case Z do
30                  servo1.write(Backward), servo2.write(Right);

31          lastCommandTime = currentMillis;

32      if (currentMillis - lastCommandTime) > BT_TIMEOUT then
33          servo1.write(90), servo2.write(90);
34          lastCommandTime = 0;
35          Print "Bluetooth timeout. Move to Neutral position";
```

(a) Front Left (W)   (b) Forward (F)   (c) Front Right (E)

(d) Left (L)   (e) Neutral Position (N)   (f) Right (R)

(g) Back Left (A)   (h) Backward (B)   (i) Back Right (Z)
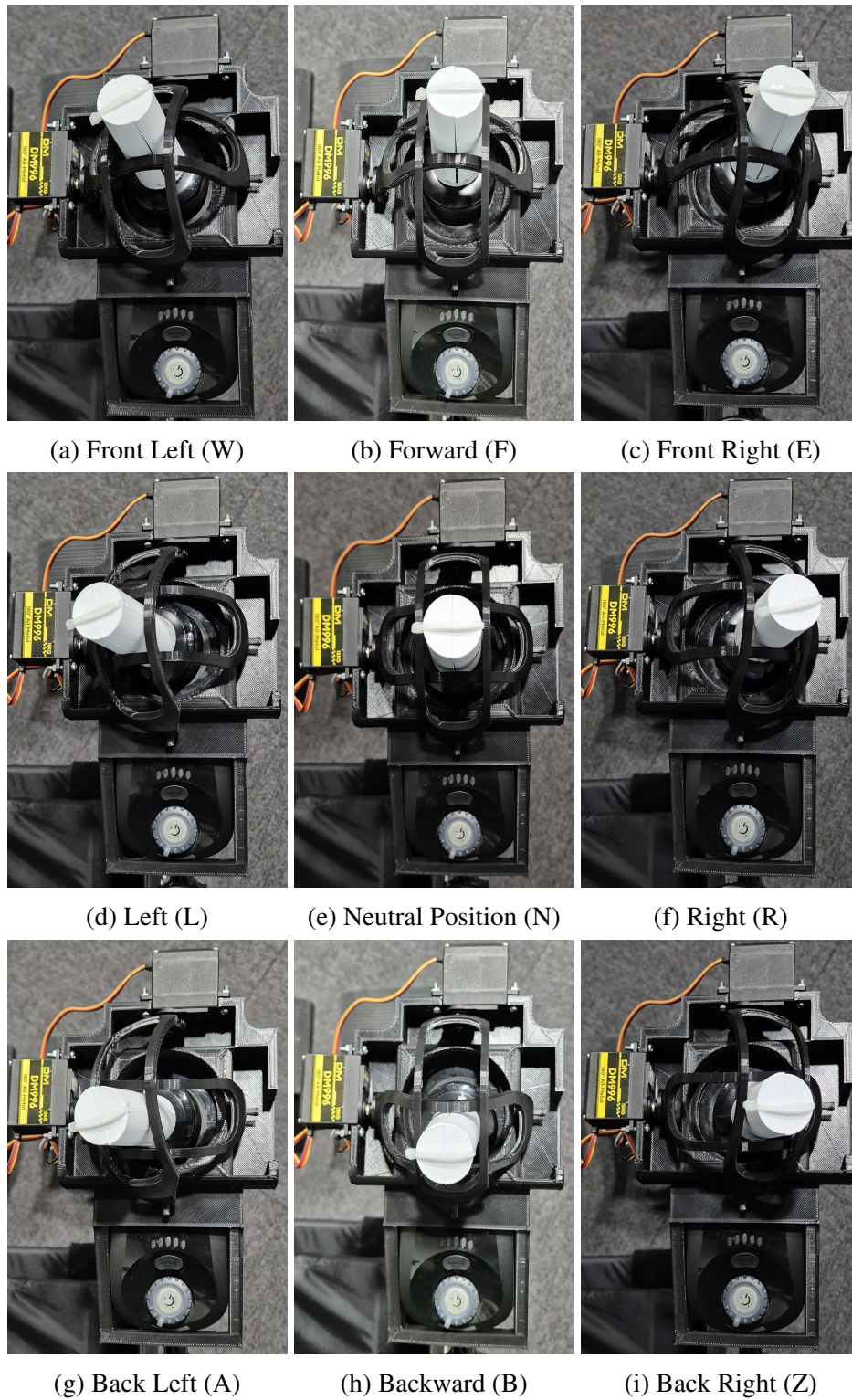
Figure 5.9: Different positions of the mechanism alongside the corresponding button labels and issued commands.

ties, and velcro to ensure it does not get dislodged. The laptop is itself rigidly fixed onto the mounting arm via velcro straps, preventing any movement of the laptop while being used. The laptop stand can be completely adjusted, and the joints are fixed into place via Allen screws to enable the device to be customized to individual settings and for ensuring that the unit stays safe and functional in use.

The camera is also positioned on an extendable monopod, which is secured tightly at the top of the wheelchair. This guarantees that the camera presents a clear and unobstructed view of the environment of the user, allowing them to move around and observe their surroundings without tilting their head. This feature is most vital as placing the laptop in front of the user would else restrict their view.

The placement of the camera can be adjusted according to the user's preferences to ensure the best possible viewing experience. The second position is positioning the camera above the back of the laptop support. This setup's placement enables a better view of the front section of the wheelchair so that the user can look straight ahead. However, it offers a closer look, capturing the close-up shot without the rest of the space. On the other hand, mounting the camera on the extendable monopod offers a broader view, offering the user a broader image of the surrounding. Lastly, the choice between these placements is a matter of personal preference and discretion of the user. User height is a critical factor in determining the choice because it may have an influence on their Point Of View (POV). Depending on where they want to look, the user will have to choose the best height for the camera and the laptop stand so that they can enjoy the most comfortable and productive view angle.

Figure 5.11 illustrates the user's perspective from the system sitting in the wheelchair. The photo presents an unobstructed view of the laptop, eye-tracker, and mounting plate, supported firmly below the laptop screen by velcro. The On/Off button is conspicuous, both as a power switch and as an emergency stop button, so the user can quickly turn off the system if needed.

On the switch's right side is a knob for speed control, where one can vary the speed of the

Figure 5.10: The image showing the wheelchair with mounted robotic controller, the laptop mount, laptop and camera.

wheelchair. There is a gradient on the knob with the left end representing the slowest and the right representing the fastest. This gradual control allows for fine-tuned adjustments based on the user's preference and needs.

Along the left side of the wheelchair is a pole, which also serves as the support for the adjustable laptop mount. The height of this pole can be adjusted to offer more adjustment to set up the laptop and other equipment properly for the user. Last, the robotic controller, another element of the integrated system, appears in the image as well to complete the gear for the wheelchair.
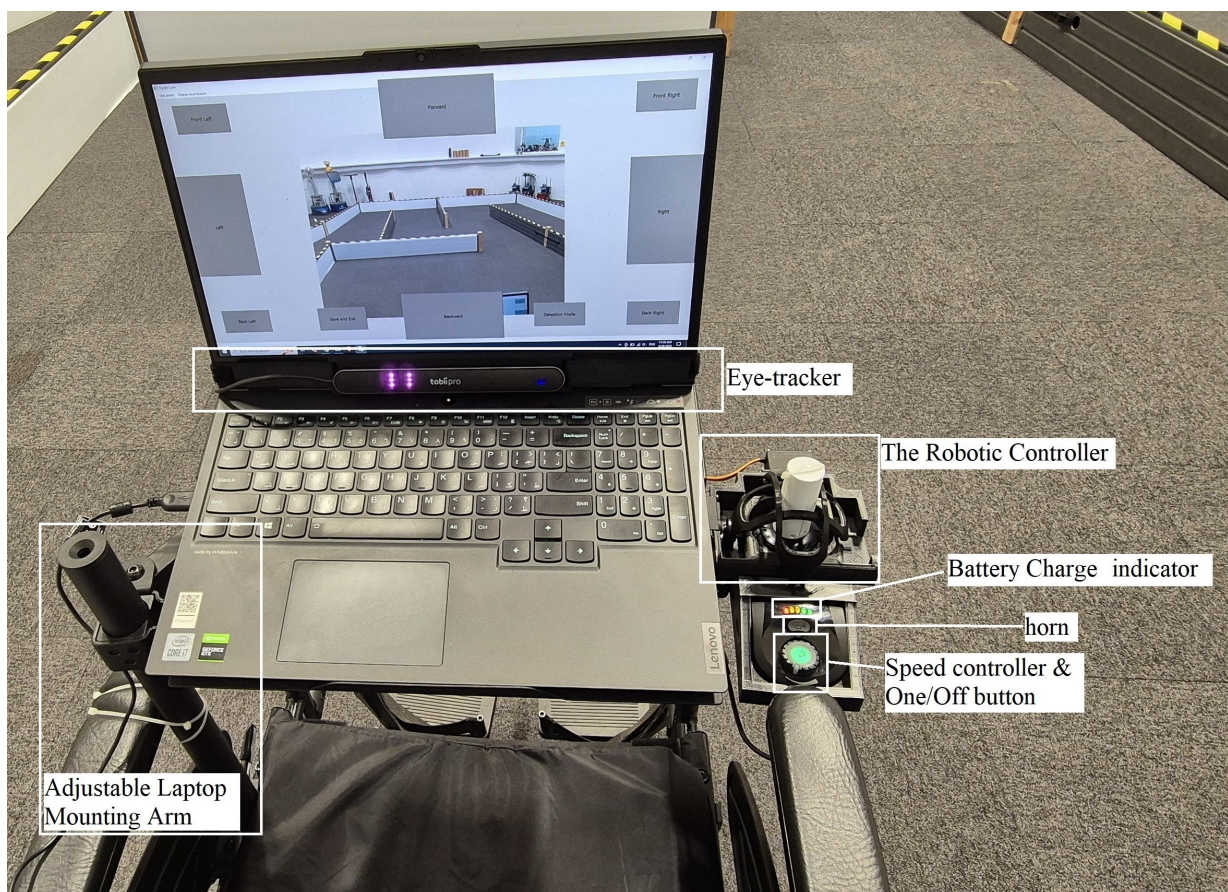
Figure 5.11: The image showing the wheelchair joystick controller such as the horn button, wheelchair's battery charge indicator, wheelchair One/Off button, the speed controller knob. The eyetracker and it's mounting bracket, the interface and the laptop mount is visible in the image.

To prevent damage to the laptop by the eye-trackers mounting plate, a removable mounting

place has been designed which can be installed on any laptop and will be tighten using velcro. This would make it easier to switch to a different laptop if needed. additionally as there is not enough gap for the mounting magnet between the laptop sides once closed,on the laptop that is currently in use, it will damage the laptop if installed on it's own.

In line with the user's safety and security as well as the equipment, we recommend users to begin by moving any adjustable items at the back of them so that they may be in a comfortable position while seated in the wheelchair. When seated, users should also tie their seatbelt to prevent being ejected from the chair when moving. Next, the laptop needs to be aligned according to the user's position and preference so that it is in the most ideal position for reading from the eye tracker and, at the same time, comfortable. After adjusting the laptop to a position of one's desire, the screws of the laptop mount need to be tightened so that it does not move around while operating the wheelchair. To enable easy maneuverability, the controller of the wheelchair should be at an extended angle and not placed parallel to the wheelchair. This allows easy movement through constricted spaces. The users will also be trained to place a hand on the emergency stop button so that they can easily perform an emergency stop in case it becomes necessary.

5.2 Wheelchair Navigation GUI

This new interface has been thoroughly re-engineered and tuned to the specific requirements of wheelchair control, plus experiential knowledge learned from previous experiments—such as feedback from the Turtlebot trial and the author's own extensive use of the system. Several key improvements have been made as a consequence of these insights. Of particular note, the interface now generates faster command responses to enable smoother and more seamless movement. There are additional directional buttons to support additional motions, existing buttons have been made larger for increased accessibility, and Bluetooth connectivity has been incorporated to enhance wireless communication with the wheelchair. This part begins with summarizing modi-

fications in the front-end interface, stressing usability enhancement and visual improvements. Secondly, the background examines the technical basis of the interface, explaining how the system runs behind the scenes to enable proper and efficient management.

The wheelchair joystick is naturally meant to provide natural and smooth direction control of 360 degrees and proportional speed control. For the sake of keeping this natural movement imitated by the joystick, this update includes the basic direction controls—Forward, Backward, Left, and Right—and adds four additional diagonal directions of Front-Right, Front-Left, Back-Right, and Back-Left. These new directions provide a less obvious and more flexible means of control, enabling the wheelchair to perform smoother curved motions rather than stiff mechanical turns. For example, instead of moving straight ahead and then turning right at once, the user can now simply press the Front-Right button to experience a smooth curved motion. This is particularly useful in tight or complex environments where precise navigation is essential. By adding these extra directions, the system not only improves maneuverability, but it also brings the control experience closer to that of an old-fashioned joystick—offering more natural, responsive, and continuous interaction. Figure 5.12 presents the eight direction commands utilized in this version.

The selection of these eight discrete directions represents a deliberate design trade-off aimed at balancing enhanced maneuverability with the specific usability constraints of a gaze-based interface. The four primary cardinal directions (Forward, Backward, Left, and Right) provide fundamental control, while the addition of the four diagonal directions offers a more granular and naturalistic means of control, enabling smoother curved motions. This is a significant enhancement over a simple four-direction system.

However, increasing the number of command buttons further would have introduced significant usability challenges. To prevent erroneous selections, a sufficient spatial separation must be maintained between adjacent gaze targets. Furthermore, because the primary method for stopping the wheelchair is to move one's gaze away from any active command button, it is es-
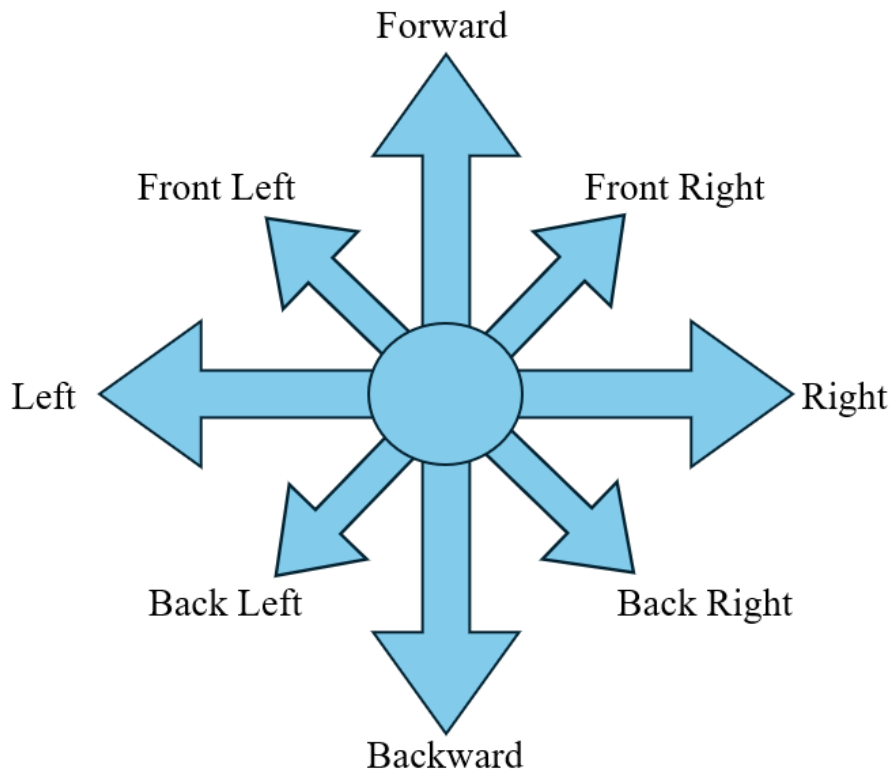
Figure 5.12: The eight directions used to navigate the wheelchair. This configuration was selected as an optimal balance between enhanced maneuverability and the usability requirements of a gaze-based interface, providing more granular control than a four-direction system while maintaining sufficient spatial separation between command buttons to minimize accidental activations.

sential to provide ample "empty" or non-active space within the GUI. Adding more directional buttons would have cluttered the interface, reducing this vital empty space and making it more difficult for users to stop the wheelchair's movement intentionally and precisely. Therefore, the eight-direction layout was chosen as the optimal configuration, as it provides a substantial improvement in control fidelity while ensuring the interface remains clear, accessible, and robust for both command activation and deactivation.

During the Turtlebot experiment, several users provided valuable feedback regarding interface design—namely that buttons were too small and it was difficult to focus their gaze accurately for extended periods of time. This was especially evident when users attempted to maintain their

gaze on a single button in an effort to trigger multiple commands, resulting in discomfort and reduced accuracy. In order to solve this issue, the main directional buttons (Forward, Backward, Left, and Right) have been made larger in the newer version. This enhances visibility and gaze accuracy, allowing users to interact with the interface easily and efficiently. However, due to the limitations of screen real estate and the imperative of maintaining a decent distance between buttons to prevent accidental activation, the four additional diagonal direction buttons that were introduced have been kept small. While smaller in terms of size, their placement has been carefully designed to be usable.

Additionally, as can be seen in Fig.5.13. The placing of the "Detection mode" and "Save and Exit" button is changed to accommodate the new directions.

As shown in Figs. 5.12 and 5.13, The interface can control the wheelchair's joystick in 8 directions. Forward, right, left and backward are the primary directions which are assigned to the bigger buttons. The other diagonal directions have the smaller buttons and are place in the corners of the screen.

The original Turtlebot interface had been implemented with a step-based motion scheme where pushing each button began an already programmed movement segment. This approach was good with pre-programmed, pre-planned paths but lacked the smoothness needed for natural, real-world control. As a result, several participants reported that the movements did not feel natural. Some users also had a complaint about imprecision in the fine-tuning, as the fixed-step strategy limited the users' capacity to deal with small-directional changes. In response to this criticism, the latest version of the interface has been redesigned to provide smoother, continuous movement. Instead of moving in stepwise manner, the wheelchair now responds in real time: provided an active command is being produced—e.g., when the user maintains eye on a button—the wheelchair will continue to move in that direction. Once the gaze is removed from the button, the motion will be stopped. This overlapping command system produces more fluid, unbroken motion, much as the experience of operating a standard joystick.
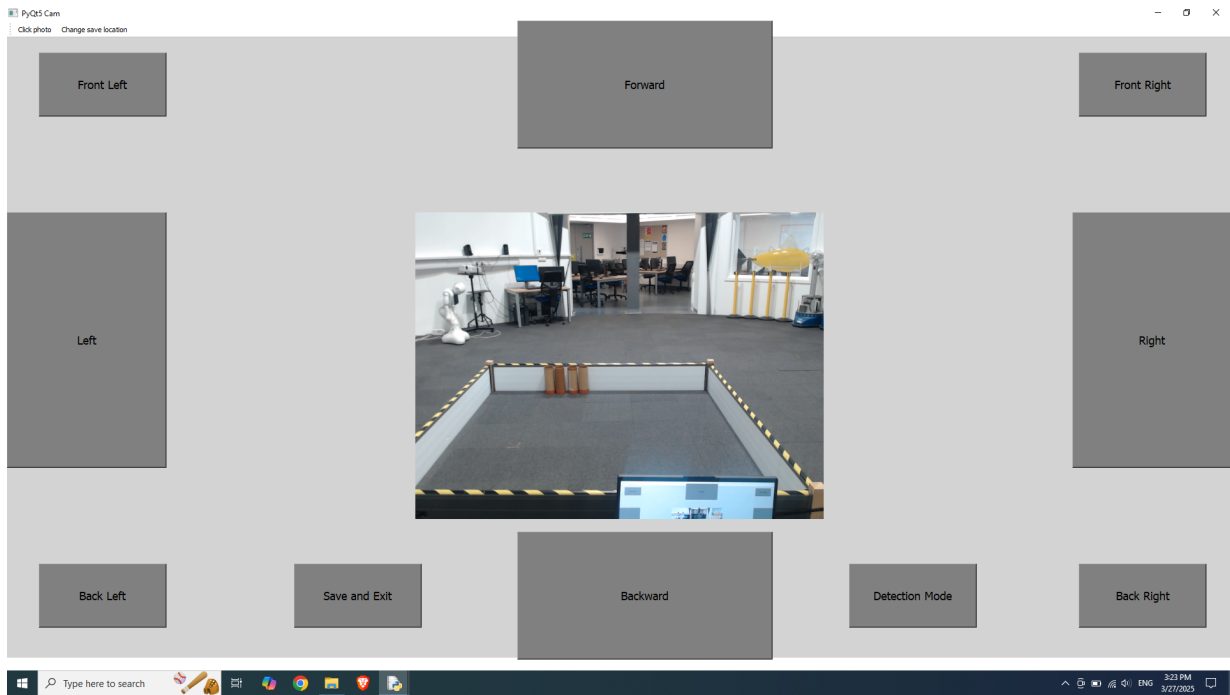
Figure 5.13: User interface for wheelchair navigation, featuring eight directional control buttons, an exit button, and a mode-switch button for activating Detection mode.

There are several important reasons behind the design of this new control approach. The primary goal is to recreate the natural feel of a traditional joystick for the users. In a real joystick, the wheelchair continues to move in a chosen direction—forward, backward, or sideways—as long as the joystick is held in that position. By mimicking this movement, the system makes it easier for users to enjoy a more comfortable and natural experience. In addition, reliance on fixed, pre-programmed steps can also be restrictive and even hazardous at times.

When a limited distance or time is only allowed for movement, users sacrifice flexibility in responding to conditions. This stiffness can make it difficult to squeeze through tight spaces or react in time to unexpected hazards, increasing the threat of collision. Sustained control, on the other hand, offers live updates, which makes movement smoother, more reactive, and ultimately safer.

On the other hand, the electric motors used in the wheelchair take approximately one second to respond and initiate movement after the joystick is pushed in a given direction. This built-in

delay can become quite frustrating for users—especially in a step-based control system—where they would need to repeatedly generate new commands just to continue moving. If the interface were constructed on discrete steps, then the lag between every motor response and command would give a staccato, unnatural sensation. Instead of smooth continuous movement, users would be subjected to continuous interruption, and precise control would be impossible and exhausting. By shifting to a system that allows continuous input—where motion is sustained as long as a button is continually triggered—the issue is alleviated.

In this version of the system, when the user's cursor hovers over a button for two continuous seconds, the button is triggered—essentially registering a click. After this initial activation, the system switches to a faster response mode: the timer is reduced to one second. So long as the user keeps the focus (cursor) on the same button, the system will continuously send commands to the wheelchair at one-second intervals. This approach offers unbroken movement without having the user constantly re-activate the button, making it a smoother and more natural process.

As mentioned earlier, the mechanism is set to move for 2 seconds for each command received, unless it is a stop command. Therefore, a 1-second interval is an optimal approach to ensure uninterrupted movement.

The "Stop" command is also sent automatically to the wheelchair as soon as the cursor leaves the active button area to allow for instant stopping of movement. To further provide safety, the wheelchair system also has a two-second built-in command timeout. This means that without any new command within two seconds after the last one—system freeze, communication delay, or disconnection—the wheelchair will stop automatically. This two-layer safety function will stop the wheelchair from self-movement. For sustained movement, the wheelchair will need to be given a new command within the time frame of two seconds.

As leaving the buttons would mean stop, and the wheelchair won't move in anyway other than selection of the buttons, the interface is not equipped with a "Stop" button.

The system operates using single-letter commands, each corresponding to a specific direction

of movement for the wheelchair mechanism. There are a total of nine distinct commands: eight represent directional inputs—forward, backward, left, right, and the four diagonal directions—as shown in Fig. 5.12, and the ninth command is dedicated to stopping the movement. This can also be seen in Fig.5.9.

The commands are sent to the wheelchair's mechanism control board over Bluetooth. The interface host PC/laptop will needs to be connected to the Wheelchair's board first before running the program. Then the program can send the commands on it's own to the named device.

5.2.1   Adaptive dwell time settings

In the TurtleBot experiment, the dwell time—i.e., how long participants had to hold their eyes on a button to activate a command—was set to a constant 2 seconds for all participants. However, feedback suggested that this was not ideal for everyone.

Some of the users found the 2-second dwell time frustrating or overwhelming and therefore enjoyed the experience less. Others, particularly those who found it difficult to keep the cursor on the button, found it frustrating. These difficulties were often caused by issues such as cursor fluctuation, drift, lighting, calibration issues, or other technical problems. Some users also found the waiting time boring, particularly in certain instances where they found the process to be unnecessarily prolonged.

On the other hand, one of the key goals of this system—particularly with the addition of pupil dilation tracking—was to create an adaptive and intuitive interface that minimizes cognitive load and does not overload the users. This highlighted the importance of an adaptive and adjustable dwell time and allows the system to dynamically modify the required fixation duration based on user behaviour and comfort.

In the non-TurtleBot systems, dwell time can be made 1, 1.5, or 2 seconds according to the user's preference and requirement. For certain users—those with intellectual disabilities who take longer to make a decision or very precisely concentrate their attention—the dwell time can

even be raised from these default settings.

This customization renders the system easy to use and usable, including individuals of varying cognitive and motor ability. The parameters can be tweaked by a caregiver or assistive technology specialist to meet the individual's specific needs and comfort level. Providing flexible dwell time, the system optimizes usability, accessibility, and overall user experience so that no user ends up rushing or disoriented when using the interface.

However, since the experiments in this study are conducted specifically on healthy adults, the maximum dwell time option is limited to 2 seconds. The rationale for this was established based on usability for the target population such that there was a balance between response efficiency and user comfort.

While longer dwell times may be beneficial to individuals with cognitive or motor impairments, they were not included in this particular study because the intention was to provide assurance of system performance under conditions of neurotypical user use. Future studies can explore how longer dwell times would impact individuals who require more processing time and therefore make the system more accessible for a wider range of users.

On the other hand, to ensure safety and prevent accidental command choice, the lowest dwell time is 1 second. The timing allows sufficient time for users to make deliberate choices, reducing the chance of involuntary eye movement, temporary fixation, or sudden perspective shifts causing undesired actions.

Having a dwell time under 1 second would lead to erroneous command selections, especially in dynamic scenarios where users can be affected by gaze instability due to external distractions, lighting conditions, or physical eye compensations. With this threshold value, the system balances responsiveness and reliability to offer a smoother and more controlled user experience.

5.2.1.1   Command selection using real-time classification model

Another method for employing adaptive dwell time is the use of the classification model outlined in Section 4.2, trained on pupil dilation patterns. This technique takes advantage of pretrained weights that have been developed from data gathered over several participants, making the adaptation process more generalized and resilient. An overview of the approach can be seen in Fig.5.14.
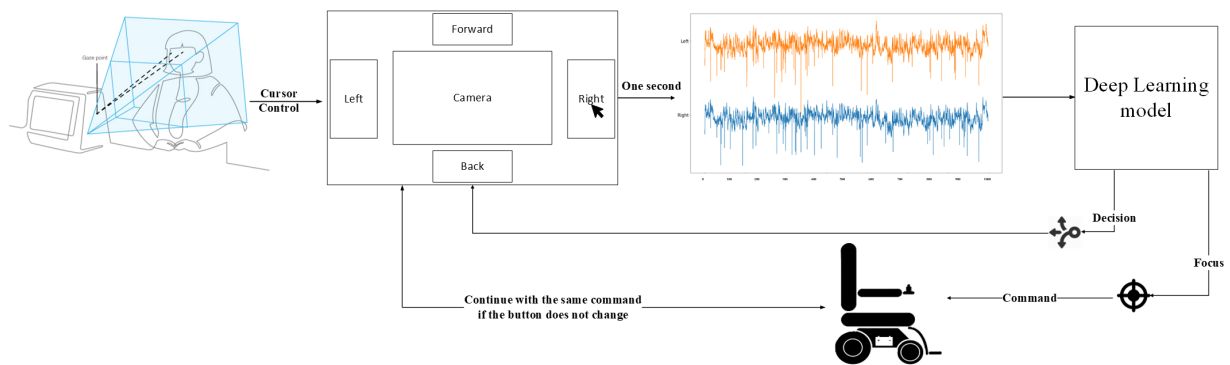
Figure 5.14: The overview of the workflow of the adaptive command selection method which is utilizing the real-time pupil dilation data.

As described in Section 4.2, the classifier operates on 2 seconds of pupil dilation data observed and normalized across users for comparability. Operating on data in fixed 2-second window style has one possible disadvantage—potentially longer dwell times during the first 2-second condition because the system would have to spend more time for processing and consideration before executing a command.

To counter this, additional tunings could be needed, i.e., making the classification algorithm even more efficient, reducing latency of data processing, or automatically updating the size of the window to adapt according to the response of every individual user. This would maintain efficient adaptive dwell time while achieving some degree of trade-off between response time and precision.

As described in Chapter 4, the model is trained on predicting decision-making and focus

states from pupil dilation signals. Decision-making, in this case, refers to when the user is considering the scenario and making the decision in what direction to move. Focus, then, implies that the user has made up their mind and is actually directing attention at a button for a choice—for 2 seconds.

Here, as the cursor or gaze moves into a button area, the system begins monitoring pupil dilation data at 1-second intervals. These data are then utilized to feed into a pre-trained classifier model to make decisions regarding what the user meant. As the initial model training had been trained on 2-second windowed inputs, this new data is normalized to 2-second time windows prior to utilization.

The classification model runs in a separate thread to allow for real-time decision-making without slowing down the experience of the user. If the model belches out a label and the classification output is "focus", the system immediately selects the button, which then fires the associated command.

This approach enhances flexibility and allows the system to distinguish between intended selections and temporary gaze fixations, therefore reducing the possibility of accidental commands without sacrificing the responsive quality of the user experience.

One drawback of this approach is model misclassification risk. If the system incorrectly classifies the user's state as "decision-making" when the user is really focusing on a button, the button will not be activated until after. To assist with coping with this, the system can be set to automatically trigger the button selection at the beginning of the third second, so that prolonged fixation will always be recognized as an intentional focus event.

The model can also be fine-tuned trained with audios of the specific user's pupil dilation pattern such that it becomes an adaptive user-focused experience.

5.3   Experiment Design

To find out the usability and acceptability of the system, an experiment was designed employing the proposed setup detailed in this chapter.

The feedback from previous experiments proved extremely valuable, and as a result of it, ideas and design improved drastically. The trial was conducted within an arena room of considerable size, chosen for a purpose of accommodating wheelchair mobility for exercise purposes unrestrictedly. A pathway to the maze using light weight boards was created with fence-boards to provide a resemblance to actual surroundings for testing and user-friendliness of the system. Figure 5.15 is a map of top-view maze and arena layout. At the beginning of the experiment, a spacious open area is provided to allow participants time for testing and familiarization. The remaining sections of the maze path are then used for the experimental trials.
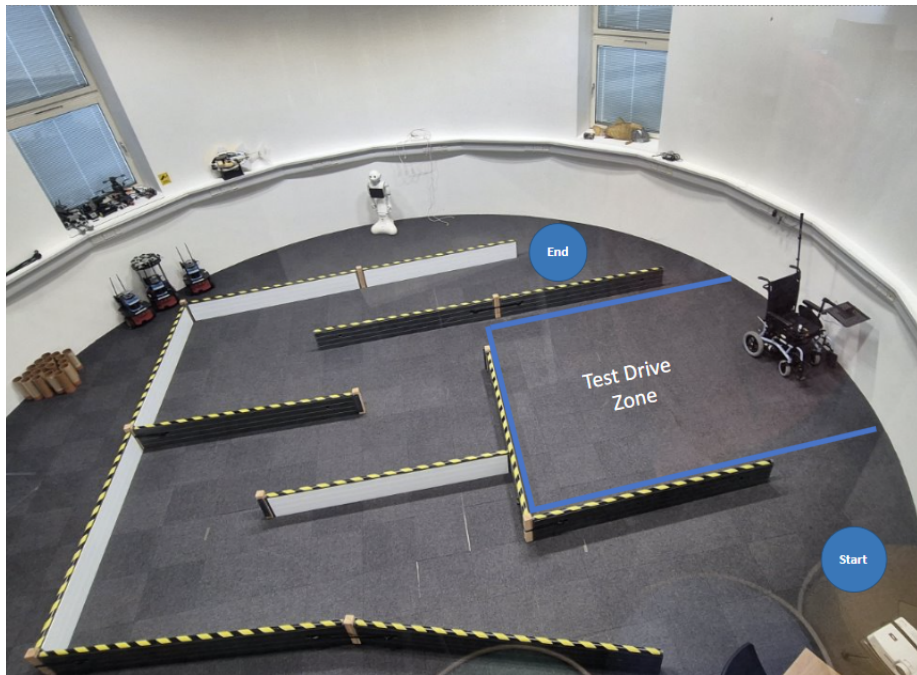
Figure 5.15: Top view of the Robot Arena showing the wheelchair experiment path and the designed test drive zone.

Once participants arrive at the venue, they will be shown a view of the path and general

explanation of the process and the experiment as well as the system. They will be given the information sheets and are encouraged to ask any questions or raise any concerns. Then the consent form will be handed out to them.

With the consent granted, they will be handed with the participant information collection form which has details about their age, wearing glasses/ lenses and Visual Analogue Scale (VAS) scale of the motivation and fatigue. The VAS questionnaires can be found on the Appendix.B these will be completed before the experiment. There is a VAS scale for fatigue for after the experiment, which will get completed after the experiment and before the questionnaire.

After they have passed through the normal introduction and consent process, they will be instructed to sit on the wheelchair, as can be seen in Fig.5.16, and adjust the laptop to a comfortable position. During this step, the participant will follow the position guide of the eye-tracker manager. The height of the laptop mount will be set based on the preference and eye-tracker measurements of the participant to maximize comfort and precision. Moreover, participants will be asked to provide feedback on camera angle and position once the interface is started. The aim is to make the camera give an even view so that the user can view both the front of the wheelchair and the road ahead, as well as the environment.

Once all the adjustments have been taken care of, the eye-tracker will be calibrated so that the measurements are comfortable as well as precise, all in an attempt to meet the individual needs of the user. Once the calibration has been completed, the volunteers will be required to test operate the system in the open field. It is done in order to acclimatize them with the system and be comfortable in maneuvering the wheelchair. They will also be able to test the camera view and request any changes required while they are doing so. Once participants feel confident and comfortable with the system, they will be asked to navigate toward the starting point of the path. At this stage, the recordings will be reset to begin collecting data for the actual experiment. Pupil recording will commence as soon as the interface is first used, but it will be specifically activated at the beginning of the experimental protocol to ensure accurate tracking during the

Figure 5.16: Image showing a user seated on the wheelchair with the mounted equipments.

trial.

The experiment path begins at the start position marked on the Fig. 5.15. Participants are instructed to follow the designed route until they reach to the end point and save their recordings by pressing the save button at the end.

Participants were instructed to complete a predefined navigation path in two separate rounds, each utilizing a distinct method of button activation. In the first round, a fixed dwell-time approach was used, requiring participants to maintain their gaze on a button for two continuous seconds to trigger a command. In contrast, the second round implemented a model-based activation method, wherein the system dynamically initiated commands based on real-time classific-

ation of pupil-related features.

Once the experiment is complete, the participants will be asked to move the mounted devices aside and exit the wheelchair. They will then be guided to a chair and table where they will complete a post-experiment questionnaire. They will first be asked to complete the VAS to assess their level of fatigue after completing the task. The subjects will also be requested to provide feedback on their experience, whether they have faced any problem or frustration during the process. Additionally, they will be requested to provide comments on the fatigue, the point at which they have begun to feel exhausted or tired. In order to gain more information, the participants will complete a more extensive questionnaire to provide feedback on their overall experience with the system and any additional comments or suggestions that they may have.

5.3.1 Participant recruitment

Ethical approval (Reference: ETH2324-2132) has been obtained for this Experiment from the university's ethics committee to ensure compliance with institutional guidance and ethical standards.

This experiment involved six healthy participants. This phase of the research was designed as a high-fidelity pilot study, with a primary focus on evaluating the system's practical performance and viability in a realistic assistive context. Given the logistical complexity of this practical, hands-on evaluation, a smaller, focused cohort is appropriate and aligns with common practice in assistive technology research for studies involving resource-intensive hardware and controlled experimental settings. Details about the participants are provided in Table 5.1.

Out of the six individuals who took part in the study, three had previously participated in the earlier Turtlebot experiment and were invited to return for this version. The final three were new participants in this experiment. This balanced composition was crucial for evaluating the generalization performance of the machine learning model introduced in Chapter 4, as it allowed for an assessment of the model's effectiveness both on users whose data patterns had contributed

to the training set and on users who were entirely novel to the system. The number of returning participants was intentionally limited to maintain this balance, ensuring the evaluation was not skewed towards those already familiar with the interface.

Table 5.1: Participant informations from wheelchair experiment.

ID	Age	Gender	Dominant Hand	Glasses	Bi/multiFocal	Eyetracking	Wheelchair
P01	28	F	R	N	-	Y	Y
P02	29	M	R	N	-	Y	N
P03	30	F	R	N	-	N	N
P04	65+	F	R	Y	Y	Y	N
P05	35-44	M	R	N	-	N	N
P06	26	M	L	Y	Y	N	N

All the subjects were healthy adults. The group was also selected to include participants from different age groups (ranging from their late twenties to over 65), providing insights into the system's usability across a varied demographic. Except for one, who had prior experience using an electric wheelchair, the remaining subjects had no experience working with a device of such type. Two of the subjects also wore glasses—both with bifocal or multifocal lenses.

5.4 Data Analysis

This section presents the data and results collected from participants during the experiment. Each participant completed the same predefined path using the same GUI design, but under two different command selection methods. In the first condition—referred to as the "Dwell Lap"—participants used a fixed 2-second dwell time to initiate commands by gazing at the buttons. In the second condition—referred to as the "Model Lap"—command selection was based on a classification model, as described in Section 5.2.1.1. The order of the laps was kept consistent across participants: all participants first completed the path using the dwell time method,

followed by the model-based method.

This section has a focus of comparing the outcomes of the experiment based on the method used, which includes the pupil responses and the performance measures. Additionally, overall system design and the subjective feedback and questionnaires has been discussed here.

5.4.1 Pupil Response

To assess the impact of the task on pupil responses, pupil dilation was recorded throughout the experiment. Various graphs were generated to identify patterns and extract meaningful insights. The data revealed several distinct trends, highlighting individual differences and potential correlations with task demands.

Figure 5.17 presents the Gaussian distribution graphs comparing pupil dialation of one eye during the dwell and the model lap. for majority of participants the peak of pupil dialation is larger or equal in the dwell lap which suggests that the dwell lap was more cognitively demanding for participants. The higer mental load is due to unfamiliarity with the system. For some participants, such as P03 and P05 the peak of the laps are almost aligned. on the other hand, P01 showed higher difference between rounds.

Figure 5.18 until Fig 5.23 present individual graphs for each participant presenting the Gaussian distribution on the top row, the histogram in the middle row and the details about the session at the bottom of the figure. The left sides are the graphs related to the dwell lap and the right side for the model lap of the participant's session. each graph contains a line representing the left eye and another for the right eye.

The analysis of pupil responses for each participant is presented using both a histogram and a Gaussian distribution. This dual visualization approach was deliberately chosen to provide a comprehensive understanding of the data. The histogram offers a direct view of the empirical frequency distribution of the raw pupil measurements, revealing the actual range and any irregularities. In parallel, the Gaussian distribution serves as an idealized model, with its peak

(a) P01 Left Pupil   (b) P02 Left Pupil   (c) P03 Left Pupil

(d) P01 Right Pupil   (e) P02 Right Pupil   (f) P03 Right Pupil

(g) P04 Left Pupil   (h) P05 Left Pupil   (i) P06 Left Pupil

(j) P04 Right Pupil   (k) P05 Right Pupil   (l) P06 Right Pupil
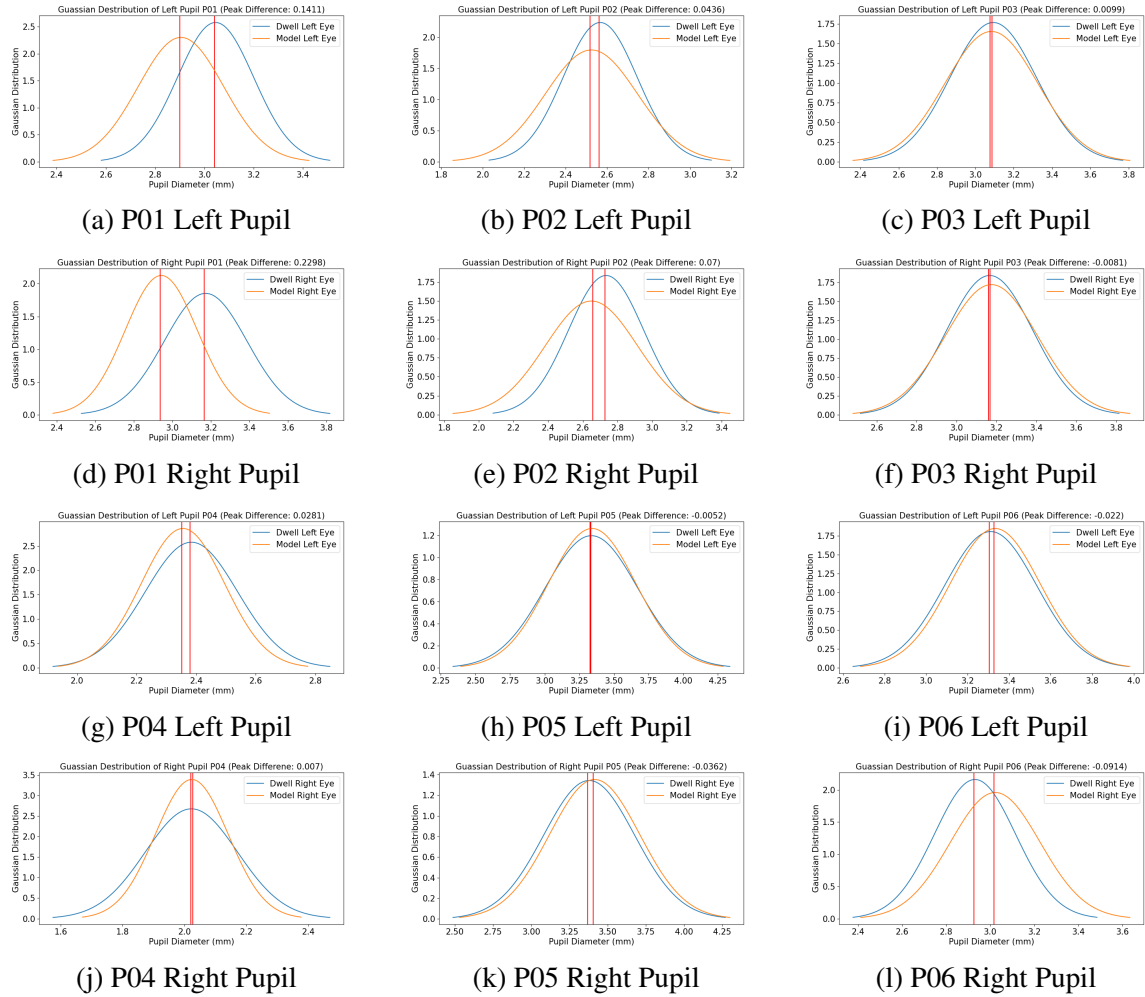
Figure 5.17: Gaussian distributions of pupil dilation for each participant, comparing the left and right pupils across experimental rounds.

providing a clear visual indicator of the mean pupil size, which is significant for intuitively comparing the central tendency between the Dwell and Model laps. Together, these plots offer a more complete picture of each participant's physiological state than a single visualization could provide.

Figure 5.18 presents the data for Participant number 1. P01 presents almost normal distribution with larger pupil dialation in dwell lap with narrower distribution of left pupil during dwell lap. The right eye presents larger pupil dilation than the left eye during the rounds. P01 completed both laps in approximately 6 minutes.
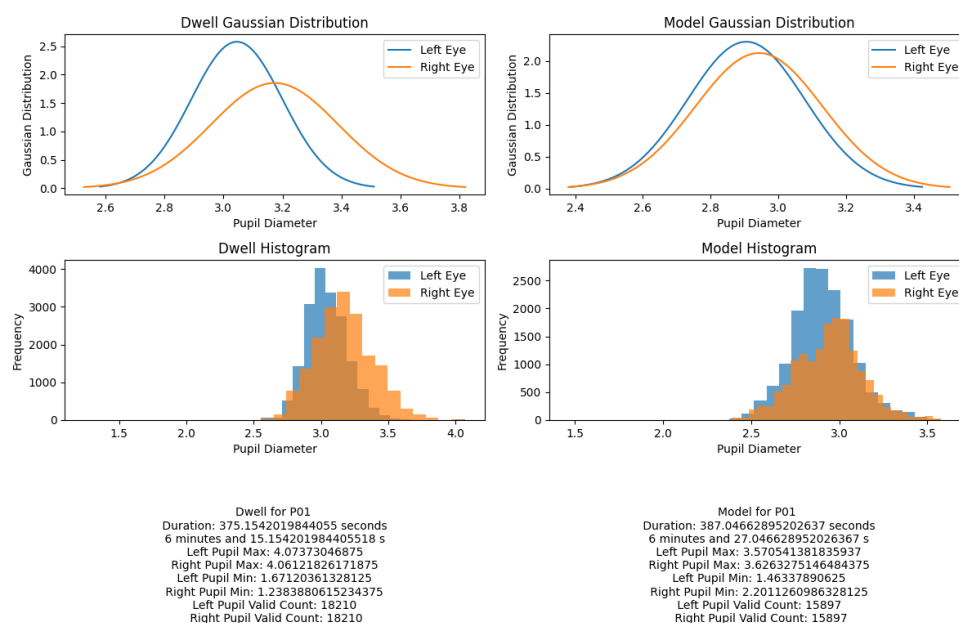
Figure 5.18: Side-by-side comparison of the histogram and Gaussian distribution of pupil diameter for participant P01 during the dwell and model laps.

Figure 5.19 illustrated the graphs related to P02. The graphs shows an elevated pupil dialation in the right eye in comparison with the left eye. Additionally, the left eye has narrower Gaussian distribution. Participant completed the dwell path in approximately 4.5 minutes whereas in less than 2.5 minutes. Although the completion time is lower in the model lap, the pupil range remained similar.
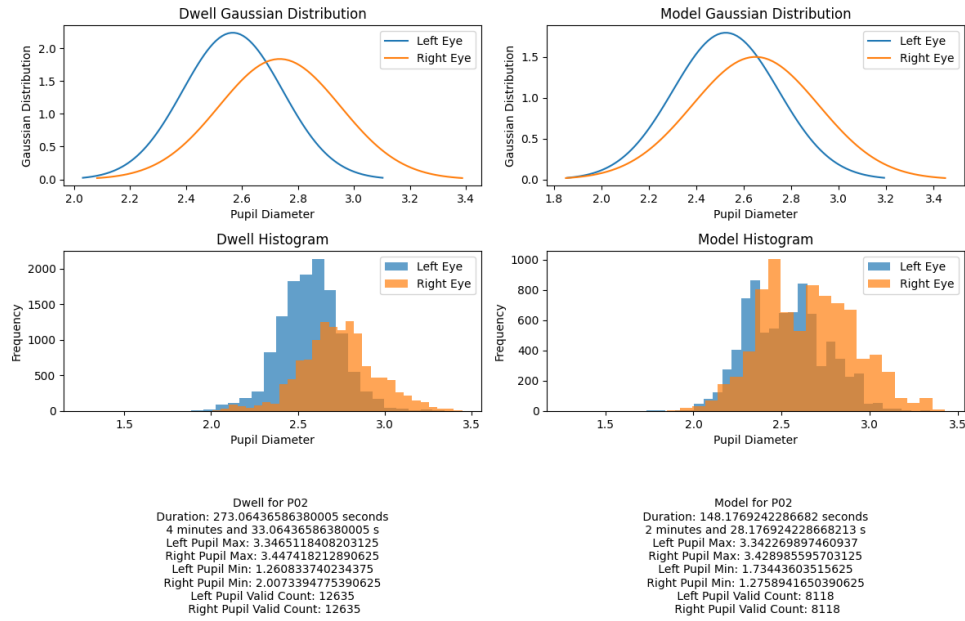
Figure 5.19: Side-by-side comparison of the histogram and Gaussian distribution of pupil diameter for participant P02 during the dwell and model laps.

P03's graphs had been presented in Fig. 5.20. The papillary data are almost similar in terms of range and distribution during the laps. The left and right eye also have similar trends, although the right eye's pupil is slightly more elevated in both rounds. P03 completed the Dwell lap in slightly less than 10 minutes and the model lap in less than 7 minutes.

Figure 5.21 illustrates the graphs for P05. The data shows a normal symmetrical distribution for both eyes during the laps. Additionally, similar to previous graphs, the right eye have an slightly larger peak diameter. P05 shows similar pupil range during the paths. The Dwell lap has been completed in approximately 6.5 minutes whereas model lap took less than 5 minutes.

For P01, P02, P03, and P05 the patterns of the pupil responses are almost similar. Mainly the right eye has slightly more elevated dialation in comparison with the left eye. The histograms has more overlapping and the main range of the dilation of the eyes are similar or close. On the other hand, P04 and P05 present different trend and patterns for the pupil dialation than the previous graphs.
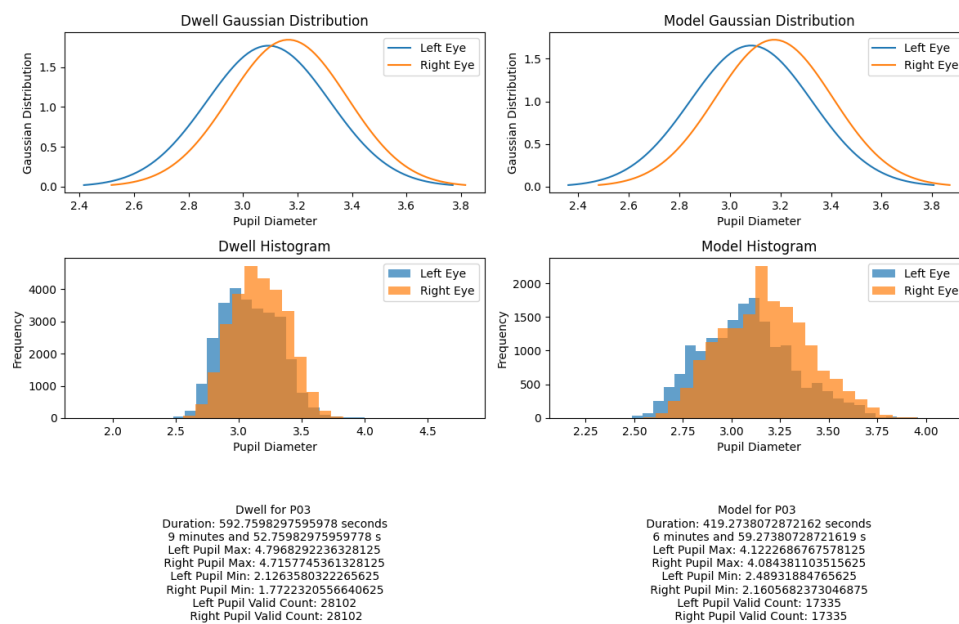
Figure 5.20: Side-by-side comparison of the histogram and Gaussian distribution of pupil diameter for participant P03 during the dwell and model laps.
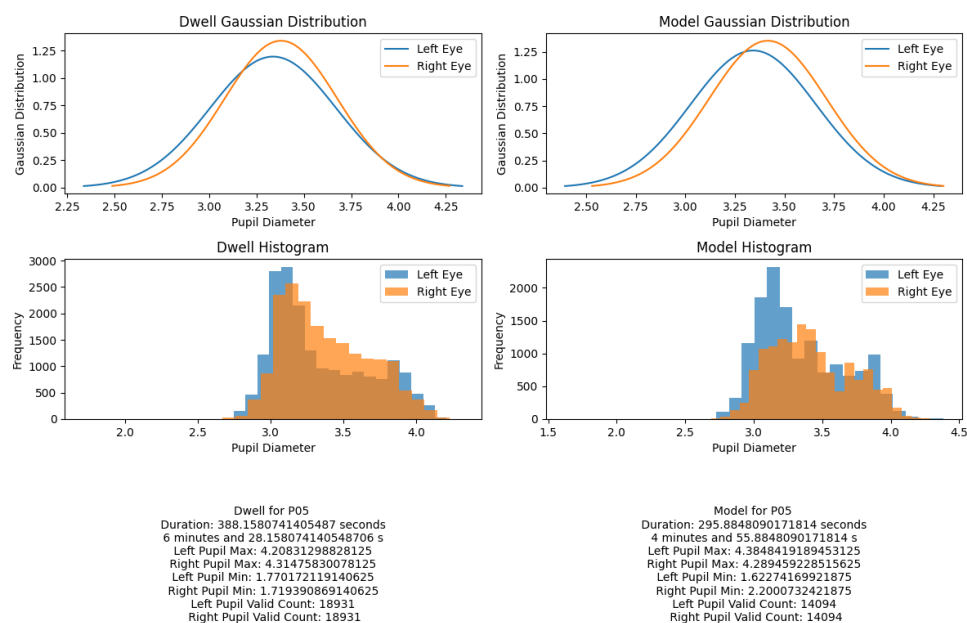
Figure 5.21: Side-by-side comparison of the histogram and Gaussian distribution of pupil diameter for participant P05 during the dwell and model laps.

Figure 5.22 Presents the pupil readings for P04 during the experimental laps. The graphs are septate and have distinct range with slight overlap. The left eye presents a higher dilation. The histogram has a small overlap. The trend has been similar in both laps. The dwell lap has been completed in approximately 8.5 minutes and the model in less than 6.5 minutes.
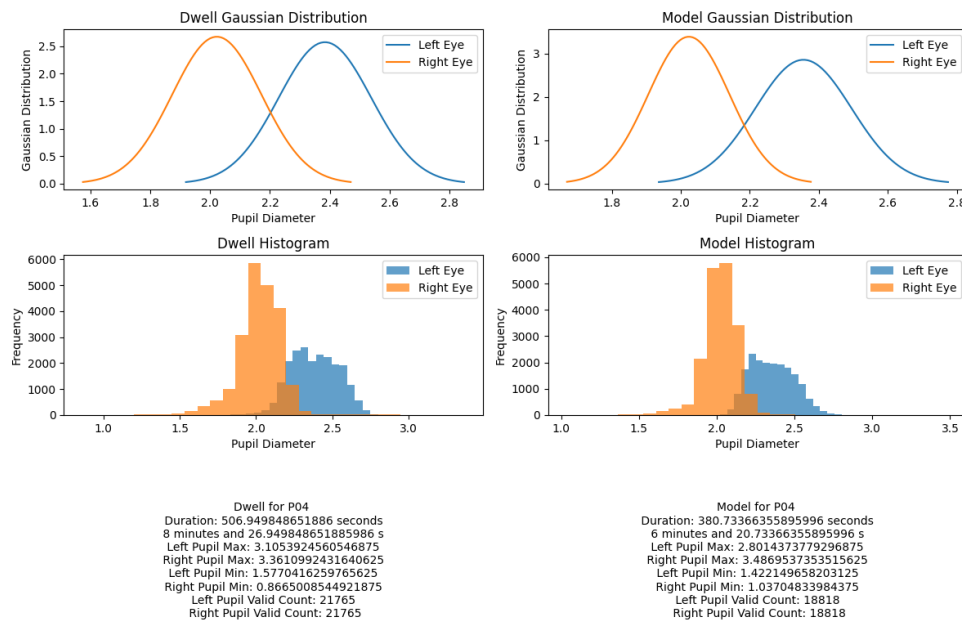
Figure 5.22: Side-by-side comparison of the histogram and Gaussian distribution of pupil diameter for participant P04 during the dwell and model laps.

Participant 6 (P06), as can be seen in Figure 5.23, have also separate graphs and dialation range. although there is a distinct separation between the graphs but there is a large overlapping area. The left eye has larger dialation in both laps. The dwell lap took slightly more than 8 minutes to complete whereas model lap took less than 3.5 minutes. This is the largest difference in completion times between participants.

These large separations in the different eye's has been observed with participants wearing glasses, specially glasses with bifocal or multi focal lenses.

These separation readings have been observed previously and tend to occur in participants wearing glasses, particularly those with bi- or multi focal lenses. Such lenses contain different
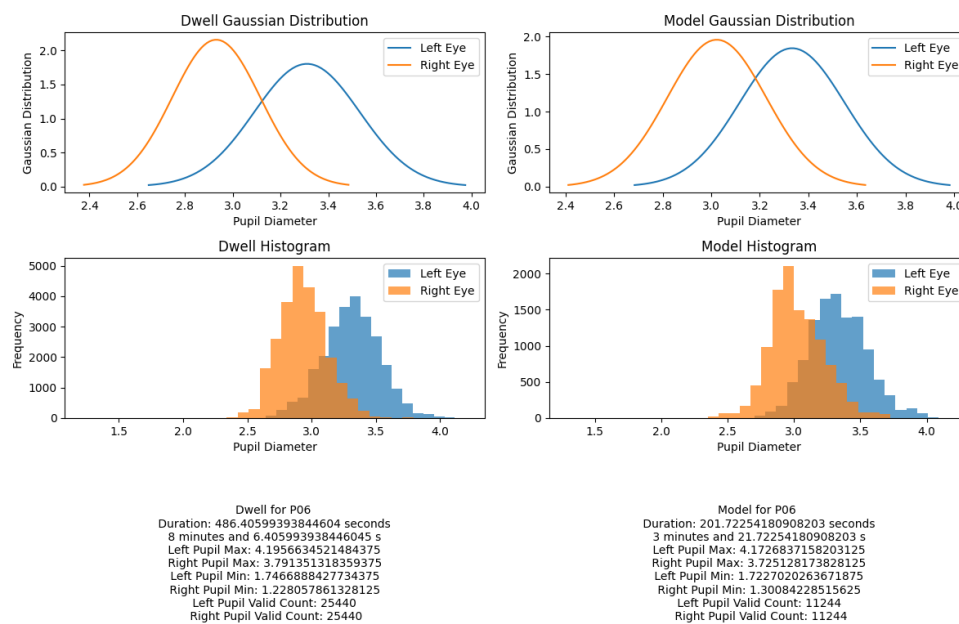
Figure 5.23: Side-by-side comparison of the histogram and Gaussian distribution of pupil diameter for participant P06 during the dwell and model laps.

optical zones that can reflect the infrared light from the eye tracker in varying ways, potentially leading to inconsistencies in pupil detection. Each optical zone may alter the reflected signal differently, which can occasionally introduce variability or affect the reliability of the pupil measurements.

5.4.2 Performance

To compare performance during the experiment, the following performance metrics were used. These measures are consistent with those previously introduced at the beginning of Section 3.3.3.

- Lap completion time: It measures the total time taken to complete the path. It's the time between the first movement command sent to the wheelchair until the last one, which will remove the time spent at the beginning for the explanations . It shows how fast users were to complete the route.

- Command Selection times: It's the time spent between each movement commands. It is influenced by the time user needed to decide on a action and the accuracy of their fixed gaze detection that the command get generated quickly.

- Number of commands: presents the number of commands needed to complete the path. as the length of the path is similar for the users, the less number of commands shows less errors and less adjustments. This counts only the navigation based commands and not the "N" commands which has been sent to stop the movement.

These performance measures not only provide us with information regarding how good each user was at utilizing the system, but also provide us with a general understanding of the system as a whole's ease of use and productivity. Quantifying both the performance of the system's users and the responsiveness of the system to its users, we understand completely how easy to use and productive the interface is. Here, we compare performance across two conditions: one using a fixed 2-second dwell time for command selection and the other using machine learning–driven classification. The comparison allows us to assess whether the smart model improves control accuracy, user satisfaction, and overall task effectiveness.

Figure 5.24 illustrates the lap completion time for participants during Dwell Lap and model Lap. The results indicate that nearly all participants were able to complete the lap faster using the model-based command selection method, except one subject who achieved almost equal completion time.

It's important to note that the reduction in lap completion time cannot be solely attributed to the model-based approach. Familiarity with the system and the wheelchair's movements likely also contributed to the shorter times. Although participants were given an opportunity to test drive the system before beginning the Dwell Lap—to reduce the impact of unfamiliarity—most opted for only a very brief trial. As a result, some level of learning or adaptation may still have influenced their performance during the Model Lap.
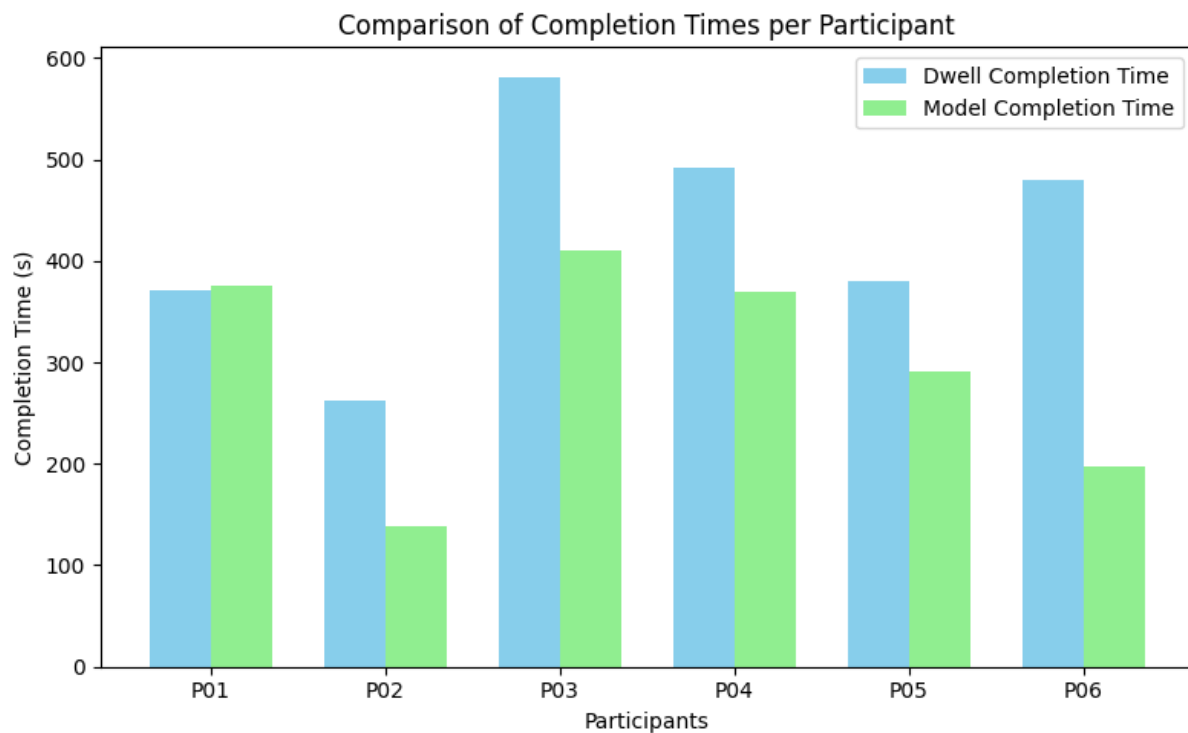
Figure 5.24: The lap completion time for participants to complete the path using the Dwell based and Model based interface.

The average time gap between each navigation command for participants is shown in Fig. 5.25. This duration represents the time elapsed between the execution of two consecutive movement commands. It includes both the decision-making period and the time required to select the next button, providing insight into how quickly and confidently users were able to interact with the system.

The model lap has the lower average command selection time for all the participants. The difference is significant for P05 and P06. It is noticable for P02 and P03 as well.

In addition to the impact of the command selection method, familiarity with the system also plays a role in the time participants spent on decision-making and selecting commands. As a result, the difference in average time between the two methods is less pronounced for participants P01 and P04, who were already familiar with the system from their previous participation in the
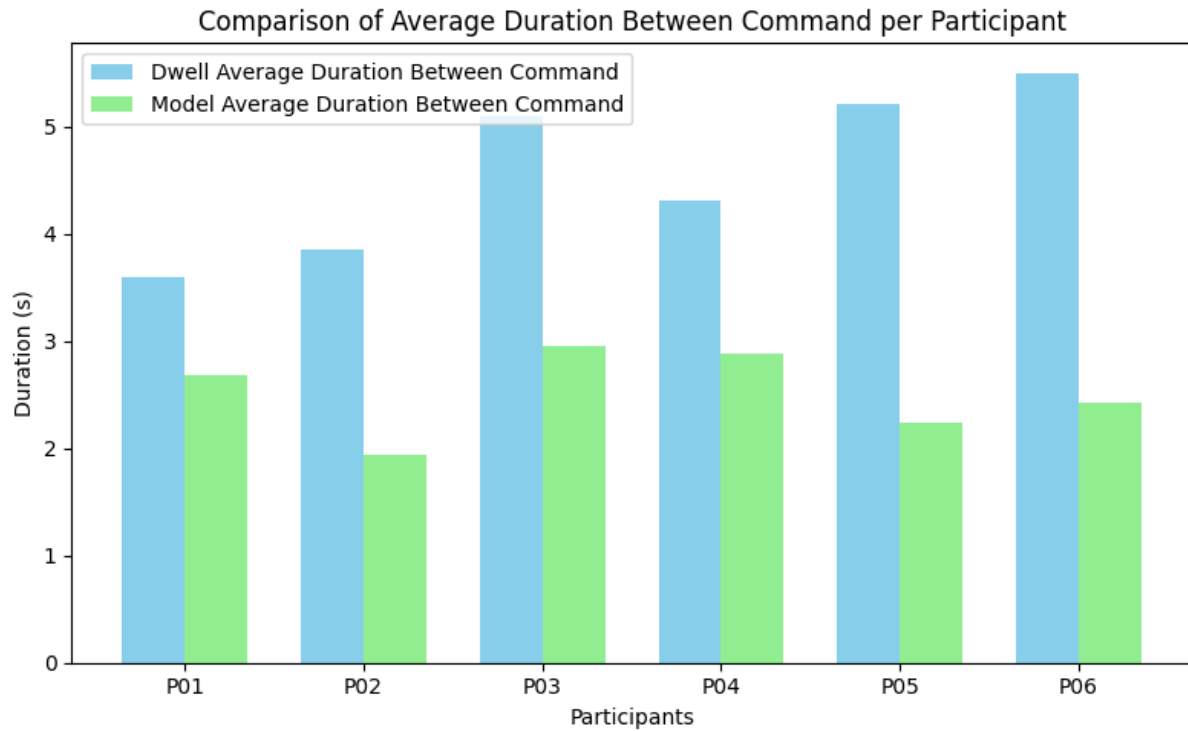
Figure 5.25: The average duration between generated commands for each participant while navigating the path using the Dwell based and Model based interface.

TurtleBot experiment.

Another important factor to consider is the number of continuous commands that are generated. With users maintaining their gaze on the same button without shifting attention too quickly, a further command is invoked every second. This chain of unbroken commands not only allows for smoother navigation but also serves as an indicator of the user's ability to maintain concentrated attention on the target. The greater the number of continuous commands, the more the level of control and degree of confidence in using the interface is elevated.

Table 5.2 illustrates the most consecutive commands that each participant produced during both laps, and the frequency with which they did so. The maximum number was for participant P02, who produced 11 consecutive commands twice during the model lap. During the Dwell lap, P03 received most consecutive commands with a peak of 8. Though P03 received a lower

peak number of continuous commands in general, they were able to execute five consecutive commands on five separate occasions during the model lap—stable performance. For all the other participants, the number of continuous commands was typically greater in the model lap than in the dwell lap, indicating better control of gaze and fluidity of interaction.

The increase in the number of continuous commands activated during the model lap suggests that the faster activation mechanism would facilitate—or feel more intuitive to—a user to possess a directional command for a longer, unbroken period. It can indicate greater user confidence or reduced cognitive effort in maintaining fixations on a selected command. particularly P03 has exceptionally longer uninterrupted series in the course of the Dwell lap rather. This would be a measure of between-person variation in attentiveness or interpersonal style. Second, how often maximum streaks happen suggests that such long streams are more than rare events; e.g., participant P01 achieved a maximum streak 12 times within one lap, just how common and powerful these prolonged interactions may under ideal circumstances get.

Table 5.2: The maximum number of the continuous generated commands for each participant in Dwell and Model lap.

Participant	Dwell	Model
P01	3 commands, 12 times	5 commands 2 times
P02	4 commands	11 commands, 2 times
P03	8 commands	5 commands, 5 times
P04	4 commands	5 commands, 2 times
P05	3 commands, 2 times	5 commands
P06	3 commands, 2 times	7 times, 2 times

The direction buttons utilized by the interface are two types: main direction buttons (Forward, Backward, Left, and Right) and diagonal direction buttons (Front-Right, Front-Left, Back-Right, and Back-Left). Table 5.3 indicates the percentage of each group of button used by participants for both laps. It can be seen that a number of the participants had a strong inclination towards the

use of main direction buttons as opposed to diagonal direction buttons. For instance, participant P04 used the main direction buttons exclusively during the model lap and used them to input 97.7% of all commands during the dwell lap.

Table 5.3: The selected button type percentage for each participant in Dwell and Model lap.

Participant	Button Type	Dwell (%)	Model (%)
P01	Main	89.4	87.9
	Diagonal	10.6	12.1
P02	Main	72.7	68.3
	Diagonal	27.3	31.7
P03	Main	72.2	71.7
	Diagonal	27.8	28.3
P04	Main	97.7	100.0
	Diagonal	2.3	0.0
P05	Main	85.1	79.4
	Diagonal	14.9	20.6
P06	Main	81.8	76.7
	Diagonal	18.2	23.3

Figure 5.26 illustrates the total number of navigation commands generated by participants during both the Dwell and Model laps. With the exception of participant P06, who produced slightly fewer commands in the Model lap, all other participants generated a higher number of commands when using the model-based control method.

Although participants issued a greater number of commands during the model lap, they completed the lap in less time. This suggests that increased familiarity with the system enhances both the effectiveness and strategic use of the control interface, allowing users to issue commands more proactively. The higher command frequency may also reflect growing confidence and intentional control over the system and their movements. As participants became more accustomed

to the interface, they made finer or more frequent adjustments, which optimized navigation and reduced completion time despite increased interaction. For instance, utilizing a larger turning radius, a behavior likely influenced by system familiarity, will result in more commands, but ultimately reduces the need for corrective manoeuvrers and shortens overall task duration.

Apart from this, the decrease in the mean choice time of commands on the model lap also agrees with increased familiarity. The decline indicates that the participants took fewer decision-making minutes, which points towards improved cognitive processing and command selection efficiency. For instance, as the users became more familiar with the system, issuing the correct command to carry out an exact turn such as path boundary avoidance was more natural and less cognitively taxing. This reduction indicates that the model is actually accelerating the interaction without requiring users to accomplish long gaze times, which can result in quicker decisions and more responsive control feedback.
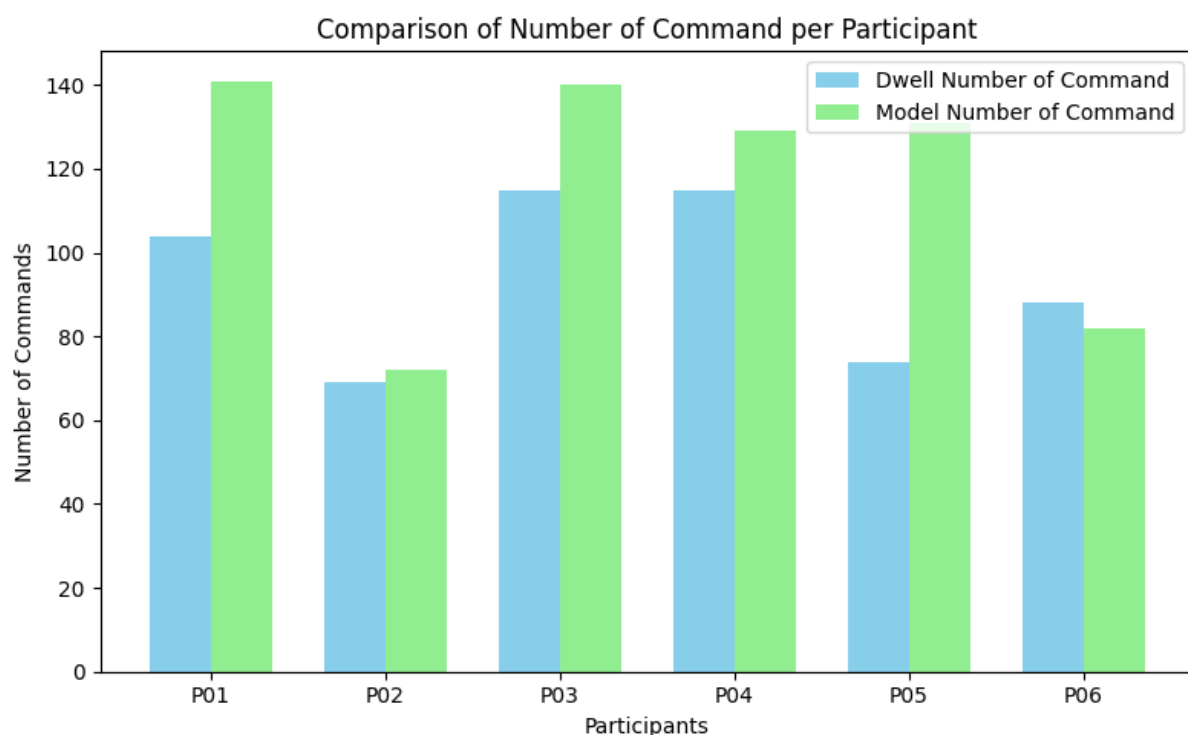
Figure 5.26: The total number of navigational commands generated for each participant while navigating the path using the Dwell based and Model based interface.

All these steps yield detailed information regarding the system's performance and design. The overall improvement observed in the performance measures reflect that the Model significantly contributed to enhancing system usability. Besides, the Model had stable performance between new and repeat users, reflecting its responsiveness.

Another reason that improves the outcomes is the more familiarization with the system and wheelchair movement dynamics. Although a few of the participants were accustomed to an older model of the gaze-based interface, none were accustomed to driving or operating an electric wheelchair. As the wheelchair is rear-wheel drive with two passive front wheels, accuracy in turning and motion requires a period of adaptation.

5.5   Usability and Acceptability

In order to assess the usability and overall acceptability of the system, feedback from the users was required. Throughout the experiment, the subjects were requested to provide their first impressions and comments regarding the system. In addition to these immediate first impressions, standard questionnaires were used in order to officially survey their experience. These were the QUEST 2.0 to measure satisfaction with assistive technology, the NASA-TLX to measure perceived workload, and the Unified Theory of Acceptance and Use of Technology (UTAUT) to measure participants' acceptance and willingness to use the system.

5.5.1   Subjective Feedback

This section will share the insights from the subjective feedbacks that has been received. Participants shared their feedback during the experiment verbally. Additionally, there was a section in the questionnaire for it.

Three of the participants had participated in the turtlebot experiment as well, there were also three new participants.

Volunteers who had used previous incarnations of the system noted noticeable improvements, in particular with regard to cursor movement. They felt that the stuttering or "jumping" movement of the cursor had been significantly reduced and that the motion was now more controlled and fluid. They liked the larger size of the principal directional buttons, reporting it an improvement over previous models. The other region of positive feedback was the addition of constant movement, which the players enjoyed because it made the system more natural and intuitive. Not only did this improve the overall ease of use, but it also enabled users to feel more in control. However, some of the returning users did comment on their preference for the wider video stream of the previous version, as they used it to navigate more conveniently. However, they all agreed that the fluid motion brought into this version felt considerably more fluid and easy to use compared to the step-based motion layout used in the former TurtleBot system.

The new users appreciated the overall design of the system, finding the interface, eye-tracking feature, and mechanism of the wheelchair's motion satisfactory. They found the system easy to use and efficient, even with minimal prior experience.

One widespread suggestion from participants was regarding the diagonal buttons' size. The majority of them found them too small and recommended increasing their size to improve usability. Interestingly, despite being smaller, some users found they preferred using the diagonal buttons instead of the main direction buttons in specific situations. They mentioned that diagonal controls were more smooth and effective when navigating tight or more complex path segments, and that made overall maneuverability improved.

In general, participants gave very positive feedback about the system, its design, and the potential applications it might facilitate. Most were enthusiastic about the potential of the system and saw real promise in its future applications. Their suggestions were mostly aimed at areas of refinement in refining the system towards a potential end product. All the respondents agreed that the system would be especially useful and acceptable to people with severe motor impairments—i.e., those who are unable to use standard systems with their limbs. They saw it not

only as a practical solution but also as an enabler that would significantly enhance autonomy and quality of life.

Additionally, they pointed out that the system is easy to use and understand. and learning to use the system wouldn't require extensive training or explanations.

5.5.2   Questionnaire

The questionnaire outcomes as well as the scales for fatigue and motivation has been explained in this section. The details can be found in Appendixes A and B.

Participants has been about their motivation about participating in the study before the task, All participants scored 10 on the sheet which represent they are highly motivated and excited about the experiment.

The scale for fatigue has been presented to participants once before using the system and once after completion of the experiment. The scale varies between 0 to 10 which 0 represents no fatigue and 10 represents worst unberable fatigue. The highest fatigue reported is 3 which represents a mild annoying fatigue. Table. 5.4 presents the outcomes of the participant responses.

P01 and P03 selected 1 as their fatigue scale for both before and after task and they didn't report elevation of their fatigue based on the task demands. P04 also had the same before and after fatigue scale but on a higher scale of 3. P02 reported scale of 2 for fatigue before the task and then 3 for after the task. P02 reported that the strain on the eye due to the effort for not blinking while using the system, made them slightly more uncomfortable than tired than before.

On the other hand, both P05 and P06 reported less fatigue for after the task. P05 reported 3 as their scale of fatigue for before the task and P06 reported 1, then they both reported 0 and no fatigue after the tasks. They both mentioned that the tasks were interesting and enjoyable therefore their mood improved so they feel better in comparison with the start of the task.

Table 5.5 shows the average responses to the NASA TLX questionnaire. The questions assess factors that contribute to task difficulty or demand. Lower values indicate a lower perceived

Table 5.4: Participant responses on scale of motivation and the before and after scale for fatigue.

Participant	Fatigue Before	Fatigue After	Motivation
P01	1	1	10
P02	2	3	10
P03	1	1	10
P04	3	3	10
P05	3	0	10
P06	1	0	10

workload, suggesting that participants found those aspects of the task less demanding.

Participants found the mental demand and effort needed for the task more demanding with -3.66 rating. Although the ratings are on the low side and shows a slightly low demand, they are the most demands in comparison with the rest of the factors.

The next demanding factors are physical demand and frustration which had average of -5.83. The strain caused on the eye is the main reason for the physical demand, the sudden jumping of the cursor or the hardness of keeping the cursor on the button is the main reason behind the reported frustrations.

Temporal demand is one of the lowest factors with -6.83 average score representing low demand. This shows that the task and the system did not make participants feel rushed or hurried.

The lowest score is for the performance, where -10 means perfect performance and +10 means failure, with average -8.5 score between participants. This confirms that the participants where able to accomplish their goals and their expectations during the task.

The overall scores shows that the system and experiment doesn't have a high task load. All the average scores are in the negative side which means they are on the lower side.

The next part of the Questionnaire, participants has been asked about their satisfaction with the system they tested during the experiment. Table. 5.6 represents the average score of the responses received for the questions. It shows that almost all participants where quite satisfied

Table 5.5: Average participant responses to the NASA TLX following the wheelchair experiment. A score of -10 indicates very low demand, while +10 indicates very high demand. For the performance, -10 corresponds to perfect performance, and +10 indicates complete failure.

Factor	Average Responses
Mental Demand	-3.66
Physical Demand	-5.83
Temporal Demand	-6.83
Performance	-8.5
Effort	-3.66
Frustration	-5.83

Table 5.6: Average participant responses to the Quebec User Evaluation of Satisfaction with Assistive Technology (QUEST) questionnaire following the wheelchair experiment. Scores range from 1 to 5, where 1 indicates 'not satisfied at all' and 5 indicates 'very satisfied'.

Question	Average Responses
Safety and security of the device	5
Easy to use	4.16
Comfortable	4.33
Effective	4.33

with the comfort, effectiveness and ease to use of the system. and all participants were very satisfied with safety and security of the system and the mounted devices.

Additionally, participants were asked to identify the three most important factors between the options that influenced their satisfaction with the device. This ranking task aimed to highlight the aspects of the system that users considered most critical when evaluating assistive technologies. The details and the number of of times each of the factors has been selected can be seen in Table. 5.7.

Based on the responses recorded during the experiments, Participants found the system safe for the independent use, easy to understand and use, effective for the intended goal, easy to set

Table 5.7: The key factors considered important for the evaluation of assistive devices, along with the number of times each factor was selected by participants as one of their top three priorities.

Factor	Number of selection
Comfort	4
Easy to use	4
Safety	4
Effective	2
Professional services	2
Adjustments	1
Service delivery	1

up, and comfortable to use.

5.6 Summary

This chapter detailed the critical transition of this research into a realistic, applied assistive context. The primary engineering contribution presented was the design and implementation of a low-cost, 3D-printable, and non-invasive robotic controller, which successfully retrofitted a conventional powered wheelchair for gaze-based navigation. The chapter also described the evolution of the user interface, incorporating the adaptive, intention-based model developed in Chapter 4 and refining the control paradigm for continuous and more naturalistic movement.

The efficacy of this integrated system was empirically validated through a pilot study with six participants. The results of this study were highly positive, demonstrating that the adaptive, pupil-informed control model was not only functional in a practical, real-world scenario but also resulted in significantly faster task completion times compared to the baseline fixed dwell-time method. The qualitative feedback further reinforced these findings, with participants reporting that the adaptive system felt more intuitive and responsive.

In conclusion, this chapter successfully validated the core hardware and software contributions of the thesis in a demanding and representative environment. It demonstrated that an accessible, low-cost hardware solution can be effectively combined with an intelligent, adaptive control model to create a powerful and usable assistive system. Having established the viability of the integrated gaze-based control for navigation, the next chapter will extend the functionality of this interface to address the equally critical challenge of assistive manipulation through the control of a robotic arm.

Chapter 6

Arm Controller: System Integration and Evaluation

Robotic arms have been engineered to replicate the action and movement of the human arm. They come in varying shapes, forms, and structures, each of which offers different DoF of movement for specific tasks. Robotic arms are utilized heavily in a variety of different industries, including industry, medicine, space exploration, and agriculture. Beyond these fields, robotic arms are also beneficial assistive tools for people with extremely severe disabilities or non-working limbs. By enabling users to perform daily tasks independently, these devices can significantly improve quality of life and foster greater autonomy.

There are some assistive arm robots available on the market such as JACO robotic arm by Kinova Robotics which are designed to be used as assistive arms, needs to be controlled manually and can be mounted on the wheelchairs or be used as stand-alone systems [95, 93]. A primary control method of assistive robotic arms on wheelchairs is a joystick, allowing users to have direct and intuitive control over the arm movement. In addition to joysticks, some of these systems have secondary control modalities in order to offer flexibility to users with varying levels of mobility. Examples of these are sip-and-puff, which respond to pressure change from the user's respiration,

and head movement, which track and interpret head movement into action.

This chapter extends the functionality of the assistive system to address the significant scientific challenge of reducing the profound cognitive load associated with manual robotic arm manipulation for users with severe motor impairments. The work presented here makes three key contributions. First, it introduces a novel, semi-autonomous control paradigm that shifts the interaction from complex, low-level joint control to high-level, object-based commands. This is achieved through the second contribution: the successful technical integration of a real-time object detection model (YOLOv5) into the existing gaze-based GUI. This allows the system to identify objects in the user's environment and present simple, actionable commands, thereby offloading the complex task of path planning from the user to the system. Finally, this chapter provides the first empirical validation of this integrated approach, directly comparing its performance and usability against a traditional manual control interface to scientifically quantify the benefits of the semi-autonomous system.

This chapter investigates the design of a hands-free interface for interacting with robotic arms, aiming to reduce the need for manual control. For the project, a 6 DoF robotic arm was purchased to conduct object handling operations and assess the usability of the custom-built control interface. The technical details of the robotic arm are described in the next section. This chapter continues with a thorough discussion of the interface built specially to control the robotic arm. Two versions of the interface have been designed: one is an extension of the current wheelchair control system in an integrated manner for use when the robotic arm will be used alongside the wheelchair or be mounted onto the wheelchair itself. The other is an experiment GUI version for self-contained control of the arm. The experimental setup that has been utilized in order to evaluate the system is explained below, followed by a detailed explanation and discussion of results obtained.

6.1   The Robotic Arm

For this project, the myCobot 320 robotic arm from Elephant Robotics was bought with funding support offered by the Colchester Catalyst Charity grant [116]. The myCobot 320 features six DoF with a working radius of 350 mm and a payload weight capacity of up to 1000 grams [117]. There is also a set of compatible gripper accessories offered by Elephant Robotics for this arm in order to address different object handling tasks. These include pneumatic suction cups, a pneumatic soft gripper, an adaptive gripper, and special object holders such as pens and smartphones [118].

Figure 6.1 shows the robotic arm with the adaptive gripper. The gripper can open up to 90 mm [119] and provides a clamping force of approximately 1 kg and can be employed to gripped small and moderately sized parts. The gripper is attached to the robotic arm with a mounting adapter and screws in a way that provides stability during use. It communicates with the system through a wired connection, offering responsive and dependable control in object handling operations.

The arm has 6 joints which cover 6 axis. The details of the joint numbering and their respective rotation directions are illustrated in Fig. 6.2. Each joint offers a rotational range of approximately $\pm 165°$, with the exception of Joint 6, which has an extended range of about $\pm 175°$.

Each axis along which motion can be independently controlled is referred to as a DoF. In the physical world, within a 3D space, the position and orientation of an object can be fully described using six parameters. The three position parameters are the X, Y, and Z coordinates, which represent the position of the object in space. Besides, the object's orientation is described in terms of three rotational components, namely, roll, pitch, and yaw. A 6 DoF robotic arm can access any position and orientation within its working space, provided that it is within the mechanical workspace of the arm. This means that not only can the robot relocate its end-effector to some point in 3D space but also orient it in a desired direction. With the constraint of motion range and joint limits, for each target position and orientation, there will typically be one possible
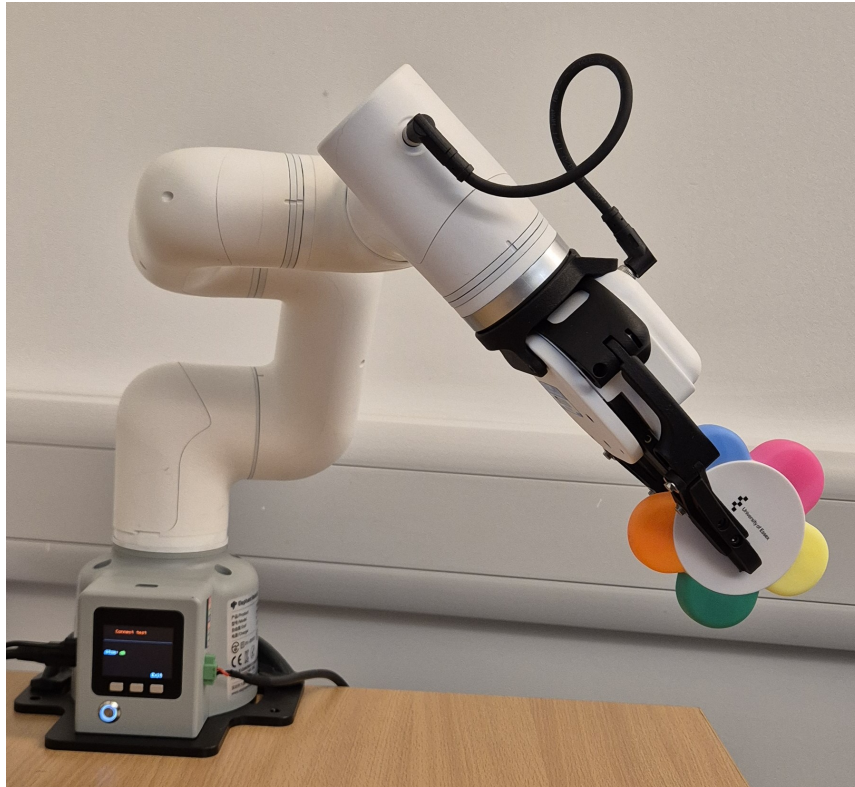
Figure 6.1: The robotic arm equipped with an adaptive gripper holding an object.

arm configuration that realizes that exact pose, although in some cases there may be more than one solution depending on the robot's configuration.

The arm movement can be executed using end-effector coordinates, which is a widely used technique known as Cartesian control. In this mode, the user or the control system specifies a target location and orientation in 3D space—X, Y, Z coordinates and roll, pitch, yaw—is given. The robotic arm will independently calculate the joint angles required via inverse kinematics and plan a path to drive the end-effector smoothly and precisely to the target pose.

Alternatively, the robot arm supports joint space control, a method where target angles are specified directly to every individual joint. In this operation mode, the user or control system specifies the target position in terms of joint positions (usually in degrees or radians), and the robot determines and traces an optimized path to that position smoothly and safely. Control of the joint space offers high-precision control and precise placement at the joint level, and it is

suitable for those tasks that involve specific arm geometries or use of low-level control programs. However, it is more difficult to determine the suitable joint angles, especially when one is trying to reach a specific end-effector pose, since the correspondence between joint angles and Cartesian position is non-linear and typically complex.
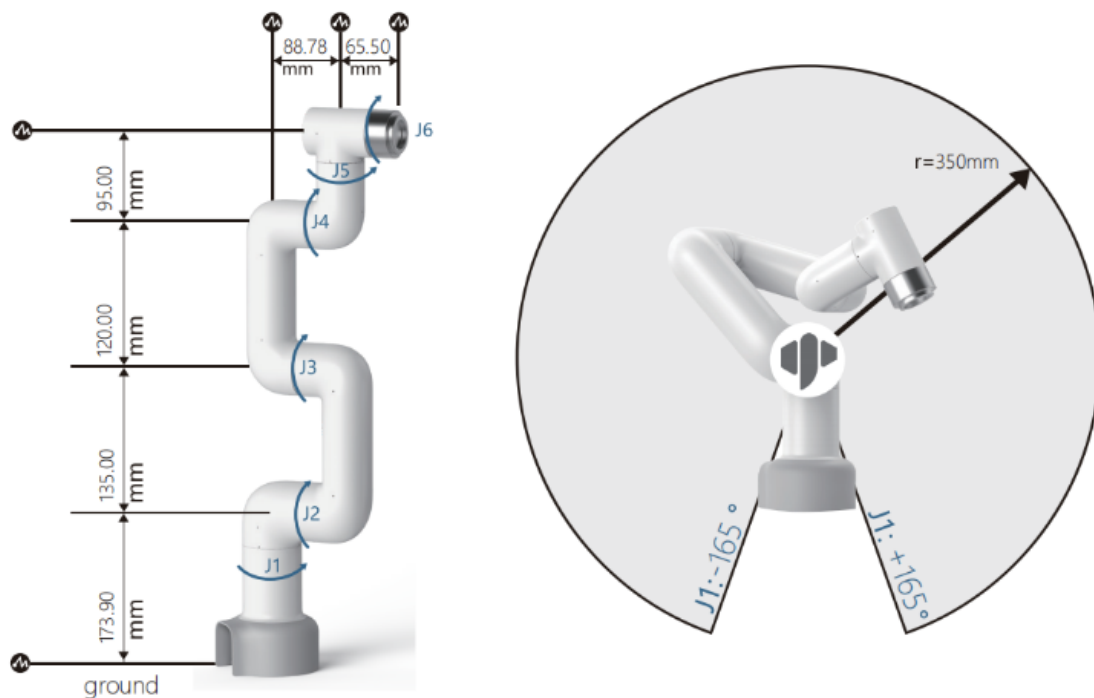
Figure 6.2: The arm's joints specification including the numbers, rotations and the area of reach. [Image from [7]]

The arm uses an M5Stack module[120] as its control unit, which is powered by an ESP32 microcontroller serving as the main processor. The MyCobot 320 robotic arm offers versatile programming and connectivity options to support a wide range of development environments and use cases. It supports several programming languages like Python, C++, C#, and JavaScript, thus making it accessible for both new developers as well as professional robotics engineers. For communication and control, the arm is equipped with Bluetooth, Wi-Fi, and USB connectivity to support wireless and wired operation. The arm possesses a 24V industrial power electrical interface, too, thus it can simply be plugged into the majority of control systems like Programmable

Logic Controllers (PLCs). The arm also includes ROS1 and Arduino support, hence its potential is unlocked for complex robotic applications as well as custom control solutions.

For this project, a GUI has been designed which will be explained in the next section. The ARM will be connected to the PC using USB connection and it uses the arm's python SDK.

6.2   GUI design

Various user interfaces have been proposed in the literature for controlling assistive robotic arms. Of these, manual control is most commonly used and includes both joint space control and end-effector control modes. Manual control gives users complete freedom to employ the arm, but could be cognitively demanding and overwhelming, especially for those with severely disabling conditions or who are using the arm extensively.

Manual arm control requires a minimal level of robot control understanding concerning concepts such as inverse kinematics, joint limits, and workspace constraints. The user must always remember how much movement to introduce to each joint and should never test the physical boundaries of the system. These kinds of requirements generate a lot of cognitive load and make it less accessible or convenient for everyday, day-to-day use over prolonged periods of time.

In order to overcome these challenges, this project proposes a new object-based control solution that reduces the cognitive burden placed on the user. Instead of micromanaging joint angles or end-effector trajectories, users provide higher-level directives by choosing objects. The robot arm then proceeds automatically by drawing on pre-programmed motion plans, enhancing usability as well as accessibility.

Two versions of the GUI that have been deployed to drive the robotic arm are introduced in this section. The first is integrated into the main system GUI for navigation of a wheelchair (described in Section 5.2). Users, within this interface, can switch from the default "Navigation Mode" to the "Detection Mode," which supports object-based control of the robotic arm.

The second implementation of the GUI was designed specifically for experimental comparison. It initially introduces participants to a joint-space control interface as a way of introducing complexity and testing their interaction with a more demanding control setup. This is followed by the introduction to the "Detection Mode" to contrast manual and intelligent object-based control techniques.

The control programs were developed in Python based on the pymycobot library, which provides a high-level interface for controlling the MyCobot 320 robotic arm. There is communication between the arm and the computer through a serial connection, which allows direct transmission of commands and feedback in real-time. The library provides functions that enable control of single joints, end-effector manipulation through end-effector coordinates, and reading the actual joint angles and end-effector position.

Next sections describes the details of the GUI versions.

6.2.1   Object Detection Enhanced ARM Controller

This GUI has been designed and have been integrated with the wheelchair navigation in a compact interface to control the assistive devices. The complete GUI configuration can be seen in Fig.6.3.

The arm controller is activated whenever the "Detection Mode" button in the wheelchair navigation GUI is clicked, as shown previously in Fig. 5.13. Upon pressing "Detection Mode" button, the system transitions into a mode that allows the user to control the robotic arm directly through the interface. The wheelchair control system and how it communicates is described in Section 5.2. This particular section is tasked with the only task of providing information about the arm interface component of the GUI.

The primary objective in the arm control design is to reduce the user's cognitive and physical workload while still enabling the successful completion of a sequence of actions. To be able to adequately demonstrate the usability and feasibility of the concept, the system has been
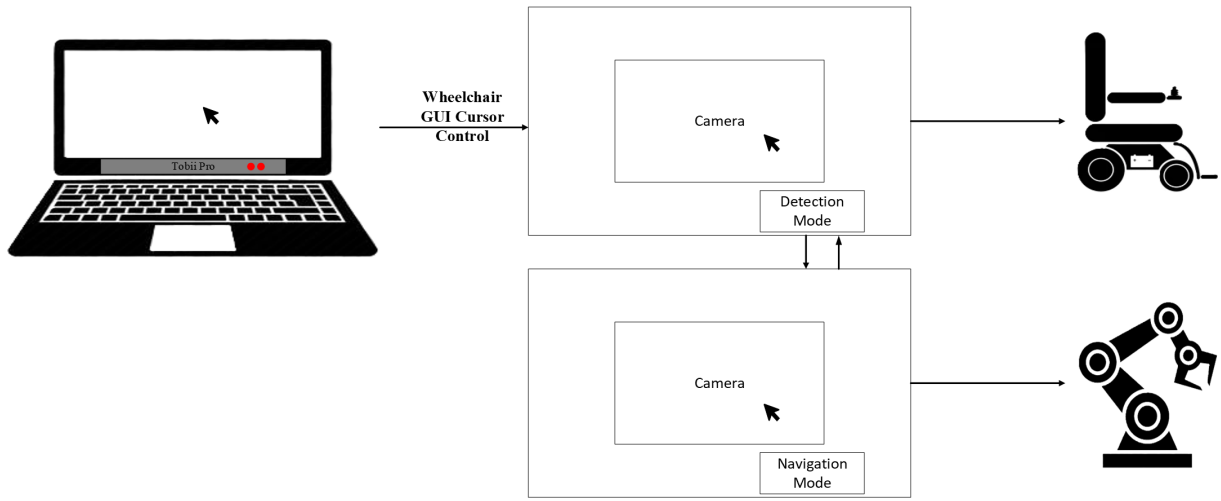
Figure 6.3: The complete configuration of the proposed GUI with the wheelchair navigation element as well as the object-detection enhanced arm controller mode.

deliberately developed to operate with a limited number of predefined objects. This focused implementation allows for a clear evaluation of the interface's usability and robustness, while laying the groundwork for future expansion to more dynamic scenarios.

GUI will initially come up in Wheelchair navigation mode, as depicted in Fig. 5.13. Here, user can control the wheelchair movement. If a user wants to shift the interface to arm control interface, then user will click on the "Detection Mode" button. Once the system shifts to the arm control interface, the GUI will shift to include a live video feed from the camera with a real-time view of the environment. There will be a "Save and Exit" button in the interface as well, where the user will be able to save their data or settings and exit from the arm control mode. The label of the "Detection Mode" button will also be changed to "Navigation Mode", where there will be an option to return to the wheelchair navigation interface. The new arm control interface is shown in Fig. 6.4 where camera view and control actions are exposed for direct hand control of the robotic arm.

When switched to detection mode, designed for pick-and-place tasks using the robotic arm, the object detection layer is activated on the camera feed. For this purpose, YOLOv5s[1] is em-

---

[1] You Only Look Once
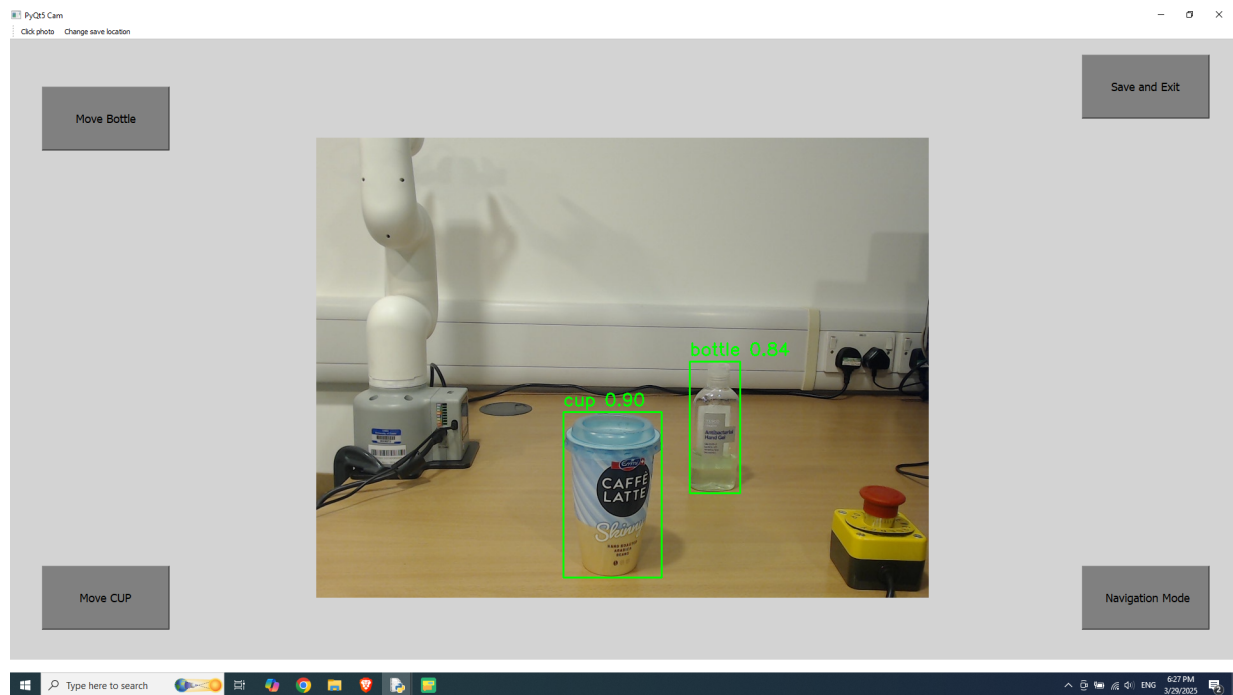
Figure 6.4: The Object Detection mode containing the main buttons, as well as the buttons related to the detected objects.

ployed as the object detection framework [121]. YOLOv5 is pre-trained on the COCO[2] dataset, which includes 80 common objects such as cars, apples, cups, cellphones, and people. Since the model detects a wide variety of objects, including those irrelevant to this project (e.g., surfboards and trains), the interface has been designed to display only predefined objects with a confidence level exceeding 70%.

In real-time object detection, it is not uncommon for a model to miss an object in a frame but pick it up in the very next. This inconsistency can cause buttons for the objects detected to flash in and out, which can be frustrating for users. Additionally, such instability can make it hard for users to provide commands, especially when using a dwell-time mechanism. In a bid to resolve this issue, the system causes buttons to only vanish when the object is unable to be detected with sufficient confidence for 20 consecutive frames. By so doing, unwarranted interruptions are prevented and buttons vanish only when the object has indeed been removed.

---

[2]Common Objects in Context
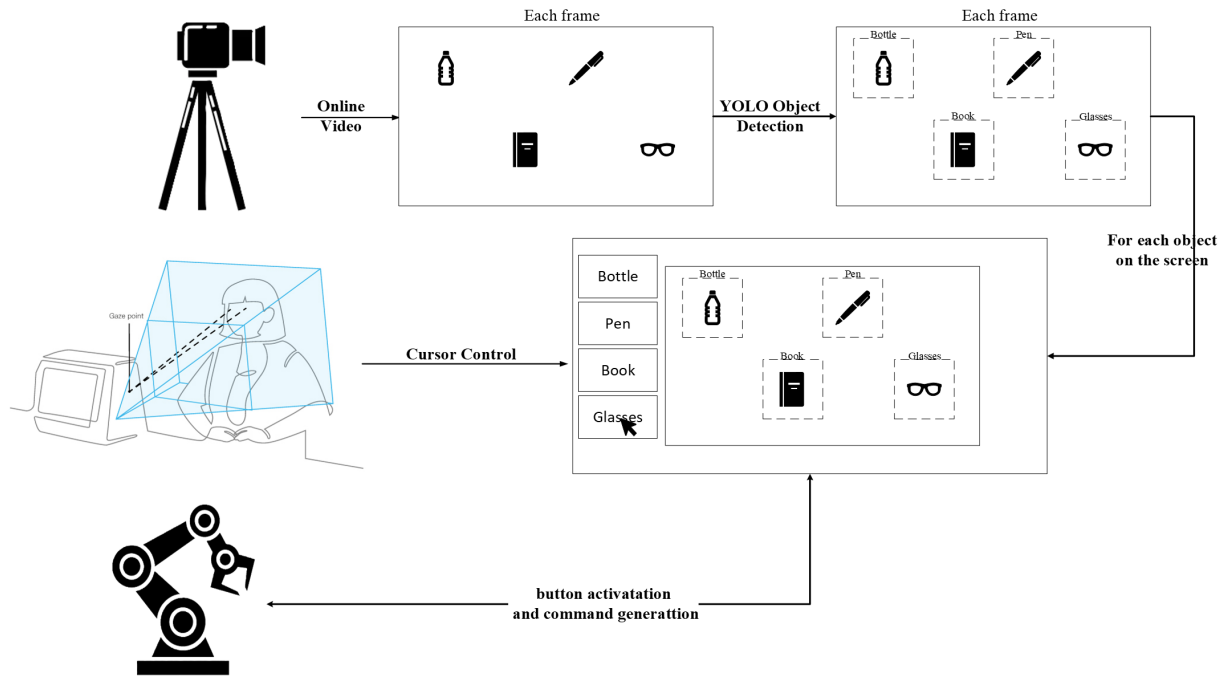
Figure 6.5: The overview of the processes behind the arm section of the GUI. Captured frames will go through the object detection layer and then the bounding boxed for qualified object will be shown around the objects on the screen. Then, the respective operation buttons of the present objects will be presented.

YOLOv5 features several model architectures in various iterations. For this project, YOLOv5s has been utilized, denoted by "s" for "small." This is one of the fastest among those available options and has sufficient accuracy to perform the intended task.

If a qualifying object is detected, a bounding box and the object name are displayed on the video stream. The corresponding button of the object also shows up on the interface. Predefined objects are assigned separate buttons on the GUI with predefined locations and callback functions, which are initially hidden until the respective object is detected. Fig. 6.4 shows the interface with a bottle and a cup being detected and outlined in the video stream. The corresponding buttons for these objects are also visible on the GUI.

By selecting an object-related button, a predefined callback function is triggered. To ensure a consistent experience across all participants and reduce complexity during the experiment, the

objects are positioned in fixed, predefined locations as well as a pre-designated placement area for placement of the objects. The path of the robotic arm for each object is pre-programmed based on these positions. A button click therefore triggers the corresponding pick-and-place action. As shown in Fig. 6.6, during any movement operation of the arm, the corresponding buttons in the interface are temporarily deactivated, and one gets an "ARM is Moving" message displayed. However, the interface and live video feed remain active, and one can watch the process live.
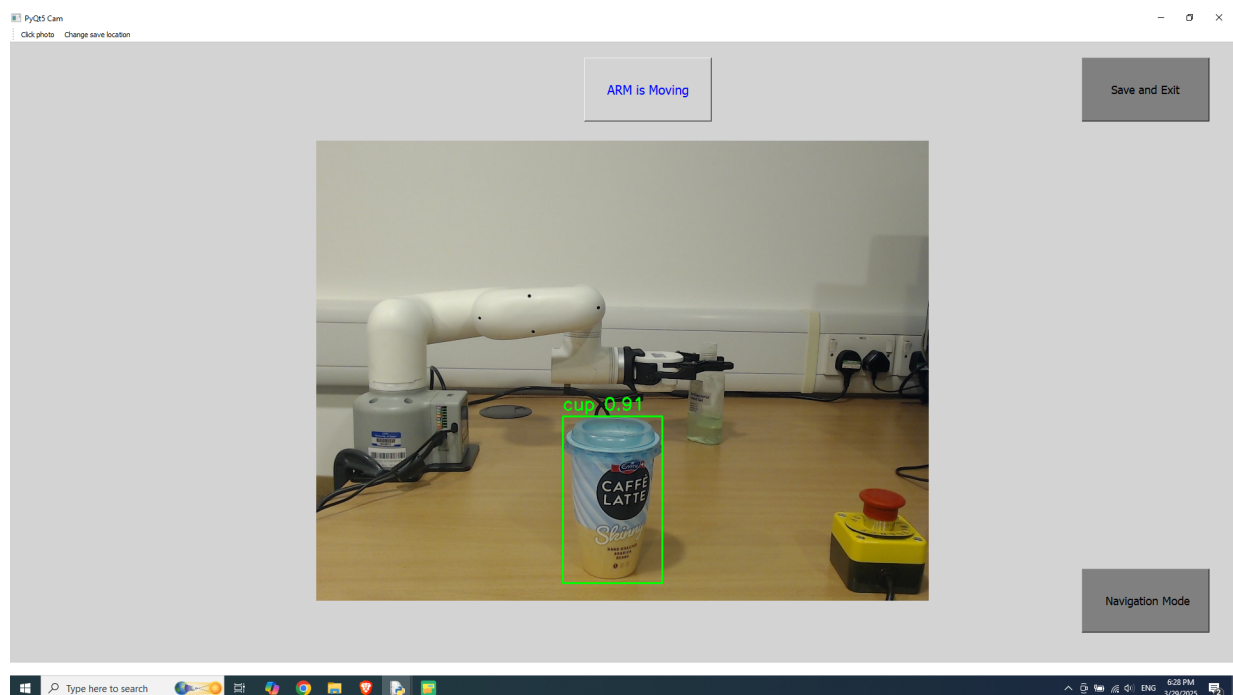
Figure 6.6: The interface showing the arm reaching for the bottle. The Image is also showing the emergency stop button on the bottom right side, as well as the cup. The interface is showing a message indicating that the arm is performing a task and all object related buttons are hidden.

The gaze-based command selection and the activation settings are same as explained in the wheelchair GUI section.

6.2.2 Experiment Version

Since the previous version of the system did not involve a series of effortful decision-making steps, nor was it lengthy enough to induce noticeable fatigue, it wasn't suitable for comparing manual control with the object-detection-assisted method. To address this, an experimental version of the interface was developed specifically to capture more meaningful data.

This experimental version allows participants to manually control joint rotations while viewing a live video feed of the working area. At any point, they can switch to the object detection mode, enabling direct comparison between the two control strategies. The design also encourages users to keep their gaze on the screen, which helps ensure accurate eye-tracking readings.

The interface continues to employ the already used 2-second dwell time for button selection. This interval was maintained specifically to provide the robotic arm enough time to complete its current activity before issuing the next command, leading to more fluid and purposeful operation.

Figure 6.7 is a screenshot of the interface with its joint control mode. Two buttons, each positioned on opposite sides of the screen, control each of the joints. The right buttons increment 10 degrees to the existing rotation of the joint, while the left buttons decrement 10 degrees.

Underneath the live video feed are three buttons taken up by gripper control. The gripper can open up to 9 cm long. The "Open" button fully opens the gripper to its widest extent (9 cm) and the "Close" button fully closes it. The "Half" button also has a mid-position of 4.5 cm. Additionally, short messages on present movements and system activities are displayed at the interface bottom to update users.

On the interface top, there are four main buttons. The "Save and Exit" button allows participants to exit the program securely. The "I'm Tired" button allows participants to flag when they are tired, enabling researchers to identify and analyze occurrences of fatigue while analyzing the data. The "Go Home" button resets all joints to their initial (zero) position and can be used if participants become frustrated or need to reset their current run.

The "Detection Mode" will change the interface to the detection mode which will add the
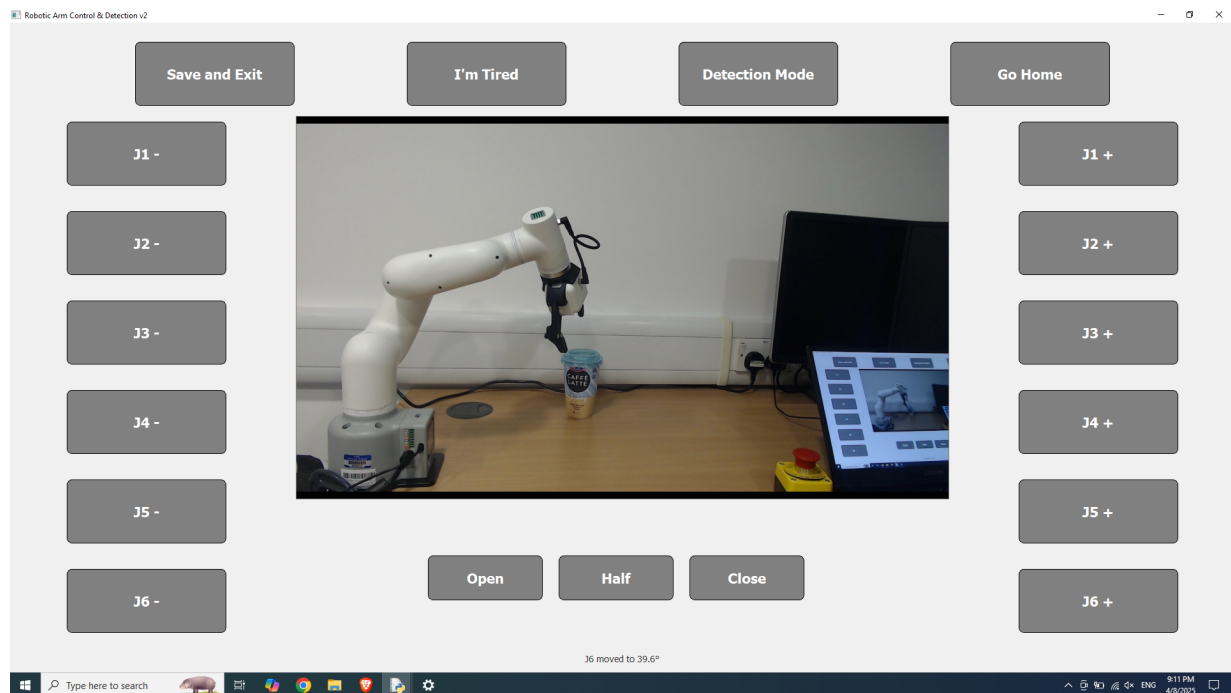
Figure 6.7: "Joint control mode of the experiment interface, displaying control buttons for each joint and the gripper.

object detection layer on top of the video. This mode is illustrated in Fig.6.8. The top buttons stay similar to the joint control mode. The buttons related to the joint control and gripper will disappear and buttons related to the detected objects will appear at the bottom of the video.

During the experiment, to keep the experiment similar for all participants, there is a defined location for the objects which both they would grab themselves or the robot will grab. The trajectories for the automated part has been pre-defined for the robot.

6.3 Experiment Design

An experiment was conducted to evaluate the usability, acceptability, and performance of the proposed method. Beyond performance measurement, the experiment aimed to obtain feedback from users on the system design and how viable it could be for actual deployment.

Manual joint control of robotic arms has been extensively used in the literature. However,
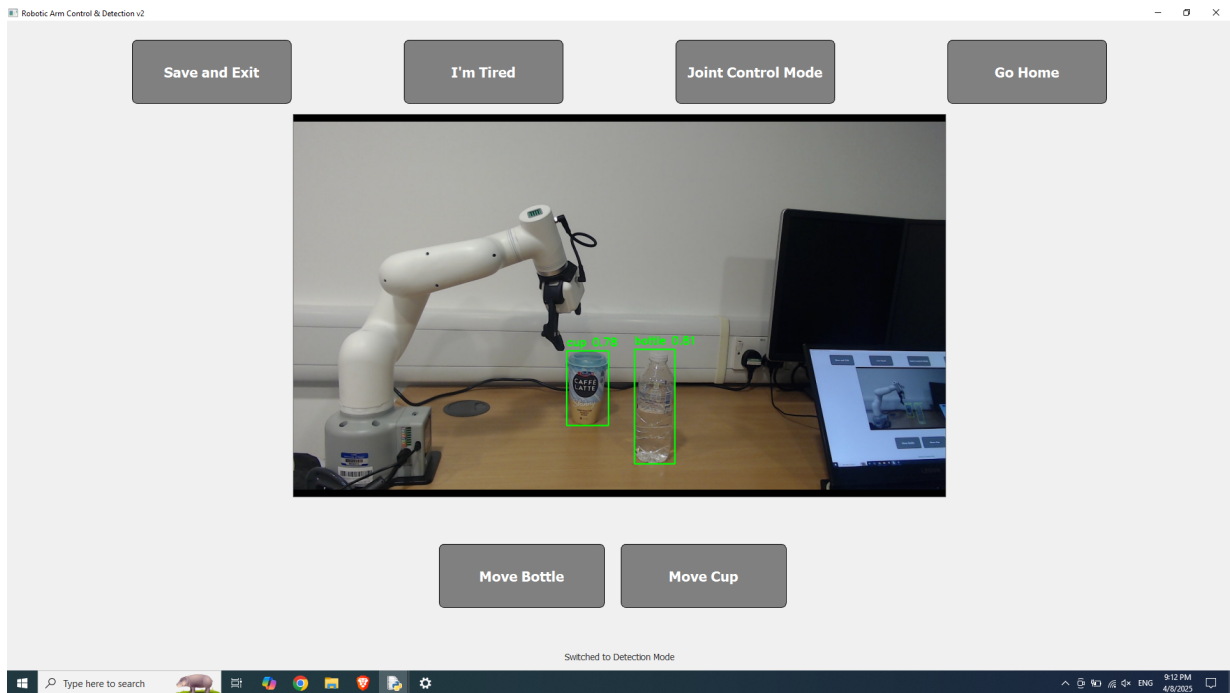
Figure 6.8: Object detection mode of the experiment interface, displaying a detected cup and bottle, along with their corresponding control buttons.

object detection-based control, as presented in this study, is focused on reducing user effort and ease of task completion. To have a fair comparison, as well as to better understand how users interact with manual and autonomous control modes in controlled environments, we set up this experimental design.

The primary aims of the experiment are to compare the user ratings of the traditional and enhanced methods, determine the acceptability of the object detection technique, and gather feedback on potential enhancements and how it may be used in real-world scenarios.

The second version of the ARM GUI, as detailed in Section 6.2.2, was utilized throughout the experiment. The arm was securely mounted on a table, providing a stable and clear working space for arm movement as well as object placement. The arrangement also provided a safe margin between the subject and the arm.

The participants were encouraged to report any sense of tiredness or frustration during the experiment. Apart from the verbal reports, they were also requested to press the "I'm Tired"

button on the interface whenever they felt extremely tired, so that the data could be tagged for later analysis.

The participant is seated in front of a laptop, clear of the operating area of the robotic arm to be safe. A stop button for the robotic arm is positioned somewhere handy at all times. A camera mounted on a tripod captures the working area and objects employed in the task.

Before conducting the experiment, subjects are explained in detail about the system and experimental procedure. A safety and risk assessment was conducted, and an emergency stop button for the robotic arm was positioned within easy reach of the participant. Prior to starting the test, the working area of the robotic arm was cleared of any obstructions, and it was ensured that participants remained at a safe distance from the arm's operational range. Following the explanation, eye tracker calibration is done. Participants are then asked to adjust their seating and posture to ensure comfort and optimal eye-tracking accuracy.

In the first half of the experiment, a single object—a bottle—is used. It is placed in a fixed, reachable position in front of the robot arm. Subjects are instructed to use the interface to reach for the object. Once they have successfully reached it, they are instructed to place the object in a target zone or near the table's edge. This is a timed test for 10 minutes or so. The participants are welcome to attempt the exercise to the best of their ability but, if they become frustrated or exhausted, can choose to skip the manual exercise and proceed to the second section of the experiment.

Additionally, there is a Home position which make the arm go to the start position. It can be used if the robot posture is hard to change or if they are not successful in reforming toward their desired formation and want to try from the start.

The object will be removed and two detection mode objects will be placed on their position. In this part, subjects will need to switch to the detection mode. Then they would select their object of choice and observe the execution of the task.

After the task, users has been asked about their thoughts on the system and how they found

the comparison of the methods. Additionally, they have been asked about their preference in the system and the control design for daily scenarios and activities. The results have been reported in the following sections of the chapter.

6.3.1 Participant Recruitment

We provided the necessary information to the participants prior to the their arrival. Additionally, all the methodology and system has been described and explained in addition to the risk assessment information. The University of Essex Ethics Committee provided ethical approval for the experiment based on the institution's policy guidelines for conducting research with human subjects.

For this experiment, three of the participants who attended the Turtlebot experiment experiment has been invited. The choice has been done to get some feedbacks about the improvements and because of their familiarity with the system and overview of the project and goals.

Written consent has been obtained from the participators before the start of the experiment. Then the system and general informations has been explained. Safety and risk assessment has been described and the Emergency stop button for the arm has been placed in participant reach. Before the test, we ensure that the arm working space is clear of the obstructions and participant is far away from the arm's working space.

The details of the participants has been found in Table.6.1. Two participants were under 30 years old and one over 65 years old.

Table 6.1: Participant information for arm control experiment.

ID	Age	Glasses	Gender
P01	U30	No	Female
P02	U30	No	Male
P03	O65	Yes	Female

6.3.2 Results

This analysis examines pupil diameter characteristics for three participants during an arm control experiment, contextualized by their demographic information. P01 and P02 were younger adults without vision correction, while P03 was an older adult requiring glasses during the experiment. All the information of participants are summarize at Table 6.1. Table 6.2 also includes summary statistics of participant pupil diameter for the session for both eyes.

Table 6.2: Minimum and Maximum pupil dilation in the data, along with Average Mean of each pupil in the arm session.

	Left eye			Right eye		
	Min	Max	Avg	Min	Max	Avg
P01	1.64	3.78	3.07	1.97	3.94	3.17
P02	1.42	3.17	2.50	1.61	3.63	2.54
P03	1.03	3.76	2.94	0.96	3.66	2.38

Table 6.3 presents the performance measures of the session. Completion time refers to the duration between the issuance of the first command in manual mode and the execution of the gripper command which is representing the time taken by participants to navigate from the home position to the object location and attempt to grasp the object. The number of commands indicates the total number of commands issued during this session by each participants. Additionally, the table includes the average command selection time, which presents the mean time participants spent between issuing the commands.

Participant P01 demonstrated the largest average pupil diameters with a range from 1.64 mm to 3.94 mm across both eyes. This larger size could suggest a relatively higher level of cognitive engagement during the task. The Gaussian and histogram plots shown in Fig. 6.9, showing reasonably symmetrical distributions reflecting a potentially focused and steady response throughout their relatively short task duration of less than 4 minutes. Notably, there is a concentration of

Table 6.3: Lap Completion and Command Analysis

Participant No	Completion Time (s)	Number of Commands	Average Selection Time(s)
P01	214.6525793	27	8.255368435
P02	563.8278167	81	7.047847709
P03	801.7663441	62	13.14371056

larger pupil dilations in the right eye.
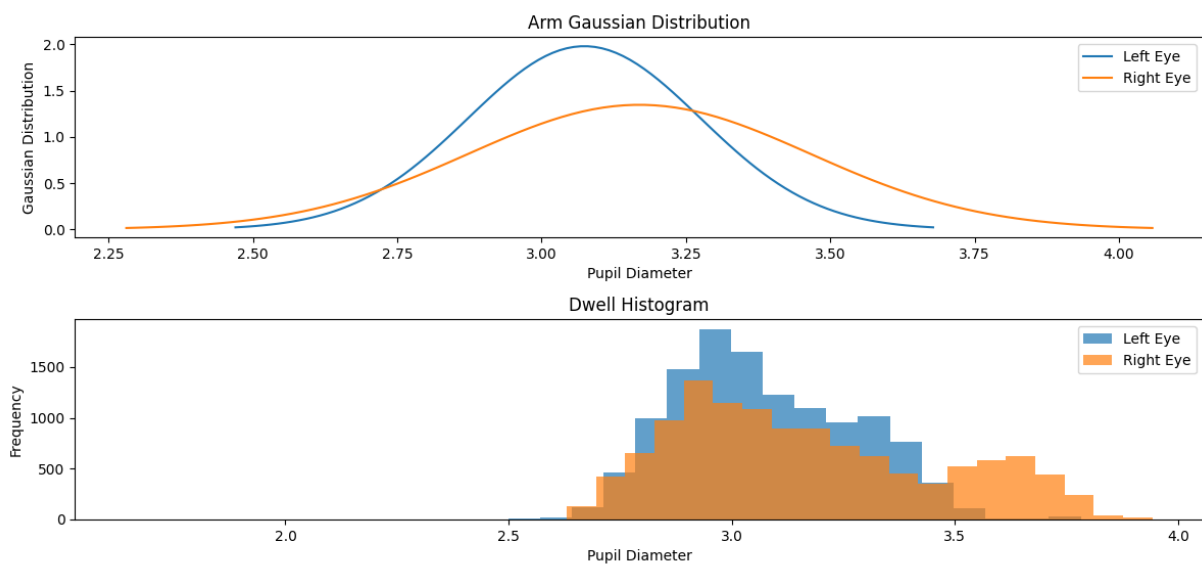
Figure 6.9: Gaussian distribution and histogram of the pupil diameter of P01 during the arm session.

Participant P02 exhibited the smallest average pupil sizes, with ranges of 1.42-3.63 mm. Their left and right eye distributions as shown in Fig. 6.10 were remarkably similar, both centered near 2.5 mm with symmetrical, bell-shaped curves in the plots. This pattern, observed over a longer session duration of about 9.4 minutes, might indicate lower average task load and a calmer, possibly more consistent engagement style compared to P01.

Participant P03 presented the most distinct and variable profile, with longest session of approximately 14 minutes. P03 showed significant asymmetry between her eyes, with the left eye
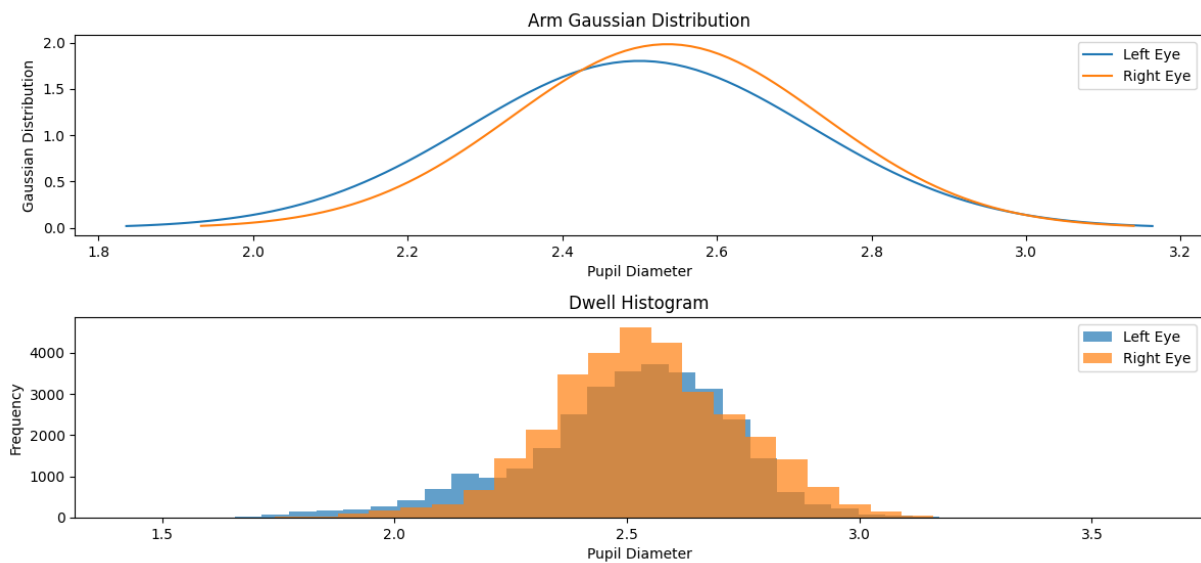
Figure 6.10: Gaussian distribution and histogram of the pupil diameter of P02 during the arm session.

having a larger average diameter (2.94 mm) than the right (2.38 mm). Their overall pupil size range was wide (0.96 mm to 3.76 mm), and the right eye's distribution appeared notably wider and more irregular in the histogram, with an average size lower than any other eye measured, as shown in Fig. 6.11.

These asymmetrical readings have been observed previously and tend to occur in participants wearing glasses, particularly those with bi- or multifocal lenses. Such lenses contain different optical zones that can reflect the infrared light from the eye tracker in varying ways, potentially leading to inconsistencies in pupil detection. Each optical zone may alter the reflected signal differently, which can occasionally introduce variability or affect the reliability of the pupil measurements.

The analysis of pupil data and performance measures in Table 6.3 collectively indicates that the manual control mode for robotic arm manipulation was a cognitively demanding and inefficient process for participants. This was empirically evidenced by the substantial time and effort required, with completion times ranging from 214 to 801 seconds (approximately 3.5 to
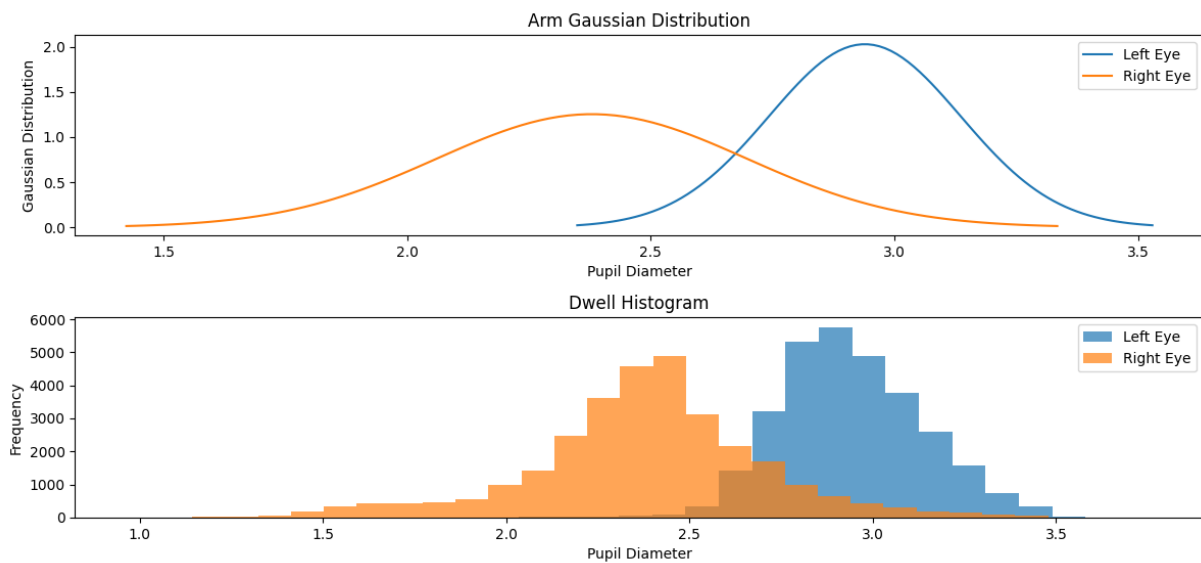
Figure 6.11: Gaussian distribution and histogram of the pupil diameter of P03 during the arm session.

13.4 minutes). Such extensive durations were further compounded by the need for users to issue a high number of discrete commands—between 27 and 81—to manually guide the arm to its target, rendering this approach impractical for repetitive daily tasks.

In contrast, the object-detection-enhanced semi-autonomous mode demonstrated a profound improvement in efficiency. The automated pick-and-place sequence, comprising movements to the home position, navigation to the object, grasping, and placement, was initiated by a single user command following object detection and consistently completed in under one minute for all participants. This dramatic reduction in task completion time is directly attributable to the system's ability to offload the complex, multi-step process of path planning from the user. By effectively transforming a challenging, multi-step manipulation task into a simple, single-command action, this approach demonstrates a substantial reduction not only in overall task duration but also in the associated cognitive effort required from the user, highlighting its immense potential for practical assistive applications in daily living activities.

6.3.2.1 Subjective Feedback

All participants reported that the manual control mode was difficult to use and cognitively demanding. Many found it challenging to memorise the joint numbers and their corresponding directions, which led to confusion during operation. Some participants described the manual mode as frustrating and even boring, particularly when used for routine tasks.

Since the controller moved the robotic arm in discrete steps, several users expressed difficulty with the step size, noting that a 10-degree increment was sometimes too small to be efficient, while at other times it felt too large for precise control. Participants suggested they would prefer continuous movement as long as the corresponding control button is pressed.

Additionally, the single camera view provided an insufficient perspective of the workspace, making it difficult to accurately judge distances and operate the arm effectively.

In contrast, participants found the automated control mode significantly easier to use and more practical for common or repetitive daily tasks. They reported that it reduced both mental effort and frustration, making the overall interaction more intuitive and efficient.

6.4 Summary

This chapter addressed the significant challenge of assistive manipulation by extending the gaze-based interface to the control of a robotic arm. The work was motivated by the profound cognitive load associated with the manual, joint-by-joint control of multi-degree-of-freedom manipulators. To overcome this, a semi-autonomous control paradigm was developed, which involved the successful technical integration of a real-time object detection model into the existing user interface. The efficacy of this novel approach was then evaluated through an experiment that directly compared its performance against a traditional manual control mode.

The results of the comparative study were conclusive. The manual control task proved to be cognitively demanding and inefficient, requiring completion times of several minutes and a high

volume of discrete user commands. In stark contrast, the semi-autonomous mode, initiated by a single gaze command, completed the entire pick-and-place sequence in under one minute. This objective data was strongly supported by the subjective feedback, in which participants described the manual mode as frustrating and difficult, while finding the object-based mode to be intuitive, efficient, and highly practical.

In conclusion, the key contribution of this chapter is the successful validation of the semi-autonomous, object-based control paradigm for assistive manipulation. It demonstrates that by offloading the complex process of path planning from the user to the system, a challenging and cognitively taxing task can be transformed into a simple, single-command action. Having now established the viability of the core components of the assistive system for both navigation (Chapter 5) and manipulation (this chapter), the following chapter will provide a general discussion of the project as a whole, synthesizing these findings to reflect on the overall scientific contributions and limitations.

Chapter 7

Discussions

This chapter provides a consolidated discussion of the key findings from the entire research project. It synthesizes the results from the preceding experimental chapters to evaluate the overall performance, usability, and scientific contributions of the developed assistive system. The discussion will reflect on the findings in the context of the initial research questions and objectives, addressing the successes and challenges encountered throughout the project's development and validation.

The eye-tracking method was generally found to be both effective and acceptable to users. In particular, the recorded pupil diameter data proved useful in detecting user intention, supporting its potential as an input signal for adaptive interfaces. However, some patterns in the data collected was highly individual-specific, these patterns remain unexplained and certain questions could not be fully addressed.

7.1 Comparative Analysis of Self-reported Demands

Table 7.1 presents an overview of the average responses across different task load factors. On the scale used, -10 represents very low demand, while $+10$ indicates very high demand. For the

performance dimension specifically, the scale is inverted: -10 indicates perfect performance, while $+10$ represents complete failure. It is important to note that the negative values across all dimensions suggest that participants generally perceived the tasks as having a low overall workload.

A detailed analysis of these values reveals two distinct trends. Firstly, there was a clear improvement in several key areas during the wheelchair experiment. The scores for Physical Demand, Temporal Demand, Effort, and Performance all decreased, indicating that the refined interface with continuous control was perceived as less physically taxing, less rushed, and more effective at helping users achieve their goals. This improvement can be directly attributed to the design enhancements made to the system following the initial TurtleBot trials.

In contrast, the scores for Mental Demand and Frustration increased. This apparent contradiction is highly significant and is likely attributable to the change in the experimental context itself. Navigating a large, physical wheelchair within a real environment carries a heightened sense of consequence compared to guiding a small robot on a printed path. The potential for real-world collisions and the need for greater situational awareness in the more realistic wheelchair task placed a higher cognitive load on the participants. Therefore, while the interface itself became more efficient and easier to use, the cognitive demands of the higher-fidelity task environment led to an increase in perceived mental demand and frustration.

This finding highlights the critical importance of evaluating assistive technologies in realistic contexts, as the task environment can have a significant impact on the user's perceived workload, independent of the interface's design.

7.2 Performance

Performance metrics showed clear improvement in the second rounds of the experiments, indicating both system effectiveness and a positive learning curve. These results suggest that the

Table 7.1: Comparison of average results from NASA TLX questionnaire from all participants during the experiments done with turtlebot and the wheelchair (value range -10 to 10).

Demand	TurtleBot	Wheelchair
Mental Demand	-4.44	-3.66
Physical Demand	-2.94	-5.83
Temporal Demand	-4.28	-6.83
Performance	-5.39	-8.5
Effort	-1.22	-3.66
Frustration	-6.89	-5.83

system is not only usable but also easy to learn, with users becoming more proficient over time.

During the wheelchair navigation task, a significant enhancement was observed in key performance indicators, particularly in lap completion time. This improvement was attributed not only to increased user familiarity but also to reduced command generation delays, made possible by the intention-based model employed in the system.

Performance can also be a key indicator of a system's usability, and in this study, it reflected not only participants' positive experiences but also their ability to effectively operate the system as intended. Across the experiments, participants were consistently able to complete the required tasks using the proposed system, demonstrating its practical applicability.

7.3 Usability and Acceptability

The initial experiment involved driving with a mobile robot using participants to control the system through a gaze-based GUI. Overall, the concept and design were received favourably. The participants liked the intuitive gaze control and the abilities of the system. While the TurtleBot as an actuality was a good prototype, a couple of the participants said it didn't particularly reflect real-life conditions, decreasing its realism to some extent.

The follow-up experiment with the use of a wheelchair worked better and interactively as a test. The volunteers were also upbeat in their responses, commenting that the arrangement was much more realistic and very closely simulated the manner in which such a system would operate in reality.

In both trials, results suggested high promise for the acceptability and usability of the system. Participants, especially those who returned for follow-up trials, saw notable improvement in design and responsiveness. Many preferred the "model lap" condition, in which there was faster command activation—making the interaction feel smoother and more responsive.

Although the participants only spent approximately 20 minutes in total using the system, there was an evident improvement in their performance. This indicates that the system is intuitive enough to be explained and taught by intended users within a matter of only a few brief sessions.

The performance enhancements noted in the wheelchair trials also illustrate the usability and practicality of the system. The results demonstrate that users can easily be trained to operate the interface and control mechanism and hence it is a viable solution for real-world implementation. The results also confirm the feasibility of the system for further testing—first with the users who utilize wheelchairs on a daily basis, then with the targeted users the system will eventually be used by user testers.

The arm experiment too gave a positive indication regarding the object-detection-based automated approach being acceptable. The method can easily enhance productivity to a significant extent and reduce time to complete everyday tasks, hence being most effective for individuals who have restricted mobility.

While automated control was very useful, participants suggested that manual control is useful in some situations—perhaps most notably on creative or delicate tasks. During discussions, some liked shared control and others liked use of the end-effector coordinates. Based on this feedback, a future version of the system could offer all three control modes—automated, joint, and coordinate-based—and allow users to select the option best meeting their needs. Also, to

accommodate individual needs and preferences, some modalities may be enabled or disabled so that users have maximum flexibility and personalization in their use of the system.

7.4 Accessibility and affordability

As mentioned in the introduction, care expenses can be very high and mostly unaffordable for most individuals. By providing affordable assistive systems and devices that promote independence, one can reduce long-term care-giving expenses to a great degree. Apart from economic benefits, these systems can also have beneficial impacts on the mental health of users by inducing a sense of independence and autonomy.

While current systems are not yet capable of giving complete independence to individuals with severe motor or upper-limb impairment, they can significantly enhance the level of independence such people can have. Through such technology, users are capable of executing a greater percentage of their daily living tasks autonomously—something that would be difficult or impossible for them to do without such systems.

Use of a wheelchair can actually give much benefit compared to the lack of access to mobility aids. The degree of benefit will, however, depend on the type of disability and specific needs of the user. The most common means of using a wheelchair is through a joystick, which will be unsuitable for users with limited hand movement or power.

For users with more serious motor impairments, one of the most affordable assistive devices currently available is the sip-and-puff controller. While affordable, such systems are extremely limited in function. They typically only offer rudimentary directional control and even limited control over speed, which can restrict the user's overall mobility experience. Eye-tracking-based systems offer a more flexible and modular solution. They can also be tailored according to the needs and requirements of the user, providing a more extensive set of control capabilities in addition to point-to-point navigation. For example, a GUI that is under gaze control can be

configured to provide numerous functions such as video conferencing, web browsing, and similar activities on the host machine. This not only enhances mobility but also supports communication and interaction, making it much more empowering and effective in daily life.

With the addition of other assistive devices such as a robotic arm, the overall level of independence of users can be greatly enhanced. While the initial cost of commercially available robotic arms such as the JACO arm is as high as $35,000 [94], most of these devices remain manually operated. Other devices, the iARM [96], are designed to be controlled by a joystick mounted on a wheelchair or by a secondary joystick mounted on the wheelchair. This leaves the option of integrating the gaze-controlled system developed in this work with these joystick-controlled robotic arm devices. The system could be adapted to control the wheelchair and the assistive arm with minimal modifications through the same gaze-controlled interface.

The system built in this project is a proof of concept for an affordable and inexpensive solution tailored to individuals with severe motor impairments. The mechanical components are all printable in 3D, and the essential parts used in the prototype can be purchased for approximately £40. In terms of eye-tracking equipment, there are many pieces of equipment available to purchase at all price points, so the configuration can be adjusted to accommodate all budgets. The whole system is thus extremely budget-friendly in relation to much that is commercially offered—especially considering the broader scope of applications supported by gaze-based input. Besides, eye-tracking technology is increasingly finding applications in mass-market applications such as gaming and user experience studies, which is cutting costs while improving accuracy and usability. Such wider availability further adds to the legitimacy of designing usable, gaze-based assistive systems for deployment in the field.

Chapter 8

Conclusion and future work

This thesis presents the development of an adaptive gaze-based human–machine interface to enhance assisted daily living, addressing critical challenges in the usability and affordability of current assistive technologies for individuals with severe mobility impairments.

First, an adaptive, intention-based activation method has been developed, utilizing real-time pupil dilation readings as an alternative to the fixed dwell-time activation commonly used in gaze-based interfaces. By detecting the user's intention to focus through pupil responses, the system adapts in real-time, offering a more personalized and responsive human-computer interaction.

The second key highlight is the design of a modular add-on robotic controller that transforms a standard powered wheelchair into a smart, gaze-controlled system. This low-cost, 3D-printable mechanism can be easily adapted for use with various wheelchair joysticks. The robotic controller is designed for quick mounting and back-drivability, ensuring that it preserves the original functionality of the wheelchair joystick while enabling intuitive gaze-based control.

Additionally, an object detection model was integrated into the gaze-controlled GUI to improve the usability and ease of operating the assistive robotic arm during daily living activities. This integration enables a semi-autonomous interaction with the assistive device, significantly reducing the cognitive load and physical effort required from the user. As a result, the system

becomes more accessible, efficient, and user-friendly-particularly for repetitive or routine tasks.

To evaluate the system's performance, usability, and acceptability, user studies were conducted at various stages throughout the project. The experiments consistently proved promising results, with participants successfully completing the required tasks and reporting positive experiences. The interface was found to be intuitive and easy to learn, even for first-time users. Performance metrics demonstrated strong user performance, which improved with familiarity and was further enhanced by the adaptive activation method. Participants also described the system as user-friendly, comfortable to operate, and effective for controlling the devices.

Overall, these findings validate the system's potential as a practical, accessible, and efficient interface for interacting with assistive devices, supporting improved independence and daily living.

8.1 Limitations of the Thesis

While this thesis successfully demonstrates the feasibility and benefits of the proposed assistive system, it is important to acknowledge the limitations that define the boundaries of its contributions and provide a clear context for future work. A primary limitation relates to the participant cohort and the experimental environment. All studies were conducted with healthy, non-disabled participants in controlled laboratory or arena settings. Although this was a necessary and deliberate choice for initial feasibility testing, safety, and model development, it means that the findings regarding usability, performance, and cognitive load cannot be directly generalized to the target clinical population, who may have different physical, cognitive, and experiential needs. Similarly, the controlled nature of the experimental environments lacks the unpredictability and complexity of real-world scenarios, such as a cluttered home or a busy public space, thereby constraining claims about the system's performance in an uncontrolled environments.

Further limitations pertain to the scope and duration of the validation. The experimental tasks

were of a relatively short duration, which precluded a thorough investigation into the effects of long-term use, such as skill retention, habituation, or genuine user fatigue—factors that are critical for a daily-use assistive device. The 3D-printable wheelchair controller, while validated as a functional prototype, has not undergone the long-term reliability and durability testing required for a final product. Finally, the semi-autonomous robotic arm control, while successful, was validated with a limited set of predefined objects in fixed locations. Consequently, the system's ability to generalize its manipulation capabilities to a wide variety of objects in unstructured and dynamic environments remains an open question for future investigation.

8.2 Future Work

With the positive and promising findings from this study, future research will focus on overcoming the still-persistent difficulties and further evolving the system to offer a fully accessible and efficient device for individuals with severe motor disabilities.

One of the key areas that has been highlighted by feedback gained through visits to stroke survivor charities and support groups is that of fatigue. Fatigue is consistently quoted as one of the most prominent issues faced by people with mobility impairments. Importantly, fatigue does not always have a noticeable effect on others, and the level of fatigue can be extremely variable between individuals, making it a very personal experience.

According to the literature, fatigue may be reflected in physiological indicators such as pupil dilation. Although the current system was evaluated through multiple experiments with healthy participants and various data were collected, none of the participants reported noticeable fatigue or cognitive overload during the trials. This may be due to the brief duration of the experiments. Therefore, longer experiments with larger durations are necessary to study the potential relationship between pupil dilation and fatigue in more detail.

In addition, future testing with actual end users—i.e., individuals with spinal cord injury

or severe motor impairments—is critical to validate the system's usability, acceptability, and overall performance in real-world contexts. The tests will provide valuable information on how the system can be refined and adapted to meet the needs of the target user group, who have complex and varied requirements.

8.2.1   Investigating Pupil Responses and the effect of User Fatigue

Future testing and measurement with individuals with motor disability might be more helpful in understanding the effect of fatigue using the system. Subject participants in experiments conducted in this project, as a whole, did not report feeling much fatigued, which placed a restriction on our ability to draw firm conclusions about its effect. Despite some reporting that their eyes were fatigued, this did not transfer to an overall sense of tiredness or mental fatigue.

One possible explanation for this could be the comparatively short duration of the test sessions. None of the participants operated the system for any long period of time, which was likely to keep fatigue-related feedback to a minimum. However, for real users who may be using this system for routine tasks over long periods of time, fatigue could become an issue. Therefore, more long-term testing is required to see how fatigue could affect usability, particularly for full-time users who are using the system as their only means of interaction.

8.2.2   Enhancing the Wheelchair Controller

Additionally, the system design can be used on other wheelchairs with slight modification, the system has been designed with mindfulness toward the cost. Therefore the system might be a potentially viable and accessible product. The plan is to explore the possibilities and options to work toward this idea. The GUI can also be a stand-alone software product used in conjunction with the mechanism. Further, since the mechanism is controlled by Bluetooth, it is also possible to create a companion mobile app. Additionally, the app can offer a significant feature to

caregivers such that they can control and drive the wheelchair remotely, reducing the effort of physical pushing and offering more convenience and security in care-giving scenarios.

There are various alternatives and options to make the GUI visually more appealing and providing more functionality. For instance, one of the ways is adding four additional directional buttons that shift the mechanism half-way through, facilitating slower movements. A second suggestion is to implement a proportional control system for the direction and speed of the joystick, whereby enables users to issue commands for the joystick in the directions based on their desired speed. These additions would offer greater flexibility and control, but would require initial testing and assessment by actual users to see if they are viable and useful.

Since the system is intended for individuals with serious motor impairments, it's also important to note that users could have cognitive impairments. In addition, since the system will be employed for extended periods of everyday use, it must be functional, reliable, and unthreatening. A cluttered or complex interface would become a barrier rather than a benefit.

While there is enormous scope for expanding the system's functionality more with additional features, the current version has been deliberately kept minimal for the purposes of testing and evaluation. The simplicity and ease have been ensured through this method, but primary functionality has been maintained as the priority and the system has been maintained in a manner that further options can be added later on according to user requirements and needs.

8.2.3 Improving Wheelchair Safety and Situational Awareness

Safety is a critical concern in the development and deployment of assistive technologies. While all participants in the study reported feeling that the current system was safe and secure, the situation may differ for individuals with complete loss of hand mobility, who are unable to operate the existing emergency stop mechanism. Therefore, future iterations of the system should include an alternative emergency stop method tailored to users with severe physical impairments. Possible solutions may include voice commands, proximity-based triggers, or a sip-and-puff

controller, which should be carefully evaluated and selected in consultation with the target user group.

Beyond emergency stopping, the final system should incorporate comprehensive safety features for obstacle detection and avoidance. Although fully automated obstacle avoidance may be the safest approach, it will perceived as restrictive, particularly in narrow or cluttered environments. alternative solutions that enhance user spatial awareness could be more effective in manual control modes. One approach would be to strategically placed proximity sensors around the wheelchair could function similarly to automotive parking sensors, offering real-time feedback about nearby obstacles. These features could be optionally enabled or disabled based on user preferences, thereby offering a customizable and flexible safety interface.

Another promising approach is the integration of additional cameras positioned at various angles, enabling users to switch between views and gain a more comprehensive understanding of their surroundings. This feature extends beyond obstacle avoidance and can support a range of additional use cases. For instance, users could benefit from improved situational awareness when interacting with pets, locating objects on the floor, or observing items placed in hard-to-see areas. Such enhancements not only contribute to safer navigation but also promote greater independence and usability in everyday activities.

8.2.4   Advancing Robotic Arm Control

Safety is still one of the primary concerns when dealing with robotic arms, especially when they are mounted on wheelchairs. One of the primary reasons why the robotic arm was not mounted in this project was due to fear of accidental motion and collision into the user or other objects. These safety concerns highlight one of the most important priorities for future research—i.e., the development of safer, lower-cost robotic arms or control interfaces that are generalizable and can be shared across platforms.

One of the concepts with promise is the inclusion of an additional depth camera and sensors

on the end-effector of the robotic arm. These sensors could be utilized in conjunction with object detection algorithms to accurately track the target object. When the object is identified, the system automatically calculates and executes the required motions, but also allow manual override or fine-tuning as needed. This type of hybrid solution—automated assistance with discretionary manual control—could be applied as an add-on to existing assistive arms, e.g., the iARM.

There are other modalities and options which can be done in this area to achieve the semi-automated object handling. There are many projects covering this area for industrial settings. It can be good to implement an approved approach in this setting but with the safety concerns in mind. Industrial systems often assume the presence of able-bodied users who can react quickly in case of unexpected behaviour from the robot. For example, emergency stop buttons or the ability to physically intervene and redirect the robot are considered sufficient in such contexts. Although with people with severe mobility difficulty, it might not be possible. As a result, the safety mechanisms must be far more robust, proactive, and autonomous.

Bibliography

[1] cornea. Available at : `https://www.cancer.gov/publications/dictionaries/cancer-terms/def/cornea`. Accessed: 2025-02-24.

[2] Tobii. Tobii Pro Nano screen-based eye tracker. Available at : `https://www.tobii.com/products/discontinued/tobii-pro-nano`. [Accessed 12-04-2025].

[3] Parastoo Azizinezhad and Anirban Chowdhury. Exploring pupil dilation as an indicator of performance in gaze-based robot navigation for assistive technology. *2024 IEEE International Conference on Modelling, Simulation & Intelligent Computing (MoSICom)*, 2024.

[4] (Accepted) Parasto Azizinezhad and Anirban Chowdhury. valuating a gaze-controlled navigation interface: A user-centered approach. In *he 47th Annual International Conference of the IEEE Engineering in Medicine and Biology Society (EMBC)*, 2025.

[5] Parastoo Azizinezhad, Hamidreza Ghonchi, and Anirban Chowdhury. Pupil diameter classification using machine learning during human-computer interaction. *2024 IEEE International Conference on Omni-layer Intelligent Systems (COINS)*, pages 1–6, 2024.

[6] Abilize pursuit. Available at : `https://www.who.int/news-room/fact-sheets/detail/assistive-technology`. Accessed: 2023-10-10.

[7] Elephant Robotics. Coordinate System; GitBook. `https://docs.elephantrobotics.com/docs/mycobot_320_m5_en/2-ProductFeature/2.1_320_M5_product/2.1.5-CoordinateSystem.html`. [Accessed 07-04-2025].

[8] Disability (2023). Available at : `https://www.who.int/news-room/fact-sheets/detail/disability-and-health`, March 2023. Accessed: 2024-11-18.

[9] Assistive technology (2023). Available at : `https://www.who.int/news-room/fact-sheets/detail/assistive-technology`, January 2024. Accessed: 2024-11-18.

[10] Assistive technology in the uk 2022 report. Available at: `https://analytics.dkv.global/AssistiveTech-in-UK-2022.pdf`. Accessed: 2023-07-26.

[11] NHS 111 Wales. Locked-in syndrome, disorders of consciousness. `https://111.wales.nhs.uk/encyclopaedia/d/article/disordersofconsciousness`. [Accessed 19-04-2025].

[12] Jesse Leaman and Hung Manh La. A comprehensive review of smart wheelchairs: Past, present, and future. *IEEE Transactions on Human-Machine Systems*, 47(4):486–499, 2017.

[13] Gabriel Pires, N Honorio, C Lopes, U Nunes, and AT Almeida. Autonomous wheelchair for disabled people. In *ISIE'97 Proceeding of the IEEE International Symposium on Industrial Electronics*, pages 797–801. IEEE, 1997.

[14] Yi-Xing Liu, Zhao-Yuan Wan, Ruoli Wang, and Elena M. Gutierrez-Farewik. A method of detecting human movement intentions in real environments. In *2023 International Conference on Rehabilitation Robotics (ICORR)*, pages 1–6, 2023.

[15] Yogesh Kumar Meena, Hubert Cecotti, Braj Bhushan, Ashish Dutta, and Girijesh Prasad. Detection of dyslexic children using machine learning and multimodal hindi language eye-gaze-assisted learning system. *IEEE Transactions on Human-Machine Systems*, 53(1):122–131, 2023.

[16] Anirban Chowdhury and Javier Andreu-Perez. Clinical brain–computer interface challenge 2020 (cbcic at wcci2020): Overview, methods and results. *IEEE Transactions on Medical Robotics and Bionics*, 3(3):661–670, 2021.

[17] Pabba Saideepthi et al. Sliding window along with eegnet-based prediction of eeg motor imagery. *IEEE Sensors Journal*, 23(15):17703–17713, 2023.

[18] Anirban Chowdhury, Ashish Dutta, and Girijesh Prasad. Corticomuscular co-activation based hybrid brain-computer interface for motor recovery monitoring. *IEEE Access*, 8:174542–174557, 2020.

[19] Andrés Úbeda, Eduardo Iáñez, and José M Azorín. Shared control architecture based on rfid to control a robot arm using a spontaneous brain–machine interface. *Robotics and Autonomous Systems*, 61(8):768–774, 2013.

[20] Qiyun Huang, Zhijun Zhang, Tianyou Yu, Shenghong He, and Yuanqing Li. An eeg-/eog-based hybrid brain-computer interface: application on controlling an integrated wheelchair robotic arm system. *Frontiers in neuroscience*, 13:1243, 2019.

[21] Md Samiul Haque Sunny, Md Ishrak Islam Zarif, Ivan Rulik, Javier Sanjuan, Mohammad Habibur Rahman, Sheikh Iqbal Ahamed, Inga Wang, Katie Schultz, and Brahim Brahmi. Eye-gaze control of a wheelchair mounted 6dof assistive robot for activities of daily living. *Journal of NeuroEngineering and Rehabilitation*, 18(1):1–12, 2021.

[22] Maged Iskandar, Gabriel Quere, Annette Hagengruber, Alexander Dietrich, and Jörn Vogel. Employing whole-body control in assistive robotics. In *2019 IEEE/RSJ International Conference on Intelligent Robots and Systems (IROS)*, pages 5643–5650. IEEE, 2019.

[23] Aarti Malhotra. Socially intelligent affective ai. In *Proceedings of the AAAI Conference on Artificial Intelligence*, volume 36, pages 12888–12889, 2022.

[24] Lian Zhang, Joshua Wade, Dayi Bian, Jing Fan, Amy Swanson, Amy Weitlauf, Zachary Warren, and Nilanjan Sarkar. Cognitive load measurement in a virtual reality-based driving system for autism intervention. *IEEE transactions on affective computing*, 8(2):176–189, 2017.

[25] Tao Xu, Hongtao Wang, Guanyong Lu, Feng Wan, Mengqi Deng, Peng Qi, Anastasios Bezerianos, Cuntai Guan, and Yu Sun. E-key: an eeg-based biometric authentication and driving fatigue detection system. *IEEE Transactions on Affective Computing*, 14(2):864–877, 2021.

[26] Päivi Majaranta and Andreas Bulling. Eye tracking and eye-based human–computer interaction. *Advances in physiological computing*, pages 39–65, 2014.

[27] Kyle Krafka, Aditya Khosla, Petr Kellnhofer, Harini Kannan, Suchendra Bhandarkar, Wojciech Matusik, and Antonio Torralba. Eye tracking for everyone. In *Proceedings of the IEEE conference on computer vision and pattern recognition*, pages 2176–2184, 2016.

[28] Oskar Palinko, Andrew L Kun, Alexander Shyrokov, and Peter Heeman. Estimating cognitive load using remote eye tracking in a driving simulator. In *Proceedings of the 2010 symposium on eye-tracking research & applications*, pages 141–144, 2010.

[29] Muneeb Imtiaz Ahmad, Ingo Keller, David A Robb, and Katrin S Lohan. A framework to estimate cognitive load using physiological data. *Personal and Ubiquitous Computing*, pages 1–15, 2020.

[30] Yao Guo, Daniel Freer, Fani Deligianni, and Guang-Zhong Yang. Eye-tracking for performance evaluation and workload estimation in space telerobotic training. *IEEE Transactions on Human-Machine Systems*, 52(1):1–11, 2022.

[31] Rahul Gavas, Debatri Chatterjee, and Aniruddha Sinha. Estimation of cognitive load based on the pupil size dilation. In *2017 IEEE International Conference on Systems, Man, and Cybernetics (SMC)*, pages 1499–1504, 2017.

[32] Maria Borgestig, Jan Sandqvist, Richard Parsons, Torbjörn Falkmer, and Helena Hemmingsson. Eye gaze performance for children with severe physical impairments using gaze-based assistive technology—a longitudinal study. *Assistive technology*, 28(2):93–102, 2016.

[33] Chi-Shin Hwang, Ho-Hsiu Weng, Li-Fen Wang, Chon-Haw Tsai, and Hao-Teng Chang. An eye-tracking assistive device improves the quality of life for als patients and reduces the caregivers' burden. *Journal of motor behavior*, 46(4):233–238, 2014.

[34] Y. K. Meena et al. Emohex: An eye tracker based mobility and hand exoskeleton device for assisting disabled people. In *2016 IEEE International Conference on Systems, Man, and Cybernetics (SMC)*, pages 002122–002127, 2016.

[35] Jonathan L Rosch and Jennifer J Vogel-Walcutt. A review of eye-tracking applications as tools for training. *Cognition, technology & work*, 15:313–327, 2013.

[36] James F Cavanagh, Thomas V Wiecki, Angad Kochar, and Michael J Frank. Eye tracking and pupillometry are indicators of dissociable latent decision processes. *Journal of Experimental Psychology: General*, 143(4):1476, 2014.

[37] Debatri Chatterjee et al. Real time estimation of task specific self-confidence level based on brain signals. *Multimedia Tools and Applications*, 80(13):19203–19217, 05 2021.

[38] Guus van Loon, Felix Hermsen, and Marnix Naber. Predicting product preferences on retailers' web shops through measurement of gaze and pupil size dynamics. *Journal of Cognition*, 5(1), 2022.

[39] Y. K. Meena et al. A hindi virtual keyboard interface with multimodal feedback: A case study with a dyslexic child. In *Proceedings of the 32nd Human Computer Interaction Conference*, 07 2018.

[40] Ritayan Mitra, Karen S McNeal, and Howard D Bondell. Pupillary response to complex interdependent tasks: A cognitive-load theory perspective. *Behavior Research Methods*, 49:1905–1919, 2017.

[41] Eckhard H Hess and James M Polt. Pupil size in relation to mental activity during simple problem-solving. *Science*, 143(3611):1190–1192, 1964.

[42] HM Simpson and Shirley M Hale. Pupillary changes during a decision-making task. *Perceptual and Motor Skills*, 29(2):495–498, 1969.

[43] Jan Willem De Gee, Tomas Knapen, and Tobias H Donner. Decision-related pupil dilation reflects upcoming choice and individual bias. *Proceedings of the National Academy of Sciences*, 111(5):E618–E625, 2014.

[44] Johan Engström, Gustav Markkula, Trent Victor, and Natasha Merat. Effects of cognitive load on driving performance: The cognitive control hypothesis. *Human factors*, 59(5):734–764, 2017.

[45] Siyuan Chen and Julien Epps. Using task-induced pupil diameter and blink rate to infer cognitive load. *Human–Computer Interaction*, 29(4):390–413, 2014.

[46] Marcel F. Hinss, Anke M. Brock, and Raphaëlle N. Roy. Cognitive effects of prolonged continuous human-machine interaction: The case for mental state-based adaptive interfaces. *Frontiers in Neuroergonomics*, 3, 2022.

[47] Pauline van der Wel and Henk van Steenbergen. Pupil dilation as an index of effort in cognitive control tasks: A review. *Psychonomic Bulletin & Review*, 25(6):2005–2015, 2018.

[48] Yuedong Wang, Graham Naylor, Sophia E. Kramer, Adriana A. Zekveld, Dorothea Wendt, Barbara Ohlenforst, and Thomas Lunner. Relations between self-reported daily-life fatigue, hearing status, and pupil dilation during a speech perception in noise task. *Ear Hear*, 39(3):573–582, May/Jun 2018.

[49] NHS. Paying for your own social care (self-funding) — nhs.uk. `https://www.nhs.uk/social-care-and-support/money-work-and-benefits/paying-for-your-own-care-self-funding/`. [Accessed 19-04-2025].

[50] NHS. Walking aids, wheelchairs and mobility scooters — nhs.uk. `https://www.nhs.uk/social-care-and-support/care-services-equipment-and-care-homes/walking-aids-wheelchairs-and-mobility-scooters/`. [Accessed 19-04-2025].

[51] NHS England. NHS England » Personal wheelchair budgets — england.nhs.uk. `https://www.england.nhs.uk/personalisedcare/personal-health-budgets/personal-wheelchair-budgets/`. [Accessed 19-04-2025].

[52] Kelsey Livesey. I need a wheelchair | how to hire or buy. `https://www.homecare.co.uk/advice/`

`i-need-a-wheelchair-what-are-my-options-nhs-hiring-and-personal-fund`
March 2025. [Accessed 19-04-2025].

[53] Assistive technology (2023). Available at : `https://www.who.int/news-room/`
`fact-sheets/detail/assistive-technology`, January 2024. Accessed:
2025-02-20.

[54] Assistive technology: definition and safe use. Available at
: `https://www.gov.uk/government/publications/`
`assistive-technology-definition-and-safe-use/`
`assistive-technology-definition-and-safe-use`, September 2024.
Accessed: 2025-02-24.

[55] The history of the wheelchair. Available at : `https://www.sciencemuseum.org.`
`uk/objects-and-stories/history-wheelchair`, July 2024. Accessed:
2025-02-24.

[56] Kay Nias. The history of the wheelchair (blog post). Available at : `https://blog.`
`sciencemuseum.org.uk/history-of-the-wheelchair/`, March 2019. Accessed: 2025-02-24.

[57] Alternative access controls. Available at : `https://www.numotion.com/`
`products-services/adults/power/alternative-access-controls`.
Accessed: 2025-02-24.

[58] Home about us press office explore incredible objects from stephen
hawking's office at the science museum. Available at : `https:`
`//www.sciencemuseum.org.uk/about-us/press-office/`
`explore-incredible-objects-stephen-hawkings-office-science-museum`,
January 2022. Accessed: 2025-02-24.

[59] Stephen hawking's wheelchair with communication system. Available at : `https://heritage.humanists.uk/object/stephen-hawkings-wheelchair-with-communication-system/`, 2016. Accessed: 2025-02-24.

[60] Abhishek Verma, Siddhant Shrivastava, and Janakarajan Ramkumar. Mapping wheelchair functions and their associated functional elements for stair climbing accessibility: a systematic review. *Disability and Rehabilitation: Assistive Technology*, 19(1):200–221, 2024.

[61] Kebo Care Mette Damm Sørensen. Why stand when you can sit? Available at : `https://levousa.com/why-stand`. Accessed: 2025-02-24.

[62] Why is assisted standing important for people with disabilities? Available at : `https://www.numotion.com/blog/february-2020/why-is-assisted-standing-important-for-people-with`. Accessed: 2025-02-24.

[63] Javeed Shaikh-Mohammed, Swostik Sourav Dash, Vivek Sarda, and S Sujatha. Design journey of an affordable manual standing wheelchair. *Disability and Rehabilitation: assistive technology*, 18(5):553–563, 2023.

[64] Quickie q700-up m standing power wheelchair. Available at : `https://www.sunrisemedical.co.uk/quickie/power-wheelchairs/q700-up-m`. Accessed: 2025-02-24.

[65] Renaldo Herdiano Putra, Ahmad Ghifari Wildan Rahman, Endah Suryawati Ningrum, and Didik Setyo Purnomo. Design and stress analysis on electric standing wheelchair. In *2017 International Electronics Symposium on Engineering Technology and Applications (IES-ETA)*, pages 112–117. IEEE, 2017.

[66] Standing wheelchair range. Available at : `https://www.wheelfreedom.com/information-centre/standing-wheelchairs`. Accessed: 2025-02-24.

[67] Jessica S Ortiz, Guillermo Palacios-Navarro, Víctor H Andaluz, and Bryan S Guevara. Virtual reality-based framework to simulate control algorithms for robotic assistance and rehabilitation tasks through a standing wheelchair. *Sensors*, 21(15):5083, 2021.

[68] Khaled M Goher. A reconfigurable wheelchair for mobility and rehabilitation: Design and development. *Cogent Engineering*, 3(1):1261502, 2016.

[69] Sushant Merai, Denish Shah, Bhavinkumar Trivedi, Poojan Joshi, and Sagarsingh Kushwah. A study and design of standing wheelchair. *Materials Today: Proceedings*, 65:3787–3792, 2022.

[70] Lotte N.S. Andreasen Struijk, Eugen Romulus Lontis, Bo Bentsen, Henrik Vie Christensen, Héctor A. Caltenco, and Morten Enemark Lund. Fully integrated wireless inductive tongue computer interface for disabled people. *2009 Annual International Conference of the IEEE Engineering in Medicine and Biology Society*, pages 547–550, 2009.

[71] Samuel Poirier, François Routhier, and Alexandre Campeau-Lecours. Voice control interface prototype for assistive robots for people living with upper limb disabilities. *2019 IEEE 16th International Conference on Rehabilitation Robotics (ICORR)*, pages 46–52, 2019.

[72] Nur Zahira Jamil, Abdelkader Nasreddine Belkacem, Sofia Ouhbi, and Abderrahmane Lakas. Noninvasive electroencephalography equipment for assistive, adaptive, and rehabilitative brain–computer interfaces: A systematic literature review. *Sensors (Basel, Switzerland)*, 21, 2021.

[73] Ioulietta Lazarou, Spiros Nikolopoulos, Panagiotis C Petrantonakis, Ioannis Kompatsiaris, and Magda Tsolaki. Eeg-based brain–computer interfaces for communication and

rehabilitation of people with motor impairment: a novel approach of the 21 st century. *Frontiers in human neuroscience*, 12:14, 2018.

[74] Arpa Suwannarat, Setha Pan-ngum, and Pasin Israsena. Analysis of minimal channel electroencephalography for wearable brain–computer interface. *Electronics*, 13(3):565, 2024.

[75] Dennis J McFarland and Jonathan R Wolpaw. Eeg-based brain–computer interfaces. *current opinion in Biomedical Engineering*, 4:194–200, 2017.

[76] Sim Kok Swee, Kho Desmond Teck Kiang, and Lim Zheng You. Eeg controlled wheelchair. In *MATEC web of conferences*, volume 51, page 02011. EDP Sciences, 2016.

[77] Junhua Li, Jianyi Liang, Qibin Zhao, Jie Li, Kan Hong, and Liqing Zhang. Design of assistive wheelchair system directly steered by human thoughts. *International journal of neural systems*, 23(03):1350013, 2013.

[78] Marley Xiong, Raphael Hotter, Danielle Nadin, Jenisha Patel, Simon Tartakovsky, Yingqi Wang, Harsh Patel, Christopher Axon, Heather Bosiljevac, Anna Brandenberger, et al. A low-cost, semi-autonomous wheelchair controlled by motor imagery and jaw muscle activation. In *2019 IEEE International Conference on Systems, Man and Cybernetics (SMC)*, pages 2180–2185. IEEE, 2019.

[79] Kosmas Glavas, Katerina D. Tzimourta, Alexandros T. Tzallas, Nikolaos Giannakeas, and Markos G. Tsipouras. Empowering individuals with disabilities: A 4-dof bci wheelchair using mi and eog signals. *IEEE Access*, 12:95417–95433, 2024.

[80] Qiyun Huang, Shenghong He, Qihong Wang, Zhenghui Gu, Nengneng Peng, Kai Li, Yuandong Zhang, Mingping Shao, and Yuanqing Li. An eog-based human–machine interface for wheelchair control. *IEEE Transactions on Biomedical Engineering*, 65:2023–2032, 2018.

[81] Qiyun Huang, Yang Chen, Zhijun Zhang, Shenghong He, Rui Zhang, Jun Liu, Yuandong Zhang, Mingping Shao, and Yuanqing Li. An eog-based wheelchair robotic arm system for assisting patients with severe spinal cord injuries. *Journal of Neural Engineering*, 16, 2019.

[82] Muhammad Ilhamdi Rusydi, Muhammad Abrar A Boestari, Riko Nofendra, Syafii, Agung Wahyu Setiawan, and Minoru Sasaki. Wheelchair control based on eog signals of eye blinks and eye glances based on the decision tree method. *2024 12th International Conference on Information and Communication Technology (ICoICT)*, pages 152–159, 2024.

[83] tobii.com. How do eye trackers work? — A tech-savvy walk-through — tobii.com. `https://www.tobii.com/resource-center/learn-articles/how-do-eye-trackers-work`. [Accessed 1-04-2025].

[84] SR Research. About Eye Tracking — sr-research.com. `https://www.sr-research.com/about-eye-tracking/`. [Accessed 1-04-2025].

[85] Tobii Eyetracker. How do tobii eye trackers work? - tobii connect. `https://connect.tobii.com/s/article/How-do-Tobii-eye-trackers-work`. [Accessed 1-04-2025].

[86] Mahendran Subramanian, Noyan Songur, Darrell Adjei, Pavel Orlov, and A Aldo Faisal. A. eye drive: Gaze-based semi-autonomous wheelchair interface. In *2019 41st annual international conference of the IEEE engineering in medicine and biology society (EMBC)*, pages 5967–5970. IEEE, 2019.

[87] Md Samiul Haque Sunny, Md Ishrak Islam Zarif, Ivan Rulik, Javier Sanjuan, Mohammad Habibur Rahman, Sheikh Iqbal Ahamed, Inga Wang, Katie Schultz, and Brahim

Brahmi. Eye-gaze control of a wheelchair mounted 6dof assistive robot for activities of daily living. *Journal of NeuroEngineering and Rehabilitation*, 18:1–12, 2021.

[88] V Viswanatha, AC Ramachandra, Gowkanapalli Lokeshwar Reddy, AV Sai Tharun Reddy, Biyyam Pranay Kumar Reddy, and Gavvala Bhanu Kiran. An intelligent camera based eye controlled wheelchair system: Haar cascade and gaze estimation algorithms. In *2023 International Conference on Applied Intelligence and Sustainable Computing (ICAISC)*, pages 1–5. IEEE, 2023.

[89] Liberator Ltd. Sip/Puff Switch with Headset - liberator.co.uk. `https://www.liberator.co.uk/sip-puff-switch-with-headset`. [Accessed 14-04-2025].

[90] Sunrise Medical. Vigo - Empowering independence with subtle movements. `https://www.sunrisemedical.com/power-wheelchairs/switch-it-electronics/head-controls/vigo`. [Accessed 14-04-2025].

[91] Michael Franz. Switch-It Vigo Gives Power Wheelchair Users Wireless Head Control — newmobility.com. `https://newmobility.com/switch-it-vigo-gives-power-wheelchair-users-wireless-head-control/`, February 15, 2024. [Accessed 14-04-2025].

[92] buildmywheelchair. Permobil Total Control Head Array. `https://buildmywheelchair.com/permobil-total-control-head-array/`. [Accessed 14-04-2025].

[93] Kinova Robotics. Jaco Robotic arm — assistive.kinovarobotics.com. `https://assistive.kinovarobotics.com/product/jaco-robotic-arm`. [Accessed 14-04-2025].

[94] Fast Company. The JACO Robotic Arm Can Scratch Your Back, Hand Out Drinks. `https://www.fastcompany.com/1720283/jaco-robotic-arm-can-scratch-your-back-hand-out-drinks`. [Accessed 14-04-2025].

[95] wevolver.com. JACO robotic arm — wevolver.com. `https://www.wevolver.com/specs/jaco`. [Accessed 14-04-2025].

[96] Assistive Innovations. iARM - Assistive Innovations — assistive-innovations.com. `https://www.assistive-innovations.com/robotarmen/robot-iarm`. [Accessed 14-04-2025].

[97] Mobility Equipment Recyclers. 2021 Permobil F3 Power Chair w/Head Array. `https://mobilityequipmentforless.com/products/permobil-f3-rehab-power-chair-17-x-20-seat-tilt-recline-power-legs-s` [Accessed 14-04-2025].

[98] Easy Living Mobility. Ottobock Juvo B5 | Made to measure — store.easylivingmobility.co.uk. `https://store.easylivingmobility.co.uk/shop/powered-wheelchairs/made-for-you-powerchairs/ottobock-juvo-b5-rear-wheel-drive-electric-wheelchair`. [Accessed 14-04-2025].

[99] Easy Living Mobility. Permobil F3 Compact Corpus Powerchair — store.easylivingmobility.co.uk. `https://store.easylivingmobility.co.uk/shop/powered-wheelchairs/made-for-you-powerchairs/permobil-f3-compact-corpus-power-chair`. [Accessed 14-04-2025].

[100] Easy Living Mobility. stand up wheelchair for sale | Permobil F5 VS — store.easylivingmobility.co.uk. `https://store.easylivingmobility.`

`co.uk/shop/powered-wheelchairs/standing-powerchairs/`
`permobil-f5-vs-standing-power-chair`. [Accessed 14-04-2025].

[101] MobilityPlus+ Ultra-Light Instant Folding Electric Wheelchair — mobilitypluswheel-chairs.co.uk. `https://mobilitypluswheelchairs.co.uk/products/`
`mobilityplus-ultra-lightweight-instant-folding-electric-wheelchair?`
`variant=40772391600286`. [Accessed 14-04-2025].

[102] dynamic controls. Dx sip and puff - installation manual. `https:`
`//www.dynamiccontrols.com/sites/default/files/2018-05/`
`sip-puff-installation-manual.pdf`. [Accessed 14-04-2025].

[103] Tom Carlson and Yiannis Demiris. Increasing robotic wheelchair safety with collaborative control: Evidence from secondary task experiments. In *2010 IEEE International Conference on Robotics and Automation*, pages 5582–5587. IEEE, 2010.

[104] Tom Carlson and Yiannis Demiris. Collaborative control for a robotic wheelchair: evaluation of performance, attention, and workload. *IEEE Transactions on Systems, Man, and Cybernetics, Part B (Cybernetics)*, 42(3):876–888, 2012.

[105] Tobii pro nano specifications. Available at : `https://www.srlabs.it/`
`en/scientific-research/hardware-products/tobii-pro-nano/`, Jul 2024. Accessed: 2024-11-18.

[106] Gaze - tobii pro sdk documentation. Available at: `https://developer.`
`tobiipro.com/commonconcepts/gaze.html`. Accessed: 2024-11-18.

[107] Pupil diameter - tobii pro sdk documentation. Available at: `https://developer.`
`tobiipro.com/commonconcepts/pupildiameter.html`. Accessed: 2024-11-18.

[108] Emanual Robotis. Turtlebot 3 e-Manual. `https://emanual.robotis.com/docs/en/platform/turtlebot3/features/`. [Accessed 13-04-2025].

[109] Tobii pro nano user manual. Available at: `https://go.tobii.com/tobii-pro-nano-user-manual`. Accessed: 2024-11-18.

[110] Navid. Mohammadi Foumani et al. Deep learning for time series classification and extrinsic regression: A current survey. *ACM Computing Surveys*, 56(9):1–45, 2024.

[111] Keiron O'shea and Ryan Nash. An introduction to convolutional neural networks. *arXiv preprint arXiv:1511.08458*, 2015.

[112] Serdar Baltaci and Didem Gokcay. Stress detection in human–computer interaction: Fusion of pupil dilation and facial temperature features. *International Journal of Human–Computer Interaction*, 32(12):956–966, 2016.

[113] MG995 Servomotor | openimpulse.com. `https://www.openimpulse.com/blog/products-page/product-category/mg995-servomotor-2/`. [Accessed 26-03-2025].

[114] ESP32 Wi-Fi & Bluetooth Modules I Espressif — espressif.com. `https://www.espressif.com/en/products/modules/esp32`. [Accessed 26-03-2025].

[115] Esp32 datasheet. `https://www.espressif.com/sites/default/files/documentation/esp32-wroom-32_datasheet_en.pdf`. [Accessed 26-03-2025].

[116] Colchester catalyst charity. `https://colchestercatalyst.co.uk/`. [Accessed 07-04-2025].

[117] Elephant Robotics. Elephant Robotics myCobot 320 M5 2022. `https://shop.elephantrobotics.com/`

`en-gb/collections/mycobot-pro-320/products/`
`commercial-and-economic-six-axis-collaborative-robot`. [Accessed 07-04-2025].

[118] Elephant Robotics. myCobot 320 collection. `https://shop.`
`elephantrobotics.com/en-gb/collections/mycobot-pro-320`.
[Accessed 07-04-2025].

[119] Elephant Robotics. myCobot Pro Adaptive Gripper For myCobot 320. `https://shop.`
`elephantrobotics.com/en-gb/collections/mycobot-pro-320/`
`products/mycobot-pro-adaptive-gripper-black-white`. [Accessed 07-04-2025].

[120] M5Stack - Modular Rapid ESP32 IoT Development Board - ESP32 dev kits. `https://m5stack.com/`. [Accessed 07-04-2025].

[121] Glenn Jocher. ultralytics/yolov5: v7.0 - yolov5 sota realtime instance segmentation, nov 2022.

[122] Neville A Stanton, Paul M Salmon, Laura A Rafferty, Guy H Walker, Chris Baber, and Daniel P Jenkins. *Human factors methods: a practical guide for engineering and design*. CRC Press, 2017.

[123] Agency for Healthcare Research and Quality. Nasa task load index | Digital Healthcare Research — digital.ahrq.gov. `https://digital.ahrq.gov/health-it-tools-and-resources/evaluation-resources/workflow-assessment-health-it-toolkit/all-workflow-tools/nasa-task-load-index`. [Accessed 1-04-2025].

[124] NASA. The nasa tlx tool: Task load index — humansystems.arc.nasa.gov. `https://humansystems.arc.nasa.gov/groups/TLX/`. [Accessed 1-04-2025].

[125] Sandra G Hart and Lowell E Staveland. Development of nasa-tlx (task load index): Results of empirical and theoretical research. In *Advances in psychology*, volume 52, pages 139–183. Elsevier, 1988.

[126] Louise Demers, Rhoda Weiss-Lambrou, and Bernadette Ska. Development of the quebec user evaluation of satisfaction with assistive technology (quest). *Assistive technology*, 8(1):3–13, 1996.

[127] Quebec User Evaluation of Satisfaction with Assistive Technology — sralab.org. `https://www.sralab.org/rehabilitation-measures/` `quebec-user-evaluation-satisfaction-assistive-technology`. [Accessed 1-04-2025].

[128] Louise Demers, Rhoda Weiss-Lambrou, and Bernadette Ska. The quebec user evaluation of satisfaction with assistive technology (quest 2.0): an overview and recent progress. *Technology and disability*, 14(3):101–105, 2002.

[129] Viswanath Venkatesh, Michael G Morris, Gordon B Davis, and Fred D Davis. User acceptance of information technology: Toward a unified view. *MIS quarterly*, pages 425–478, 2003.

[130] Dr. Nele A.J. De Witte and Dr. Tom Van Daele. Questionnaire: UTAUT — thomasmore.be. `https://thomasmore.` `be/en/care-and-well-being-people-and-well-being/` `questionnaire-utaut`. [Accessed 1-04-2025].

[131] Viswanath Venkatesh, James YL Thong, Frank KY Chan, Paul Jen-Hwa Hu, and Susan A Brown. Extending the two-stage information systems continuance model: Incorporating utaut predictors and the role of context. *Information systems journal*, 21(6):527–555, 2011.

Appendix A

Questionnaire

Questionnaires are structured tools used to collect data in an organized and systematic manner. A wide range of questionnaires exists across various fields, each designed to evaluate different types of information, such as user experiences, opinions, perspectives, or behaviours. Asking appropriate and well-formulated questions is essential for drawing meaningful and reliable conclusions. Standardized and widely accepted questionnaires not only ensure the use of validated and well-established questions but also enable comparison of results across different studies, thereby enhancing the reliability and generalizability of the findings.

In this study, the NASA Task Load Index (TLX) was used to assess the workload and demands associated with the experiment and the proposed system. It compares various contributing factors such as mental demand, physical demand, temporal demand, effort, frustration, and performance. These questions provide valuable insights into the system's design and the cognitive and physical load associated with its use.

To evaluate the acceptability and satisfaction with the proposed system, Quebec User Evaluation of Satisfaction with Assistive Technology (QUEST) 2.0 and Unified Theory of Acceptance and Use of Technology (UTAUT) questionnaire has been used. Quest2.0 focuses on the satisfaction with the assistive devices as well as the importance of the factors associated with the

ATs. The UTAUT model focuses on the acceptance and use of technologies and has been widely applied in various studies to assess the adoption of new technologies, such as learning platforms, workplace systems, mobile devices, and more.

In addition to the standardized questionnaires, a set of custom feedback questions was developed to address specific aspects of the proposed system and the experimental setup. These questions aimed to gather participants' suggestions and opinions, which were not covered by the standard instruments, providing further insights into user experience and potential areas for improvement.

For this study, the standard questions included in the questionnaire were either taken directly from the original sources or adapted to suit the context of the experiment, while maintaining the integrity and intent of the original constructs. The sources includes NASA-TLX[122, 123, 124, 125], QUEST2.0[126, 127, 128], UTAUT [129, 130, 131].

Table.A.1 presents the questions asked as well as the range of the possible answer for each question. In NASA questions section 1, The answer range from -10 defining low demand and +10 defining high demand. The next section askes to choose between each pair of the choices. QUEST Section one askes about the satisfaction. 1 determines not satisfied and 5 is representing highly satisfied. UTAUT rages from 1 meaning strongly disagree to 7 meaning strongly agree.

Table A.1: Survey Questions and Answer Ranges

Questionnaire	Number	Question	Range
NASA	S1 Q1	Mental Demand: How mentally demanding was the task?	-10,10
NASA	S1 Q2	Physical Demand: How physically demanding was the task?	-10,10
NASA	S1 Q3	Temporal Demand: How hurried or rushed was the pace of the task?	-10,10

NASA	S1 Q4	Performance: How successful were you in accomplishing what you were asked to do?	-10,10
NASA	S1 Q5	Effort: How hard did you have to work to accomplish your level of performance?	-10,10
NASA	S1 Q6	Frustration: How insecure, discouraged, irritated, stressed, and annoyed were you?	-10,10
NASA	S2 Q1	Mental Demand or Physical Demand	1,2
NASA	S2 Q2	Temporal Demand or Performance	1,2
NASA	S2 Q3	Effort or Frustration	1,2
NASA	S2 Q4	Mental Demand or Temporal Demand	1,2
NASA	S2 Q5	Effort or Physical Demand	1,2
NASA	S2 Q6	Performance or Frustration	1,2
Quest	S1 Q1	Degree of Satisfaction with The dimensions (size, height, length, width) of your assistive device?	1,5
Quest	S1 Q2	Degree of Satisfaction with The weight of your assistive device?	1,5
Quest	S1 Q3	Degree of Satisfaction with The ease in adjusting (fixing, fastening) the parts of your assistive device	1,5
Quest	S1 Q4	Degree of Satisfaction with How safe and secure your assistive device is?	1,5

Quest	S1 Q5	Degree of Satisfaction with The durability (endurance, resistance to wear) of your assistive device?	1,5
Quest	S1 Q6	Degree of Satisfaction with How easy it is to use your assistive device?	1,5
Feedback	Q1	How would you rate the total experiment today?	1,5
Feedback	Q2	How would you rate the control over the mouse cursor?	1,5
Feedback	Q3	How would you rate the speed of the robot?	1,5
UTAUT	Q1	Using the technologies daily would enable me to accomplish my goals more quickly	1,7
UTAUT	Q2	Using the technologies would improve my occupational performance for daily living	1,7
UTAUT	Q3	Using the technologies enhances the effectiveness of the treatments that I receive	1,7
UTAUT	Q4	I would find the technologies useful as an upgrade of previous/basic version of the assistive device	1,7
UTAUT	Q5	Use of the technologies can increase the quality of my daily life	1,7
UTAUT	Q6	Use of the technology can increase the quantity and quality of my daily tasks/activities	1,7
UTAUT	Q7	Use of the technology would make it easier to perform my daily tasks	1,7

UTAUT	Q8	Learning to operate the technologies would be easy for me	1,7
UTAUT	Q9	I would find the technologies easy to use and to understand	1,7
UTAUT	Q10	Completing operations such as set-up, calibration, and adjustments does not take too much time	1,7
UTAUT	Q11	Learning to use technologies does not take too long	1,7
UTAUT	Q12	I believe that it is easy to get the technologies to do what I want them to do	1,7
UTAUT	Q13	People who influence my decisions think that I would benefit from using the technology (Ex. Family members, caregivers, therapist, etc.)	1,7
UTAUT	Q14	I think that I should use the technologies with help / in presence of someone	1,7
UTAUT	Q15	In general, the community has supported the use of the new assistive technologies	1,7
UTAUT	Q16	People in my community who use the recent technologies have more independence than those who do not	1,7
UTAUT	Q17	I prefer to have the opportunity to test the technologies	1,7
UTAUT	Q18	I find participation in research is easy to do	1,7
UTAUT	Q19	I have / have been given the necessary resources to use the device	1,7

UTAUT	Q20	I have / have been given the necessary knowledge to use the device	1,7
UTAUT	Q21	There is assistance available for technological difficulties	1,7
UTAUT	Q22	Using the device is compatible with my needs	1,7
UTAUT	Q23	I find the assistive device safe for my daily independent use	1,7
UTAUT	Q24	I intend to use the technologies once available	1,7
UTAUT	Q25	I predict I would use the technologies once available	1,7
UTAUT	Q26	I plan to use technologies once available	1,7
UTAUT	Q27	I am planning to use the technologies to improve my perceptual function	1,7
UTAUT	Q28	I am planning to use the technologies to improve my cognitive function	1,7
UTAUT	Q29	I am planning to use the technologies to improve my motor function	1,7
Age	Age	U or 1 for Under 50 and O or 2 for Over 50 years old	1,2
Glasses	Glasses	Are You Wearing Glasses or contact lenses? Y or 1, 2 or N	1,2

Appendix B

The VAS Questions

The Visual Analogue Scale (VAS) is a widely used tool for capturing psychological and subjective measures. The inclusion of visual elements, such as emojis, assisted participants in interpreting the scale accurately and selecting appropriate responses.

In the wheelchair-based experiment, two specific scales were employed. The fatigue scale was administered twice: first, prior to the task to establish a baseline, and again upon task completion to evaluate the impact of system usage on the user's fatigue level. Additionally, the motivation scale was used before the experiment to gauge participants' initial engagement and willingness to interact with the system.
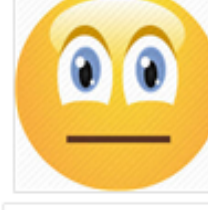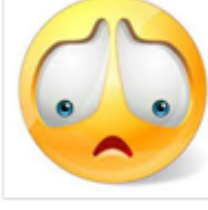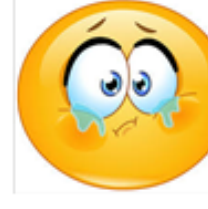
Figure B.1: The VAS questionnaire for fatigue. It has been used once before the experiment and once after completing the experiment, To determine the effect of the experiment and system on the users.
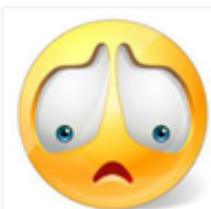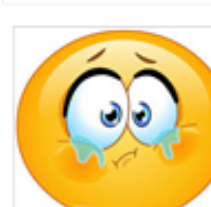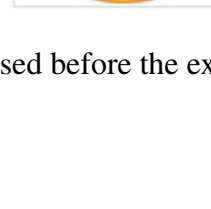
Figure B.2: The VAS questionnaire for motivation. This has been used before the experiment

Appendix C

List of Publications

1. P. Azizinezhad, H. Ghonchi and A. Chowdhury, "Pupil Diameter Classification using Machine Learning During Human-Computer Interaction," 2024 IEEE International Conference on Omni-layer Intelligent Systems (COINS), London, United Kingdom, 2024, pp. 1-6, doi: 10.1109/COINS61597.2024.10622128.

2. P. Azizinezhad and A. Chowdhury, "Exploring Pupil Dilation as an Indicator of Performance in Gaze-Based Robot Navigation for Assistive Technology," 2024 International Conference on Modeling, Simulation & Intelligent Computing (MoSICom), Dubai, United Arab Emirates, 2024, pp. 513-518, doi: 10.1109/MoSICom63082.2024.10881597.

3. (Accepted) P. Azizinezhad and A. Chowdhury, "Evaluating a Gaze-Controlled Navigation Interface: A User-Centered Approach," The 47th Annual International Conference of the IEEE Engineering in Medicine and Biology Society (EMBC), Copenhagen, Denmark, July 2025.